

Diamond-based devices

From detectors to bio-sensors and single-photon emitters

Paolo Olivero

Physics Department & NIS inter-departmental centre
University of Torino

INFN Section of Torino

olivero@to.infn.it

Cogne, 14 February 2014



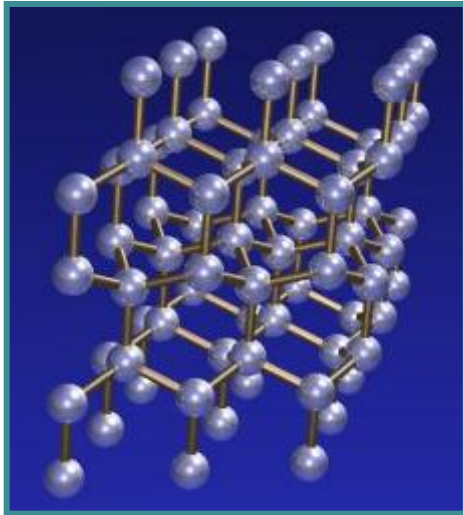
Outline

- Diamond
- IBL in diamond
 - Basic concepts
 - State of the art
- Current research activities @ UniTo & INFN-To
 - **Electrical** features
 - Radiation detection
 - Biosensing
 - Quantum Optics
- Conclusions

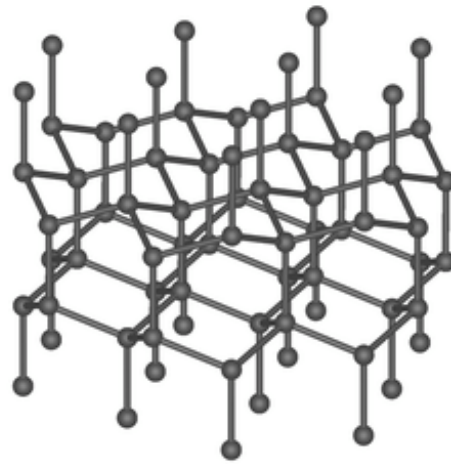
-
- Diamond
 - IBL in diamond
 - Basic concepts
 - State of the art
 - Current research activities @ UniTo & INFN-To
 - **Electrical** features
 - Radiation detection
 - Biosensing
 - Quantum Optics
 - Conclusions

Diamond

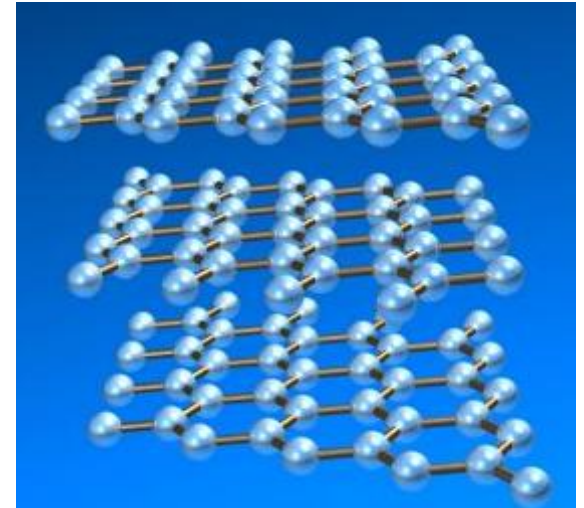
αδάμας (indestructible)



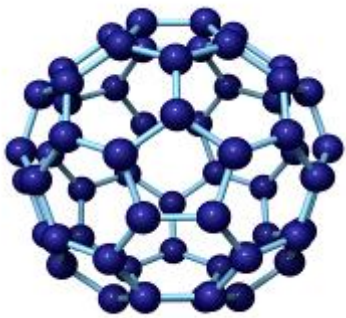
diamond



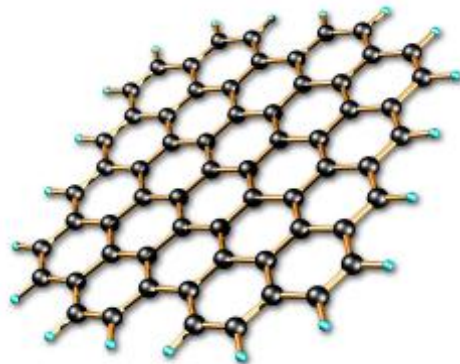
lonsdaleite



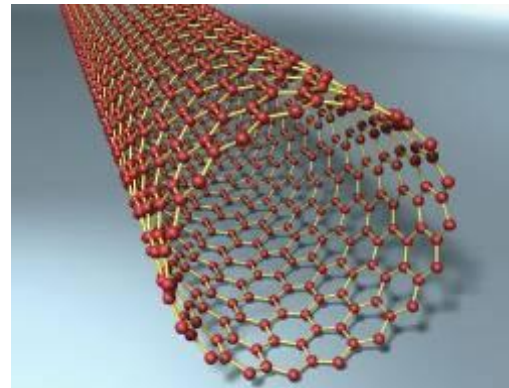
graphite



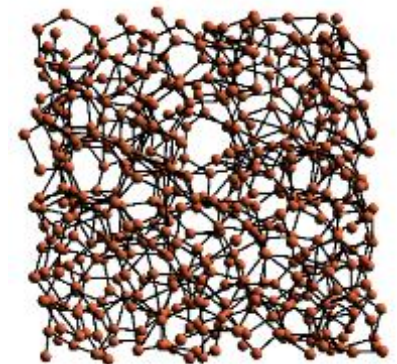
fullerene



graphene



nanotube



amorphous carbon **4**

Diamond

Carbon

The periodic table shows elements grouped into metals, non-metals, and noble gases. Carbon (C) is located in group 14, period 2. A blue box highlights the element Carbon (C) in the periodic table.

IA	IIA	METALLI										NON METALLI										VIIIA				
1	2	METALLI DI TRANSIZIONE										13	14	15	16	17	18	NON METALLI						2		
1 H		3 Li	4 Be											5 B	6 C	7 N	8 O	9 F	10 Ne							10 Ne
11 Na	12 Mg											13 Al	14 Si	15 P	16 S	17 Cl	18 Ar							18 Ar		
19 K	20 Ca	21 Sc	22 Ti	23 V	24 Cr	25 Mn	26 Fe	27 Co	28 Ni	29 Cu	30 Zn	31 Ga	32 Ge	33 As	34 Se	35 Br	36 Kr							36 Kr		
37 Rb	38 Sr	39 Y	40 Zr	41 Nb	42 Mo	43 Tc	44 Ru	45 Rh	46 Pd	47 Ag	48 Cd	49 In	50 Sn	51 Sb	52 Te	53 I	54 Xe							54 Xe		
55 Cs	56 Ba	57 La	72 Hf	73 Ta	74 W	75 Re	76 Os	77 Ir	78 Pt	79 Au	80 Hg	81 Tl	82 Pb	83 Bi	84 Po	85 At	86 Rn							86 Rn		
87 Fr	88 Ra	89 Ac	104 Unq	105 Unp	106 Unh	107 Uns	108 Uno	109 Une	110 Uun	111 Uuu											118 Og					

47 Ag numero atomico 107,868 simbolo nome dell'elemento massa atomica

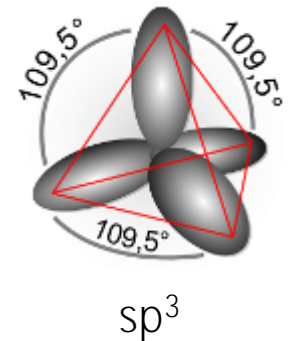
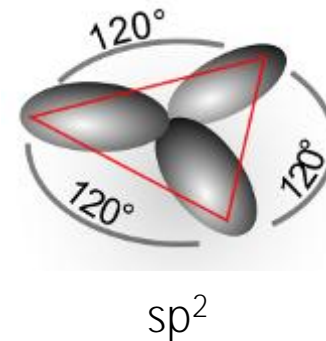
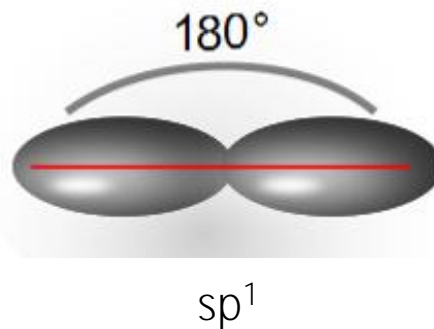
metalli caratteristiche intermedie non metalli

* I valori tra parentesi indicano il numero di massa dell'isotopo più stabile.

6
C
Carbon
12.0107

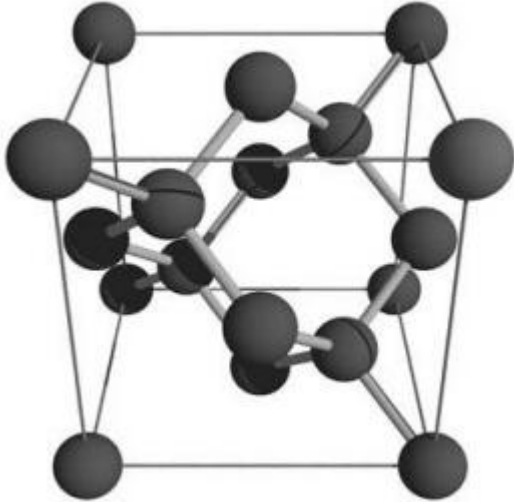


Three types of hybrid orbitals



Diamond

Crystal structure

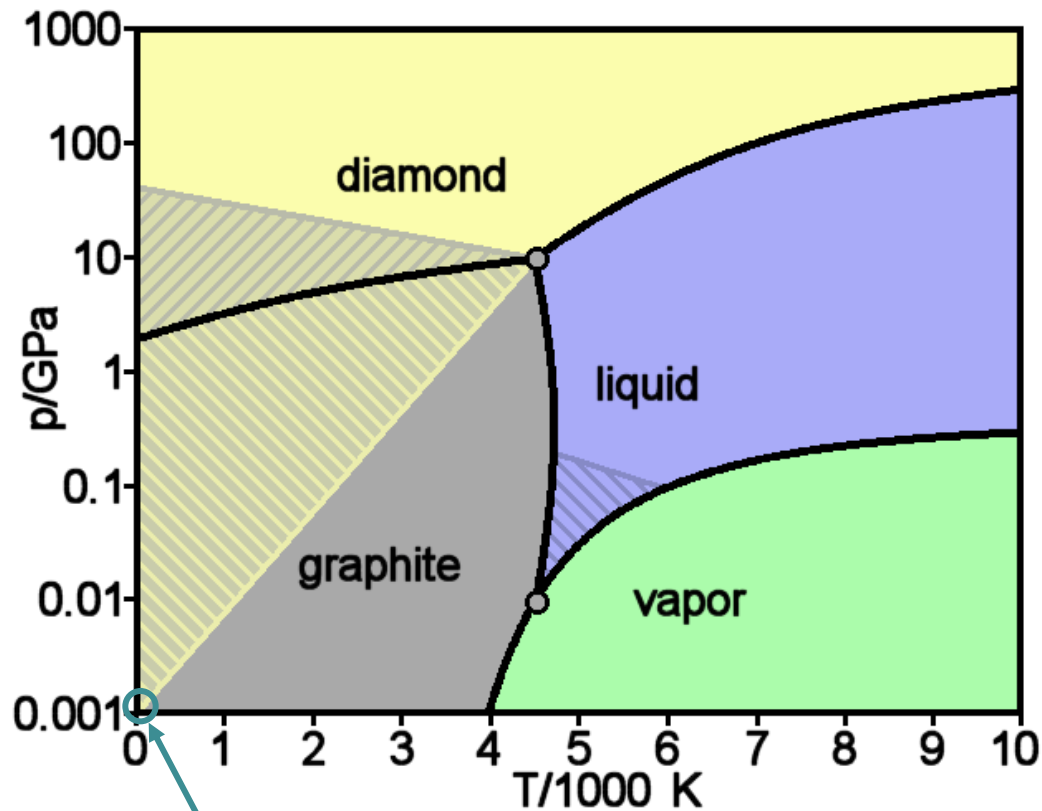


- Lattice: face-centered cubic
- Base: $\{ (0, 0, 0); (\frac{1}{4}a, \frac{1}{4}a, \frac{1}{4}a) \}$
- Crystal: diamond

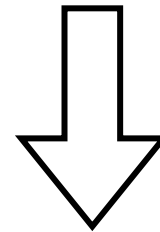
- Bond length: 1.54 Å
- Cell parameter: 3.57 Å
- Atomic density: 1.77×10^{23} atoms cm^{-3}

Diamond

Phase diagram of Carbon



Room pressure and temperature:
diamond is meta-stable



Natural diamond forms at high
pressure and temperature

Diamond

Synthesis techniques

High Pressure High Temperature (HPHT)



- growth from a diamond seed
- graphite with catalytic elements (Ni, Fe, ...)
- single-crystals: good structural properties, impurities

Diamond

Synthesis techniques

High Pressure High Temperature (HPHT)



- growth from a diamond seed
- graphite with catalytic elements (Ni, Fe, ...)
- single-crystals: good structural properties, impurities

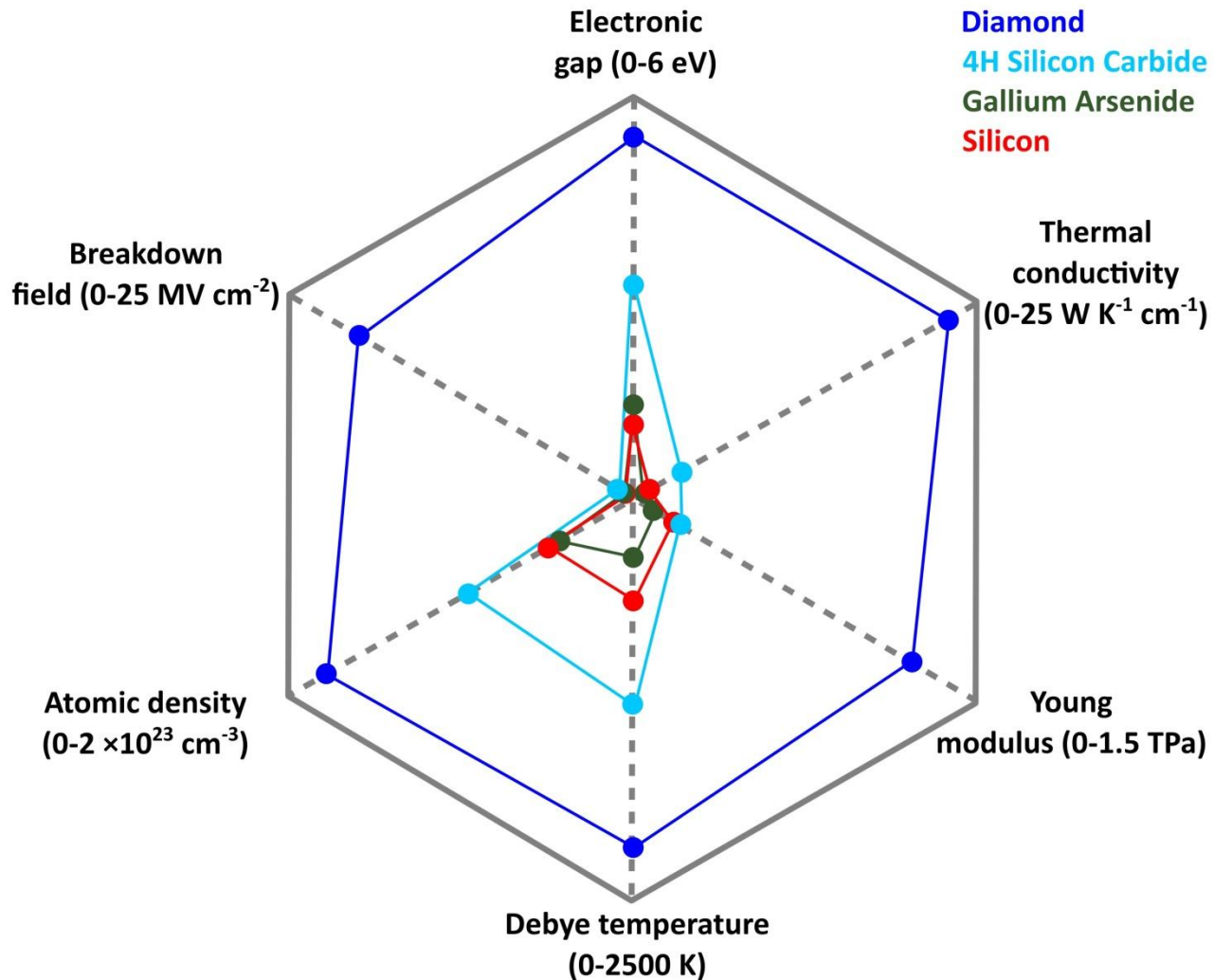
Chemical Vapor Deposition (CVD)



- low pressure and temperature
- C- and H-containing plasma
- selective etching of non-diamond phases
- homoepitaxial **growth** → **high purity** single crystals

Diamond

Extreme physical properties



Diamond

Other properties

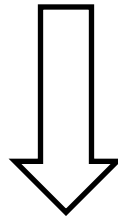
- high carriers mobility
- high breakdown field
- radiation hardness
- wide band-gap → broad transparency, low leakage currents
- chemical inertness
- bio-compatibility
- tissue-equivalence
- surface functionalization → negative electron affinity, 2D hole gas
- appealing luminescent centers
- ...

-
- Diamond
 - IBL in diamond
 - Basic concepts
 - State of the art
 - Current research activities @ UniTo & INFN-To
 - **Electrical** features
 - Radiation detection
 - Biosensing
 - Quantum Optics
 - Conclusions

IBL in diamond

Diamond: a **hard** material for micro-fabrication:

- Mechanical hardness
- Chemical inertness
- Optical transparency



Ion beam lithography

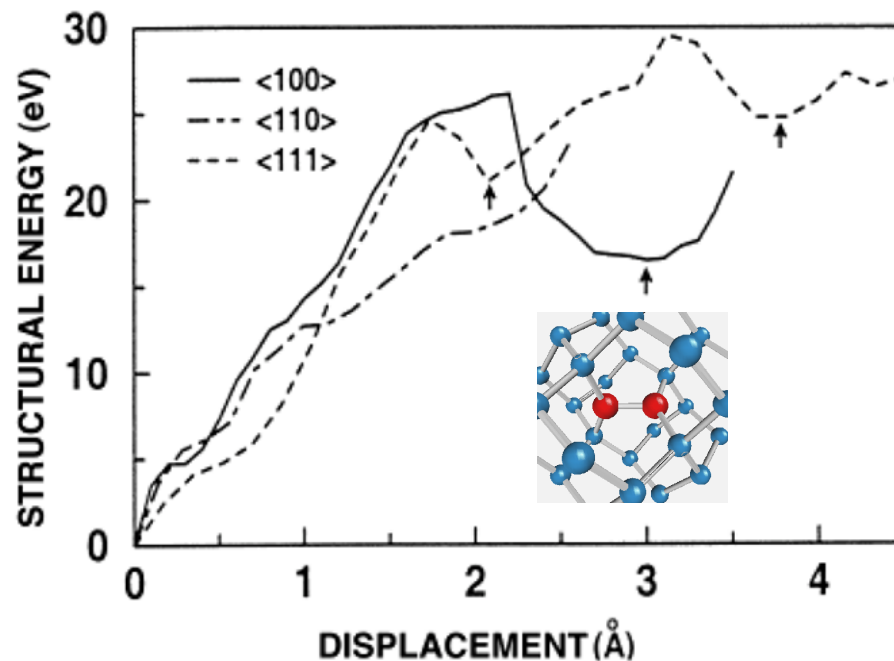
IBL in diamond

Electronic energy loss →

No effects (thermal spikes, coulomb explosions) reported so far

Nuclear energy loss →

Significant structural effects on a **meta-stable** material

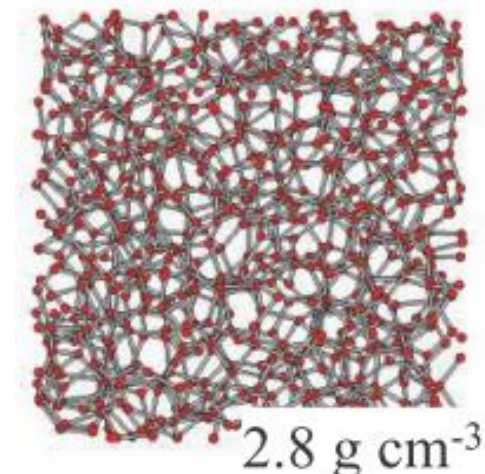
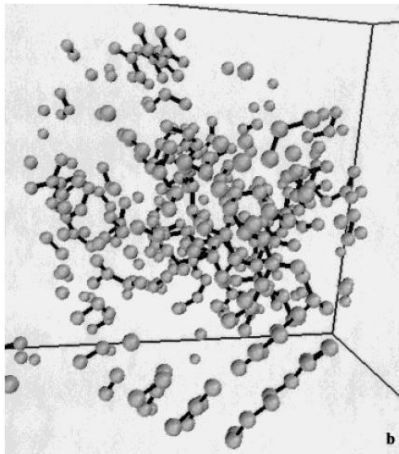


Atom displacement → Formation of an sp^2 -bonded split interstitial

IBL in diamond

A crude linear approximation: $\rho_{\text{vac}} = (\text{linear damage density})_{\text{SRIM}} \times (\text{fluence})$
 $[\#_{\text{vac}} \text{ cm}^{-3}] \quad [\#_{\text{vac}} \#_{\text{ion}}^{-1} \text{ cm}^{-1}] \quad [\#_{\text{ion}} \text{ cm}^{-2}]$

- Non-linear effects (defect-defect interaction, self-**annealing**, ...) **are ignored.**
- At high implantation fluences the defect density is not realistic (over-estimated density of point-defects)
- More advanced approaches: Atomistic simulations



IBL in diamond

A crude linear approximation: $\rho_{\text{vac}} = (\text{linear damage density})_{\text{SRIM}} \times (\text{fluence})$
 $[\#_{\text{vac}} \text{ cm}^{-3}] \quad [\#_{\text{vac}} \#_{\text{ion}}^{-1} \text{ cm}^{-1}] \quad [\#_{\text{ion}} \text{ cm}^{-2}]$

- Non-linear effects (defect-defect interaction, self-**annealing**, ...) **are ignored**.
- At high implantation fluences the defect density is not realistic (over-estimated density of point-defects)
- More advanced approaches: Semi-analytical / empirical models

Crystal-TRIM (04/1D - last revision May 2004)

developed by Matthias Posselt ¹⁾ ²⁾



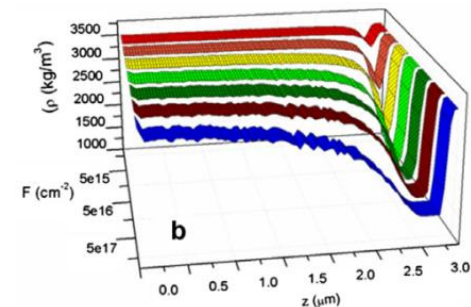
Nuclear Instruments and Methods in Physics Research B 166-167 (2000) 364-373



www.elsevier.nl/locate/nimb

Radiation defects and their annealing behaviour in ion-implanted diamonds

Johan F. Prins ^{a,*}, Trevor E. Derry ^b

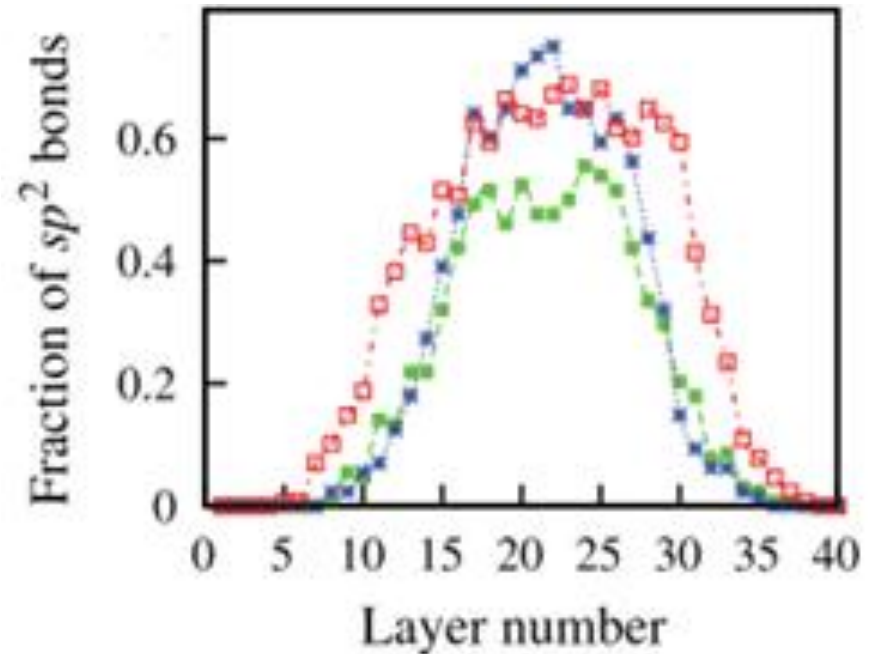
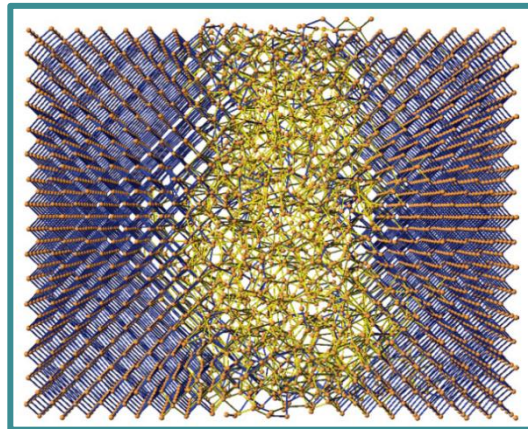
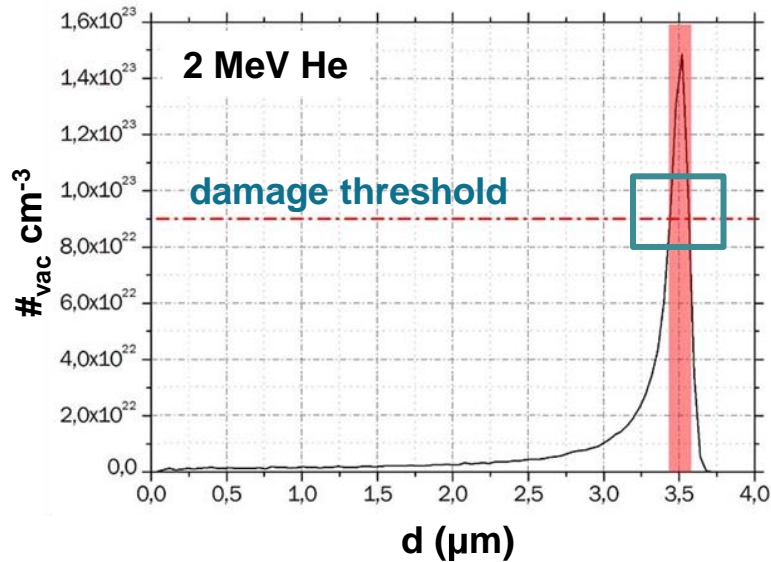


@ : Institute of Ion Beam Physics and Materials Research (Dresden),

Department of Physics – University of Pretoria, Solid State Physics Group – University of Torino

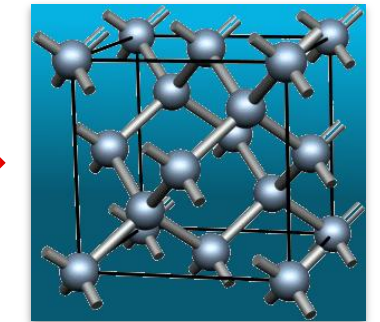
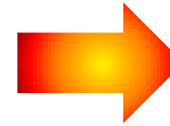
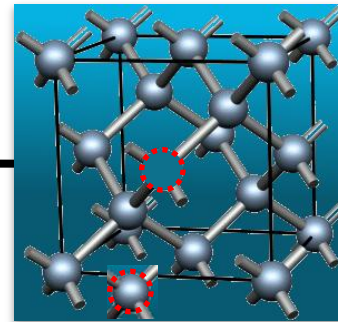
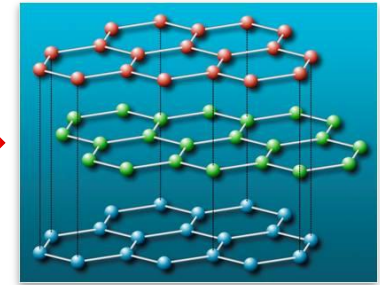
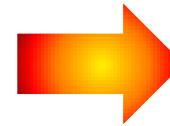
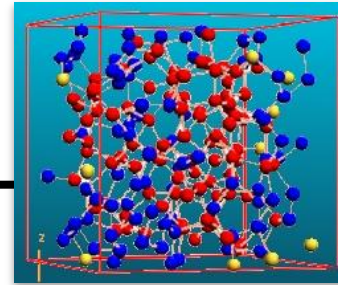
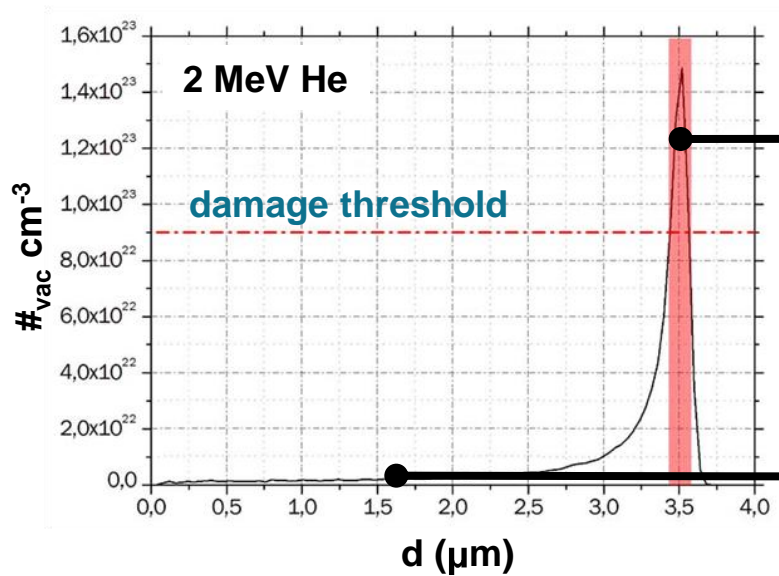
IBL in diamond

High fluence implantation → **Formation of an amorphous carbon layer**
where the damage density exceeds a **threshold value**



IBL in diamond

Thermal annealing



- Above threshold: amorphous carbon

→ polycrystalline graphite

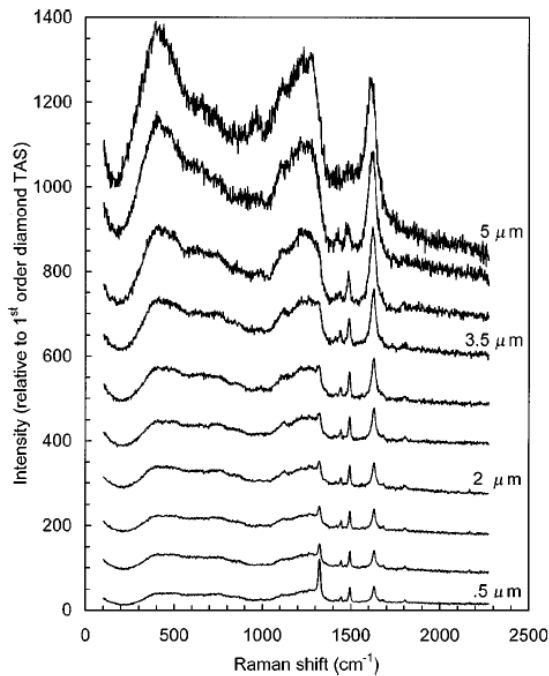
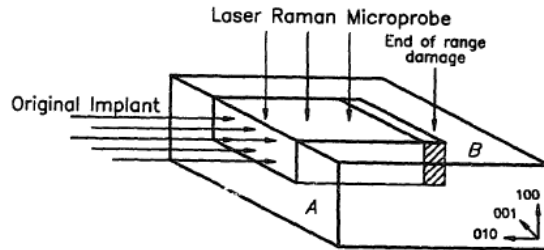
- Below threshold: diamond with Frenkel defects

→ diamond

IBL in diamond

Experimental evidences

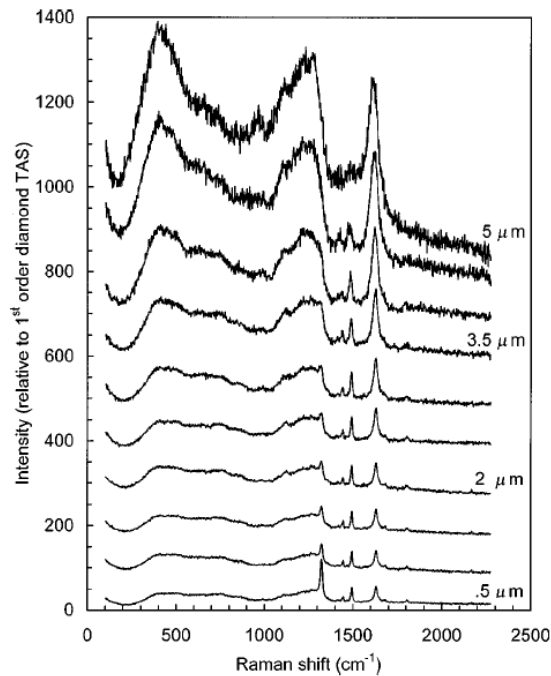
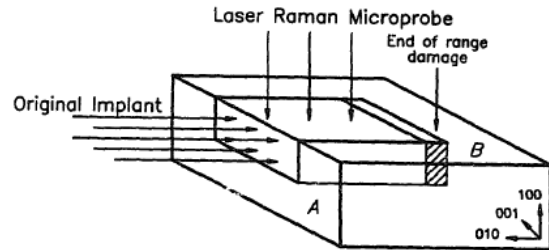
Cross-sectional μ -Raman



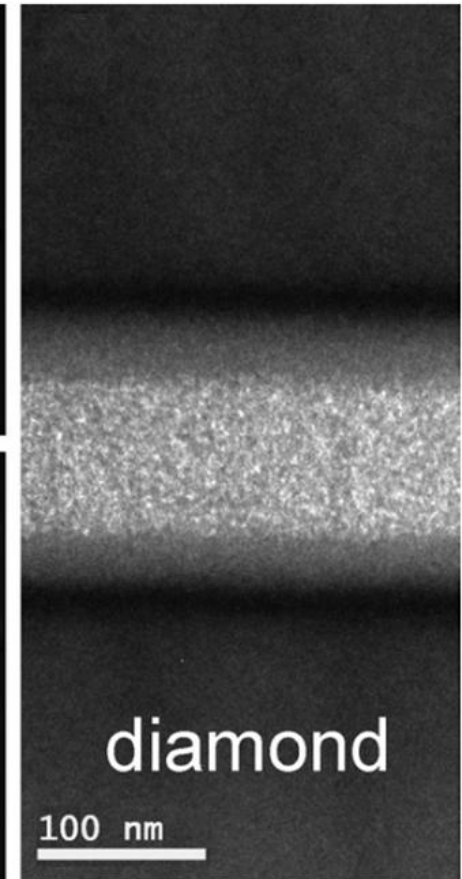
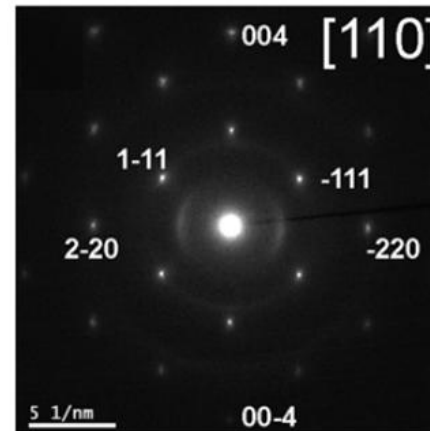
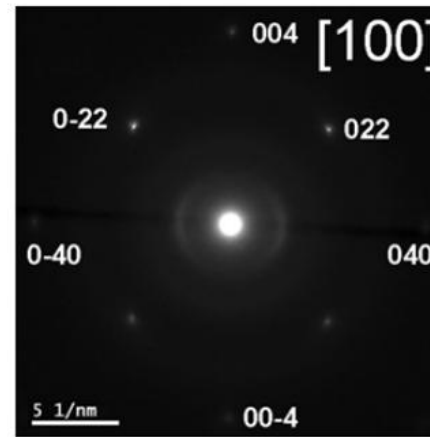
IBL in diamond

Experimental evidences

Cross-sectional μ -Raman



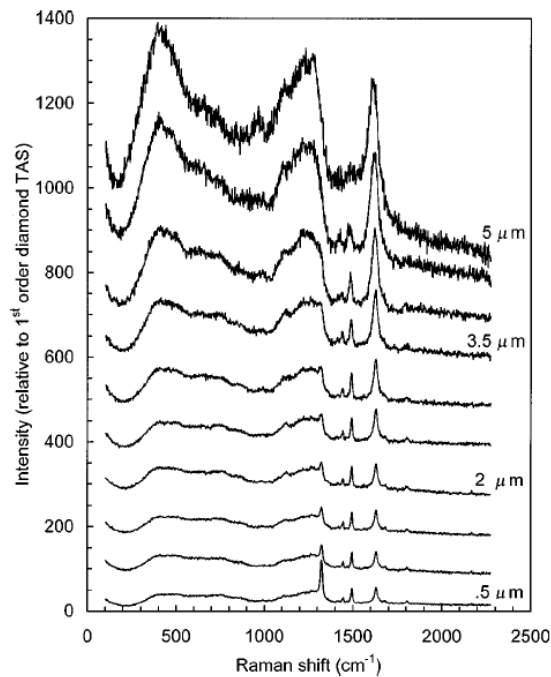
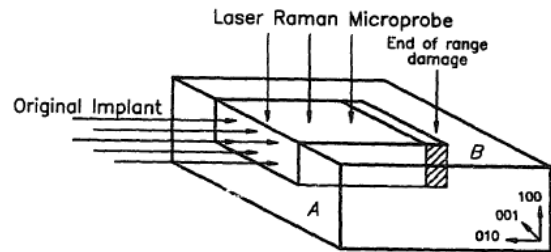
Cross-sectional TEM



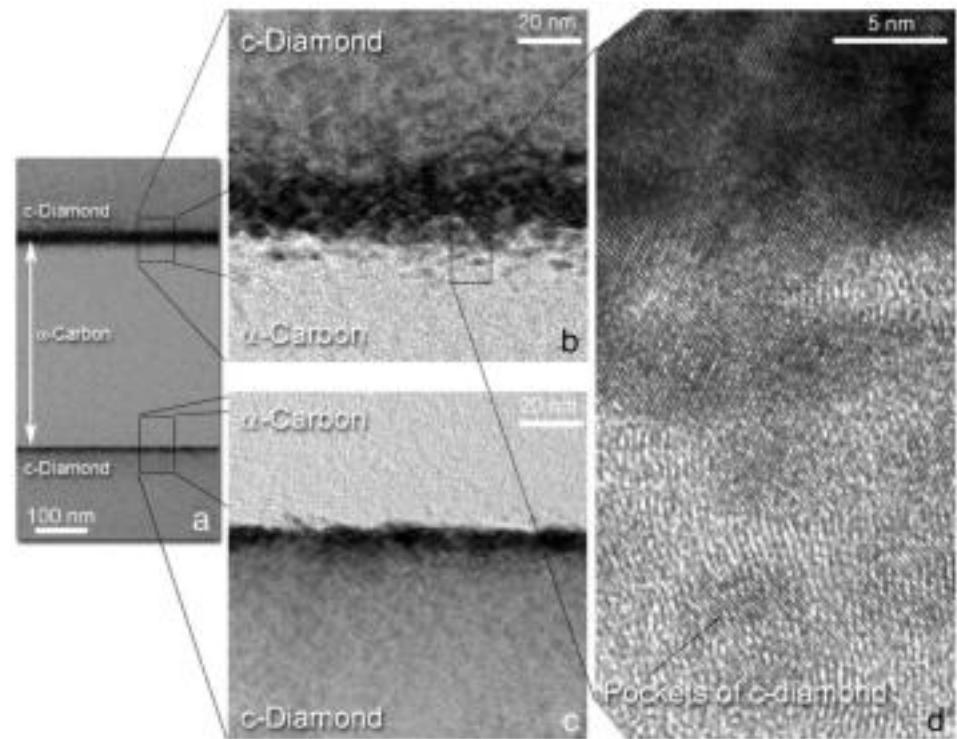
IBL in diamond

Experimental evidences

Cross-sectional μ -Raman

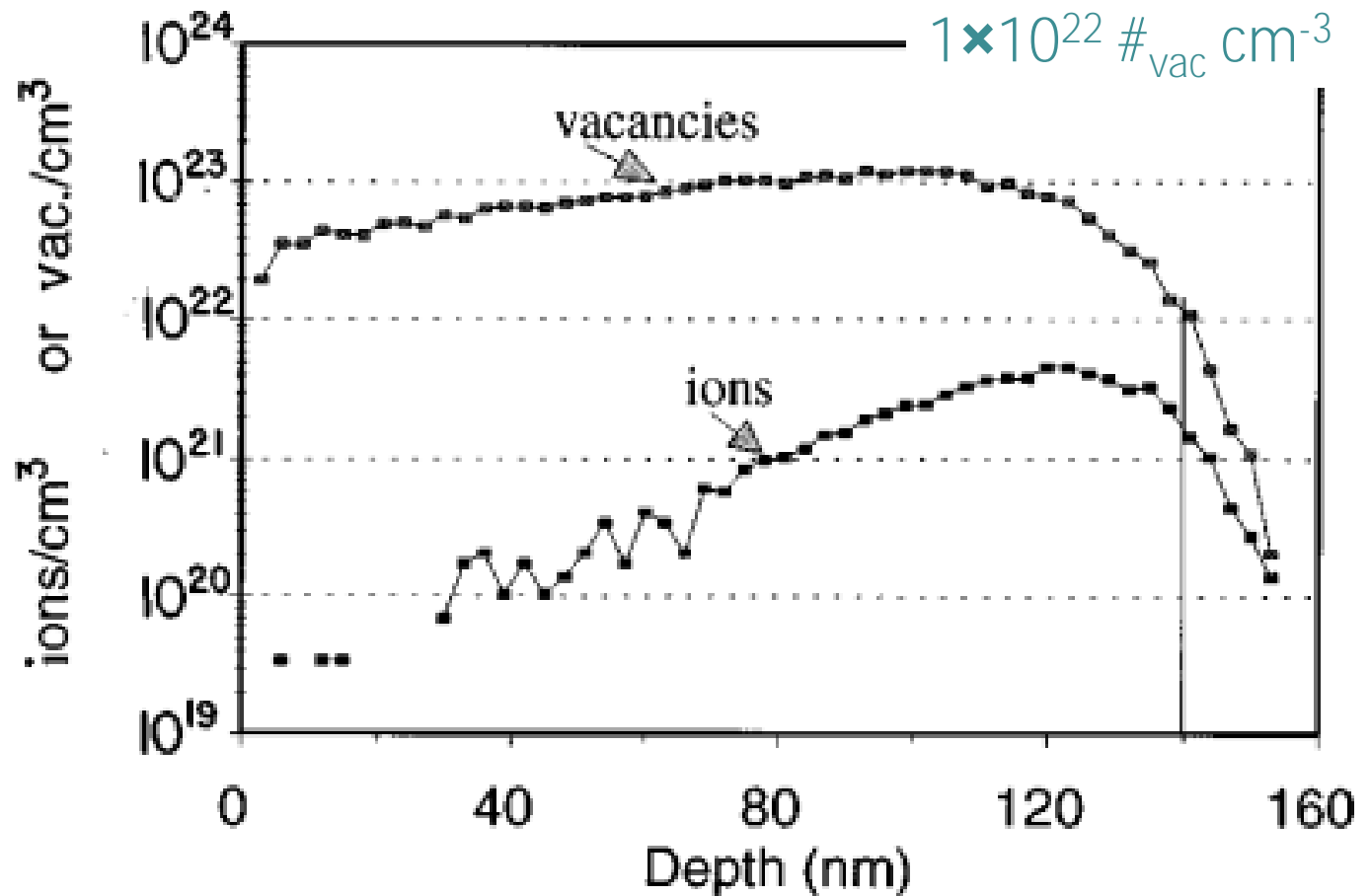
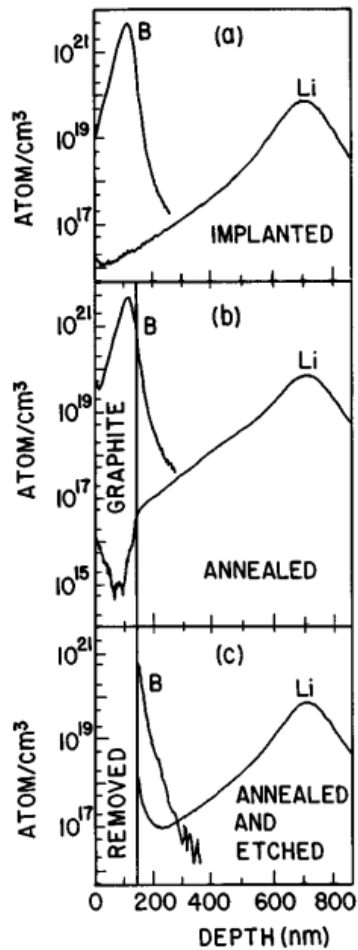


Cross-sectional TEM



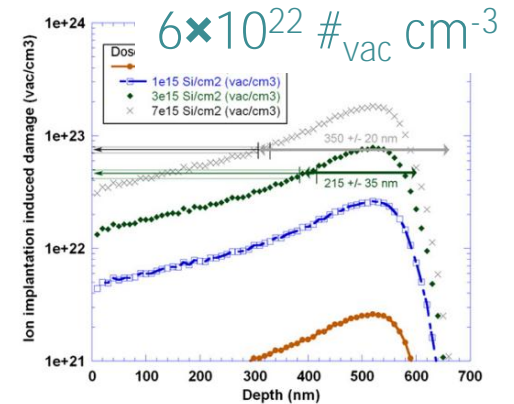
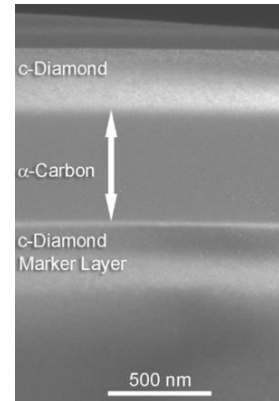
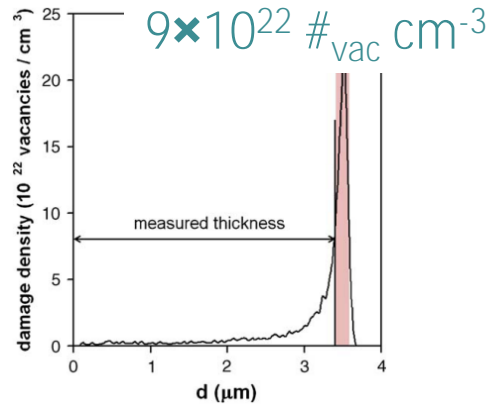
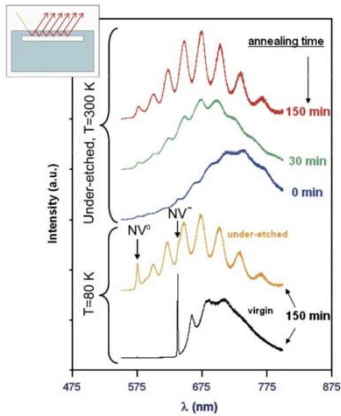
IBL in diamond

Graphitization threshold



IBL in diamond

Graphitization threshold

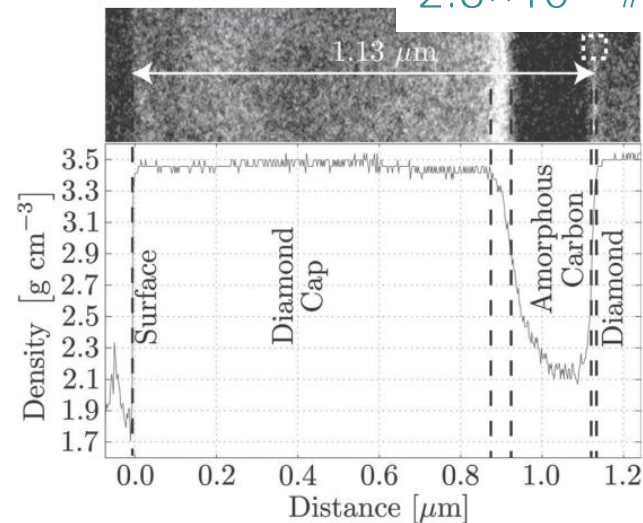
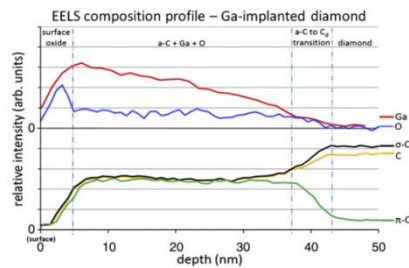
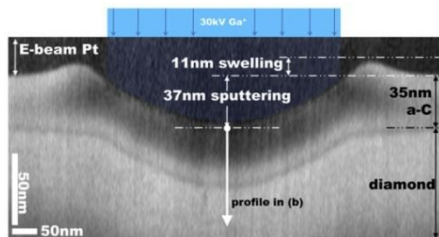


@ : School of Physics – University of Melbourne

@ : Uni. of Florida & Australian National Uni.

$2 \times 10^{22} \#_{\text{vac}} \text{cm}^{-3}$

$2.8 \times 10^{22} \#_{\text{vac}} \text{cm}^{-3}$



@ : University of New South Wales

@ : School of Physics – University of Melbourne **24**

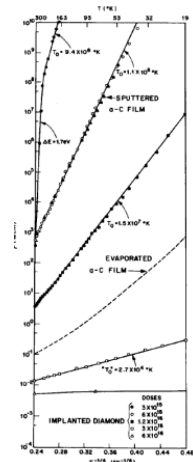
IBL in diamond

Electrical properties

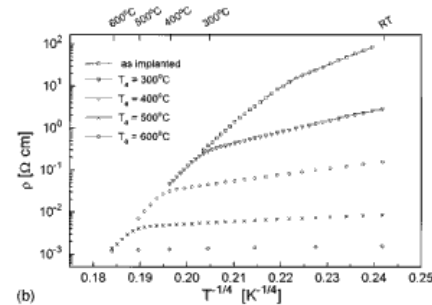
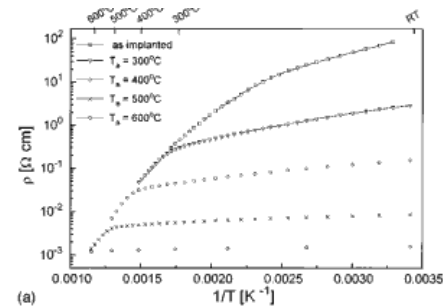
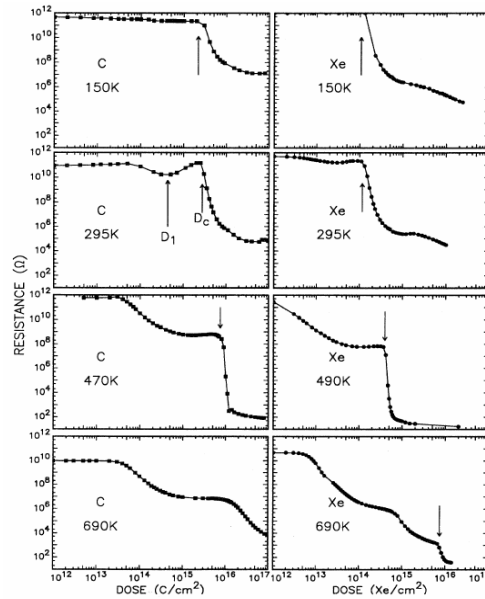
→ First works on ion-implantation-induced graphitization (70's)

V. S. Vavilov et al., *Radiat. Eff.* 22, 141 (1974)

J. J. Hauser et al., *Appl. Phys. Lett.* 30, 129 (1977)



→ Studies on conduction mechanisms in graphitized / heavily damaged diamond

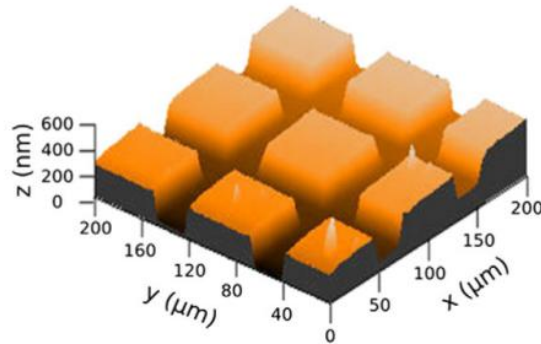


S. Praver et al., *Phys. Rev. B* 51, 15711 (1995)

IBL in diamond

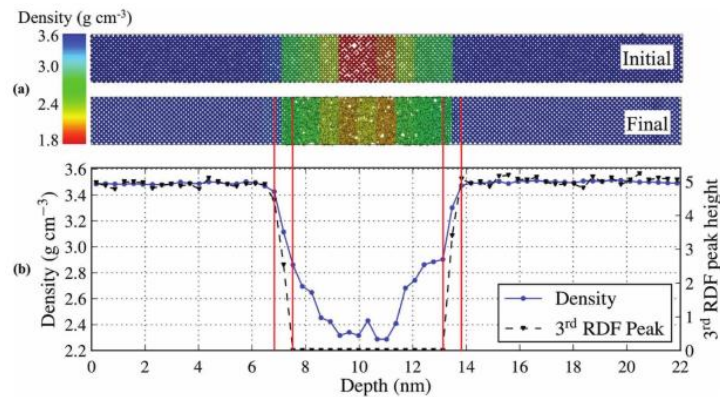
Deformation and stress

→ Surface swelling



@ : UniTo, INFN Torino

→ Internal stresses and graphitization



-
- Diamond
 - IBL in diamond
 - Basic concepts
 - State of the art
 - Current research activities @ UniTo & INFN-To
 - **Electrical** features
 - Radiation detection
 - Biosensing
 - Quantum Optics
 - Conclusions

IBL in diamond – State of the art

The diamond lift-off technique

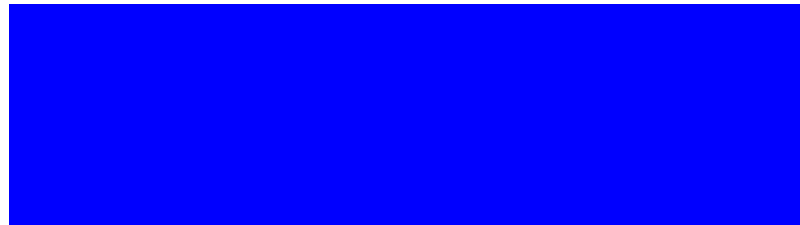
Single-crystal diamond plate liftoff achieved by ion implantation and subsequent annealing

N. R. Parikh, J. D. Hunn, E. McGucken, and M. L. Swanson
University of North Carolina, Chapel Hill, North Carolina 27599-3255

C. W. White
Oak Ridge National Laboratory, Oak Ridge, Tennessee 37831-6048

R. A. Rudder, D. P. Malta, J. B. Posthill, and R. J. Markunas
Research Triangle Institute, Research Triangle Park, North Carolina 27709-2194

Appl. Phys. Lett. **61** (26), 28 December 1992 3124



IBL in diamond – State of the art

The diamond lift-off technique

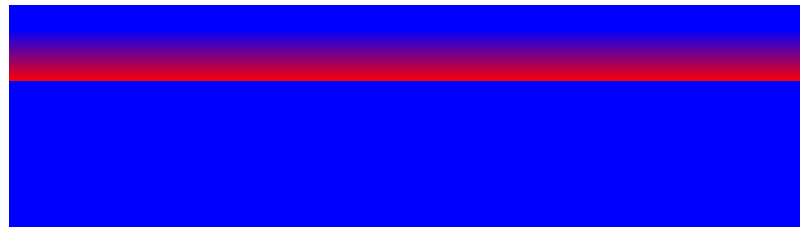
Single-crystal diamond plate liftoff achieved by ion implantation and subsequent annealing

N. R. Parikh, J. D. Hunn, E. McGucken, and M. L. Swanson
University of North Carolina, Chapel Hill, North Carolina 27599-3255

C. W. White
Oak Ridge National Laboratory, Oak Ridge, Tennessee 37831-6048

R. A. Rudder, D. P. Malta, J. B. Posthill, and R. J. Markunas
Research Triangle Institute, Research Triangle Park, North Carolina 27709-2194

Appl. Phys. Lett. **61** (26), 28 December 1992 3124



- MeV ion implantation

IBL in diamond – State of the art

The diamond lift-off technique

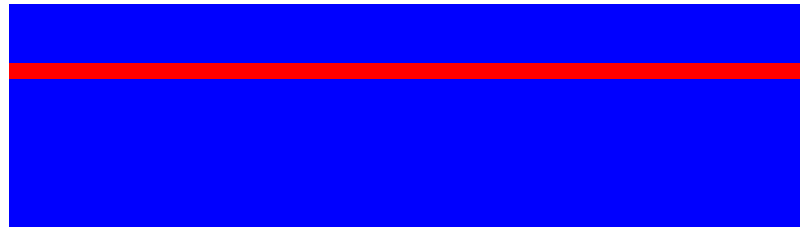
Single-crystal diamond plate liftoff achieved by ion implantation and subsequent annealing

N. R. Parikh, J. D. Hunn, E. McGucken, and M. L. Swanson
University of North Carolina, Chapel Hill, North Carolina 27599-3255

C. W. White
Oak Ridge National Laboratory, Oak Ridge, Tennessee 37831-6048

R. A. Rudder, D. P. Malta, J. B. Posthill, and R. J. Markunas
Research Triangle Institute, Research Triangle Park, North Carolina 27709-2194

Appl. Phys. Lett. **61** (26), 28 December 1992 3124



- MeV ion implantation
- Thermal annealing

IBL in diamond – State of the art

The diamond lift-off technique

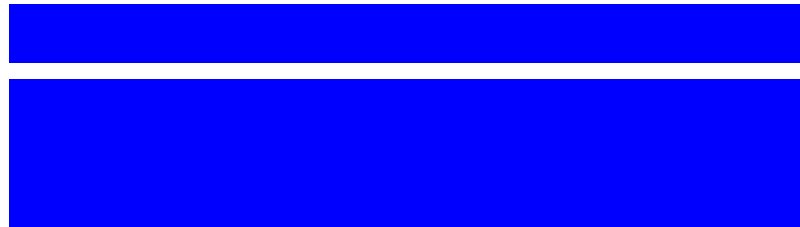
Single-crystal diamond plate liftoff achieved by ion implantation and subsequent annealing

N. R. Parikh, J. D. Hunn, E. McGucken, and M. L. Swanson
University of North Carolina, Chapel Hill, North Carolina 27599-3255

C. W. White
Oak Ridge National Laboratory, Oak Ridge, Tennessee 37831-6048

R. A. Rudder, D. P. Malta, J. B. Posthill, and R. J. Markunas
Research Triangle Institute, Research Triangle Park, North Carolina 27709-2194

Appl. Phys. Lett. **61** (26), 28 December 1992 3124



- MeV ion implantation
- Thermal annealing
- Selective graphite etching

IBL in diamond – State of the art

The diamond lift-off technique

Single-crystal diamond plate liftoff achieved by ion implantation and subsequent annealing

N. R. Parikh, J. D. Hunn, E. McGucken, and M. L. Swanson
University of North Carolina, Chapel Hill, North Carolina 27599-3255

C. W. White
Oak Ridge National Laboratory, Oak Ridge, Tennessee 37831-6048

R. A. Rudder, D. P. Malta, J. B. Posthill, and R. J. Markunas
Research Triangle Institute, Research Triangle Park, North Carolina 27709-2194

Appl. Phys. Lett. **61** (26), 28 December 1992 3124



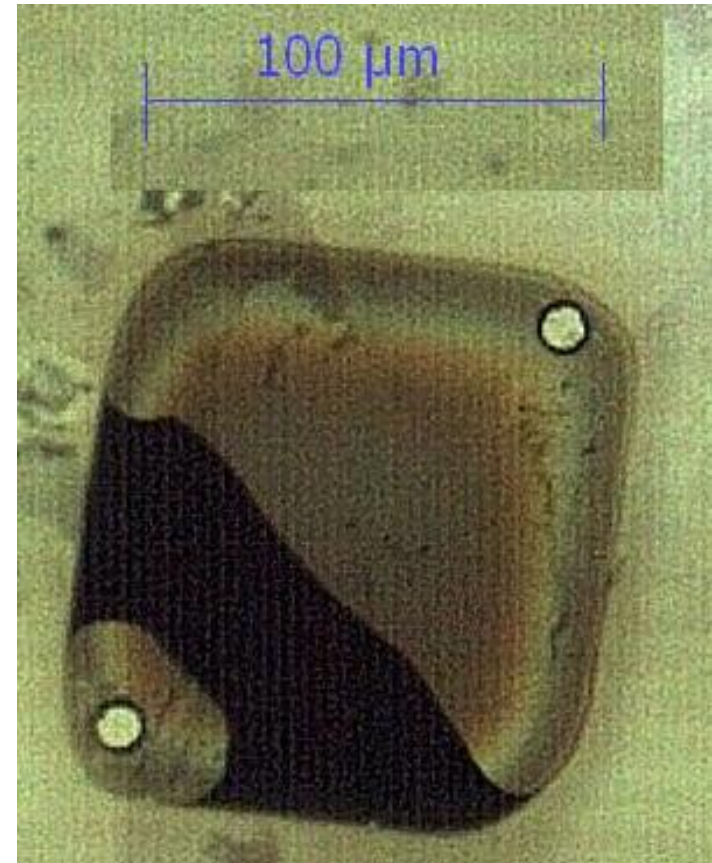
- MeV ion implantation
- Thermal annealing
- Selective graphite etching
- Lift-out

IBL in diamond – State of the art

Selective graphite etching



- Wet chemical etching
i.e.: 1:1:1 H_2SO_4 : HNO_3 : HClO_4 boiling acid
- Annealing in oxygen atmosphere
 $T = 550 - 580$ °C in air
- Annealing in ozone atmosphere
 $T = 500 - 550$ °C in air under UV illumination
- Electrochemical etching
 H_3BO_3 , non-contact Pt electrodes, $V \cong 200$ V



IBL in diamond – State of the art

Lift-off + laser micro-cutting

Fabrication of single-crystal diamond microcomponents

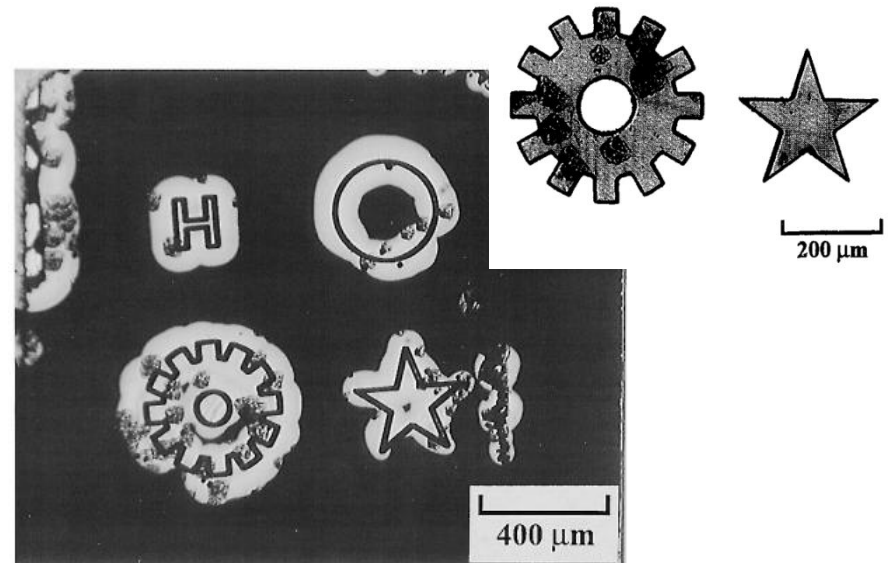
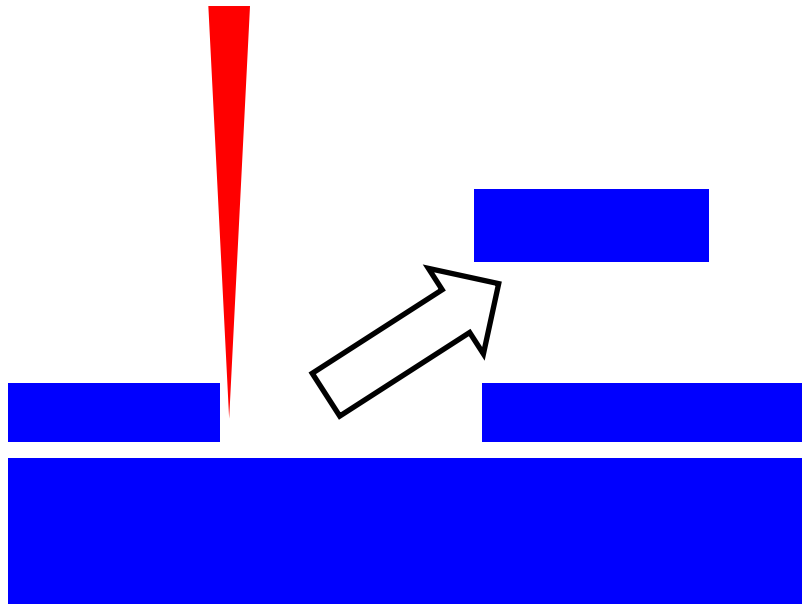
John D. Hunn, S. P. Withrow, C. W. White, R. E. Clausing, and L. Heatherly
Oak Ridge National Laboratory, Bldg 5500 MS-6376, Oak Ridge, Tennessee 37831-6376

C. Paul Christensen
Potomac Photonics, Lanham, Maryland 20705

(Received 26 August 1994; accepted for publication 7 October 1994)

We have combined a technique for the lift-off of thin diamond films from a bulk diamond with a technique for engraving diamond with a focused excimer laser to produce free-standing single-crystal diamond microstructures. One microcomponent that has been produced is a 12 tooth gear $\sim 400 \mu\text{m}$ in diameter and $\sim 13 \mu\text{m}$ thick. Other microstructures have also been demonstrated, showing the versatility of this method. This process should be applicable to producing diamond microcomponents down to spatial dimensions (width and thickness) of a few micrometers. © 1994 *American Institute of Physics.*

3072 *Appl. Phys. Lett.* **65** (24), 12 December 1994



IBL in diamond – State of the art

Lift-off + CVD growth

Diamond & Related Materials 20 (2011) 616–619



Contents lists available at ScienceDirect

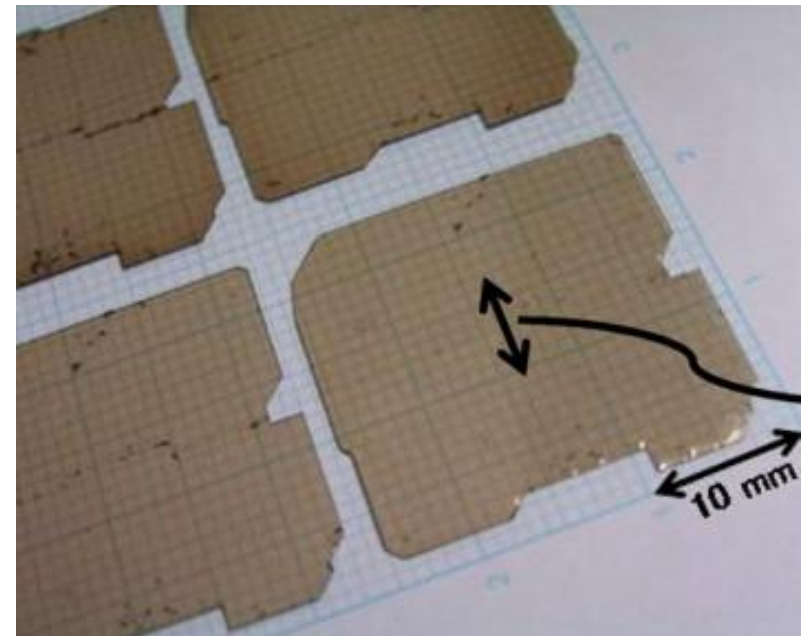
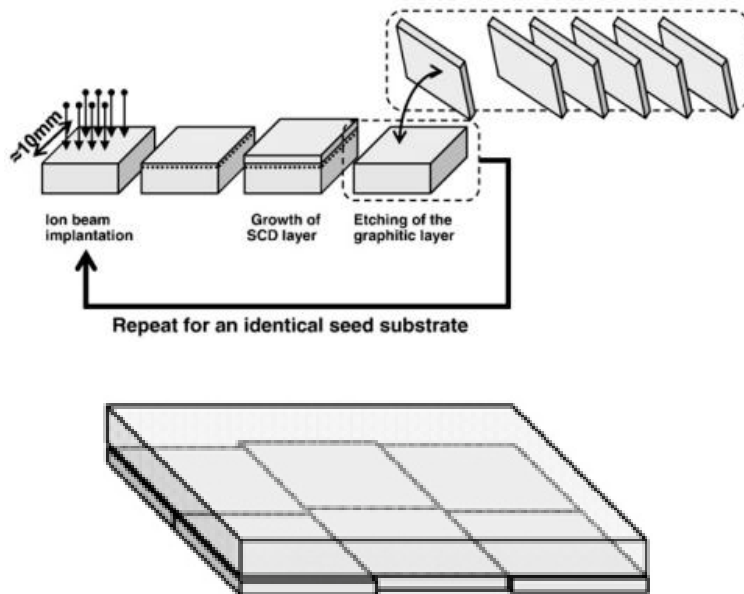
Diamond & Related Materials

journal homepage: www.elsevier.com/locate/diamond



Developments of elemental technologies to produce inch-size single-crystal diamond wafers[☆]

Hideaki Yamada^{*}, Akiyoshi Chayahara, Yoshiaki Mokuno, Nobuteru Tsubouchi, Shin-ichi Shikata, Naoji Fujimori¹



IBL in diamond – State of the art

Lift-off + CVD growth

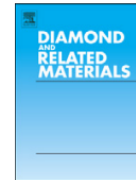
Diamond & Related Materials 24 (2012) 74–77



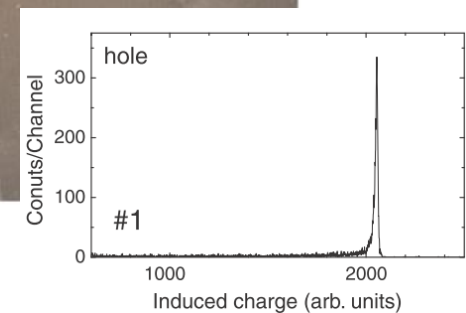
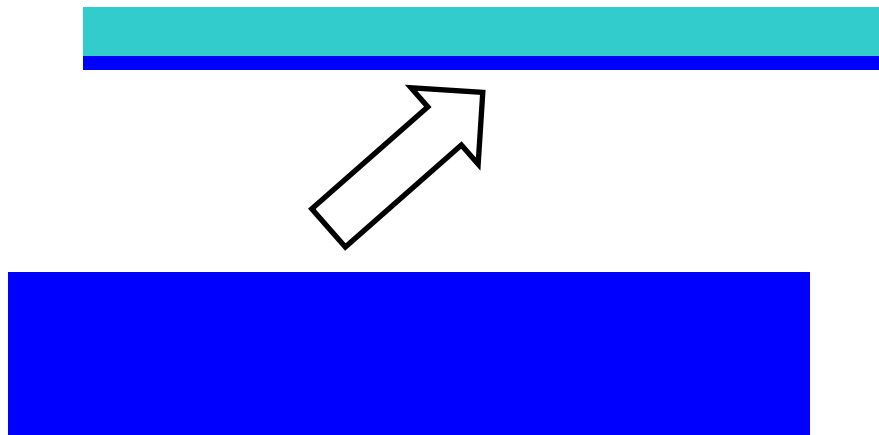
Contents lists available at [SciVerse ScienceDirect](#)

Diamond & Related Materials

journal homepage: www.elsevier.com/locate/diamond



Characterization of a sandwich-type large CVD single crystal diamond particle detector fabricated using a lift-off method[☆]



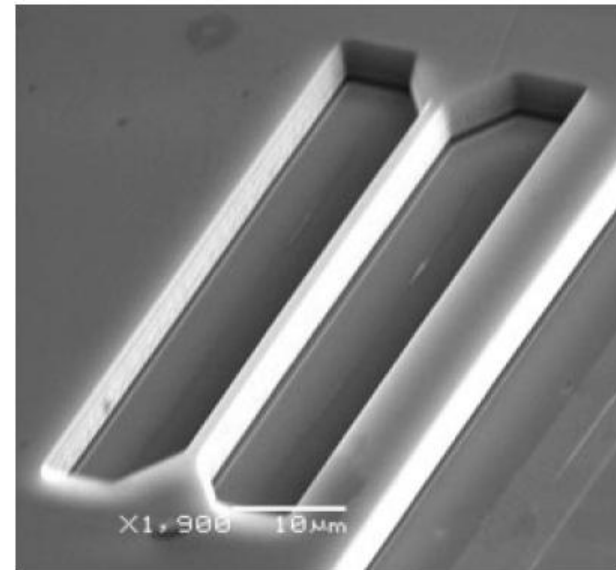
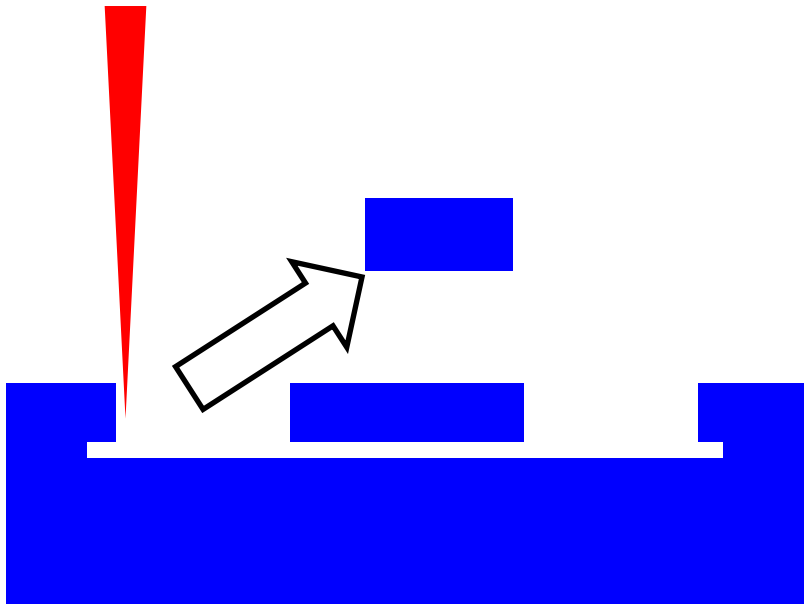
IBL in diamond – State of the art

Lift-off + Focused Ion Beam (FIB) milling

Ion-Beam-Assisted Lift-Off Technique for Three-Dimensional Micromachining of Freestanding Single-Crystal Diamond**

By Paolo Olivero, Sergey Rubanov, Patrick Reichart,
Brant C. Gibson, Shane T. Huntington, James Rabeau,
Andrew D. Greentree, Joseph Salzman, David Moore,
David N. Jamieson, and Steven Prawer*

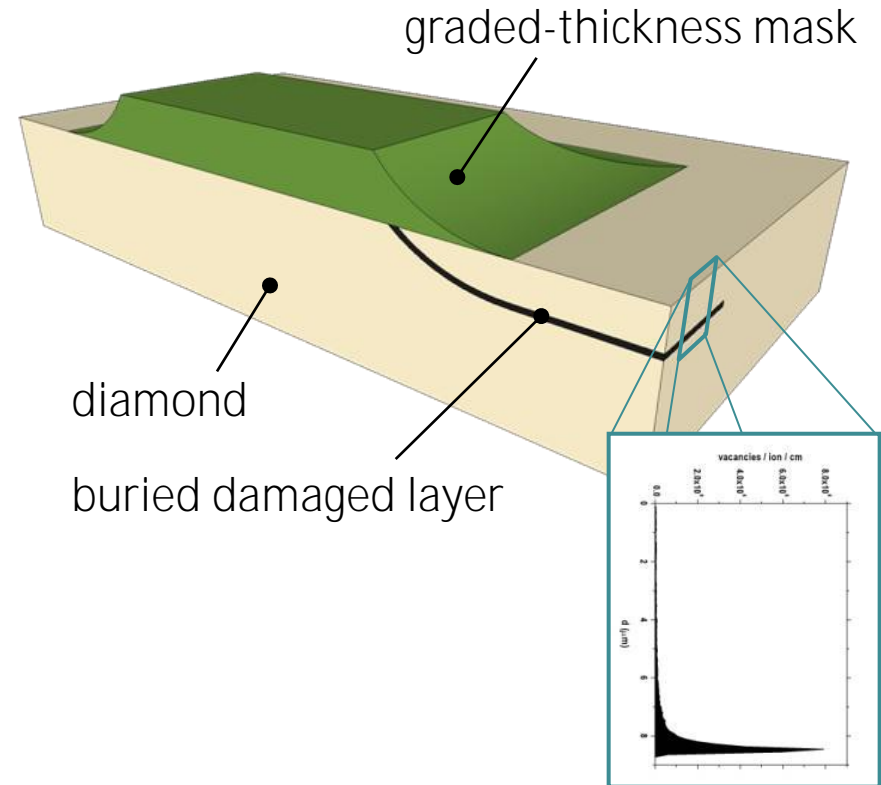
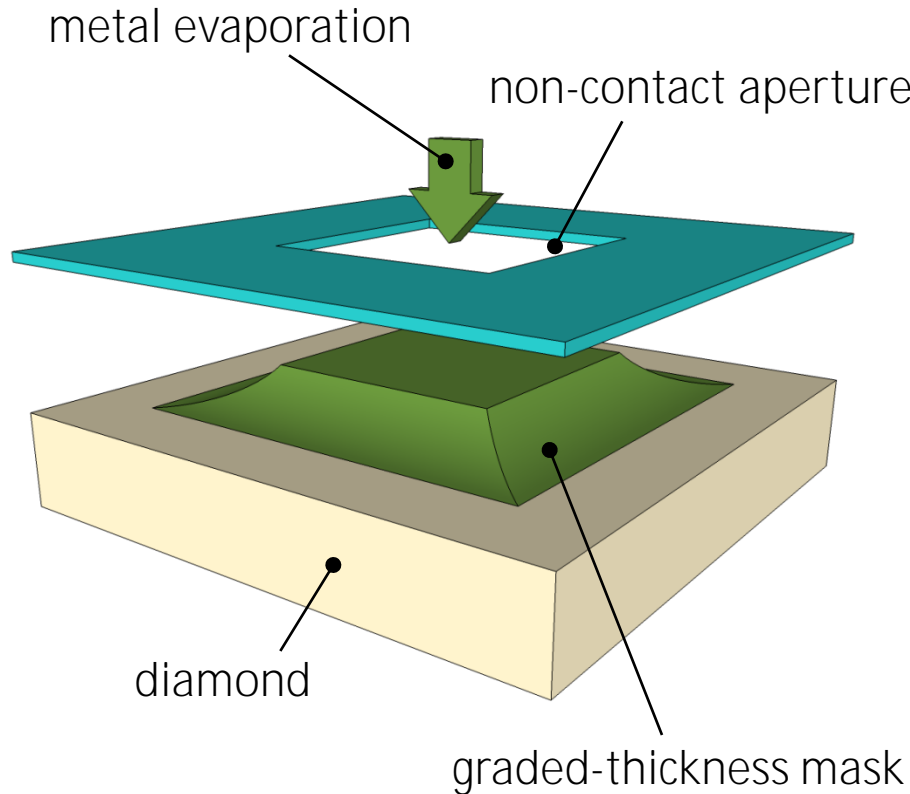
Adv. Mater. **2005**, 17, 2427–2430



-
- Diamond
 - IBL in diamond
 - Basic concepts
 - State of the art
 - Current research activities @ UniTo & INFN-To
 - **Electrical** features
 - Radiation detection
 - Biosensing
 - Quantum Optics
 - Conclusions

Electrical features

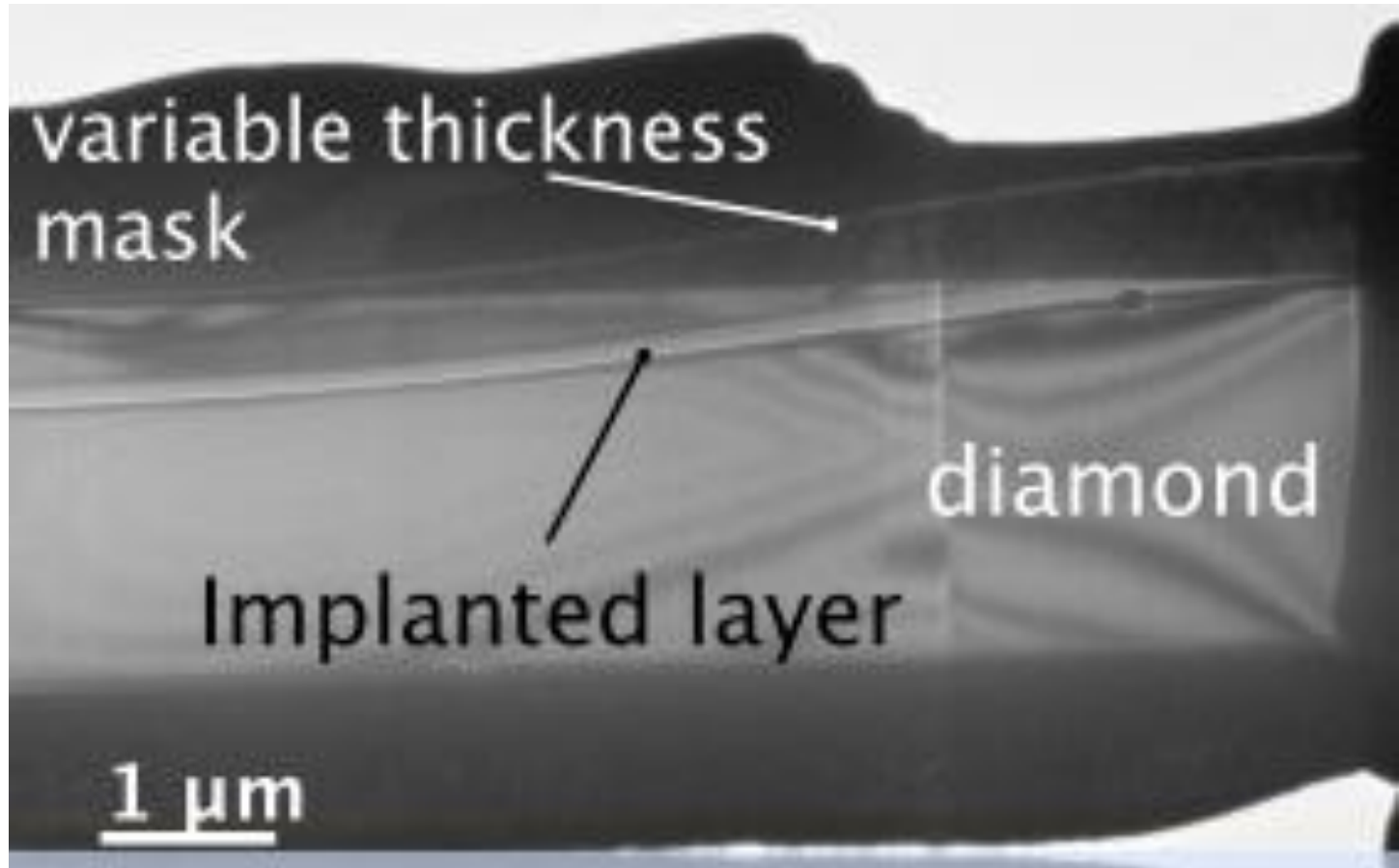
Implantation with a scanning MeV ion micro-beam through graded-thickness mask



→ **direct writing of** sub-superficial conductive microchannels in single-crystal diamond

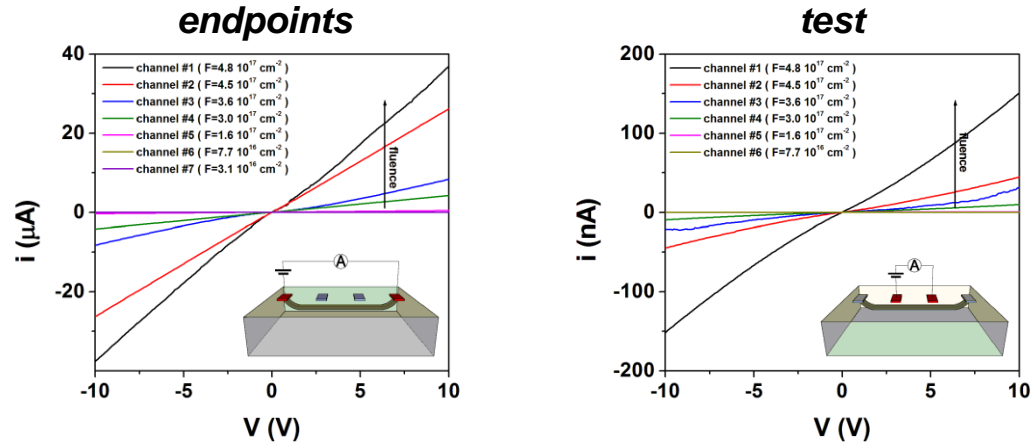
Electrical features

TEM microscopy

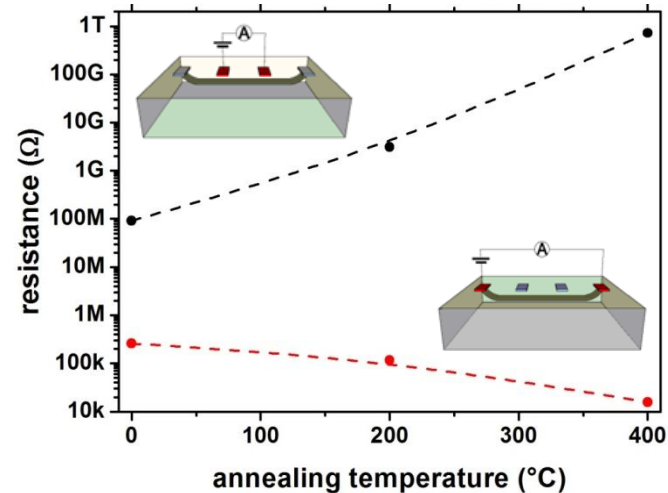
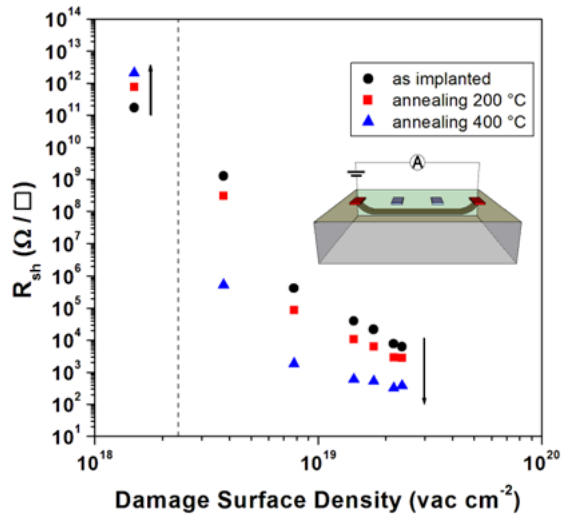


Electrical features

IV curves @ increasing fluences

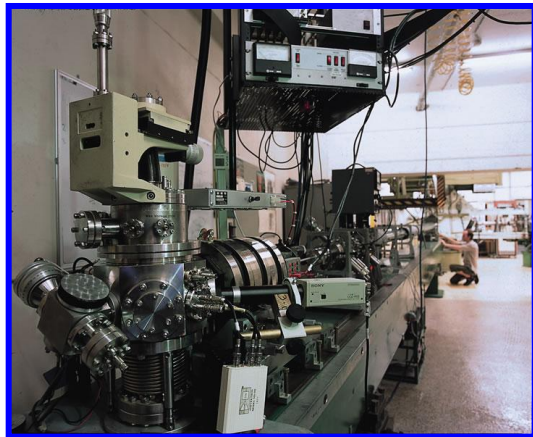


Annealing behavior



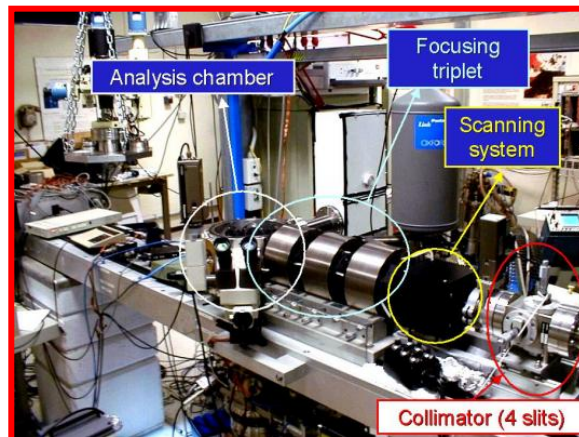
Electrical features

Ion implantation performed at the
MP2-UniMelb, LNL-AN200 and **Ruđer Bošković Institute** ion microbeam lines



Structural
TEM characterization

0.5 MeV He⁺
F=1×10¹⁷ cm⁻²



Cellular bio-sensing
3D particle detectors

1.8 MeV He⁺
F=1-10 ×10¹⁶ cm⁻²

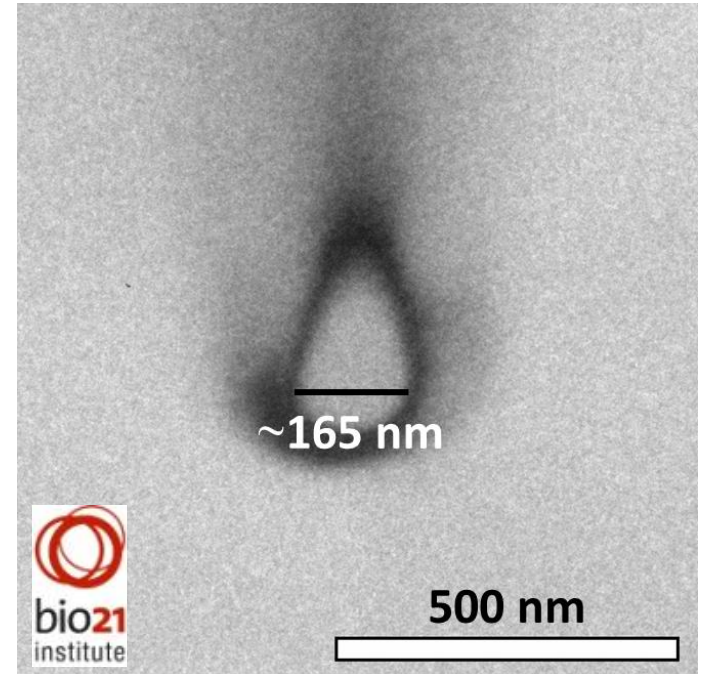
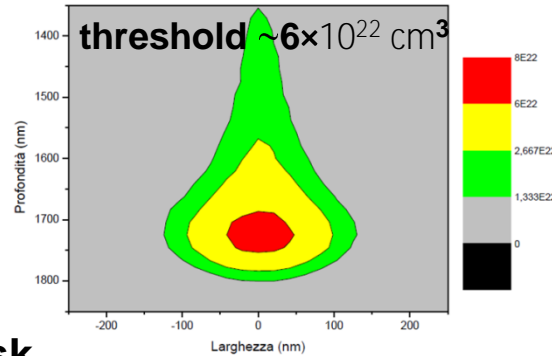
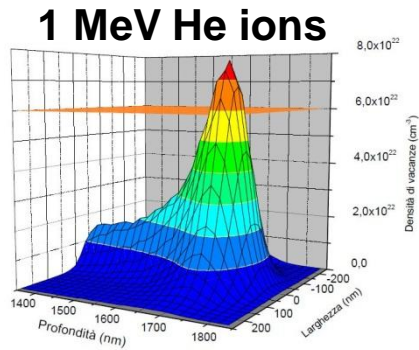


3D particle detectors

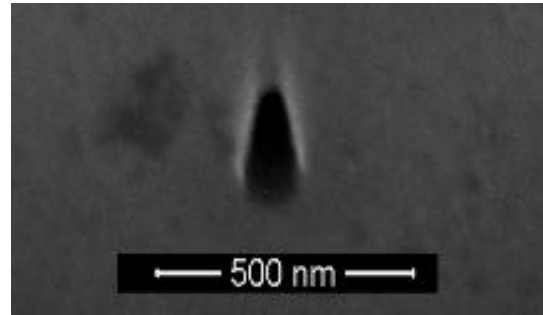
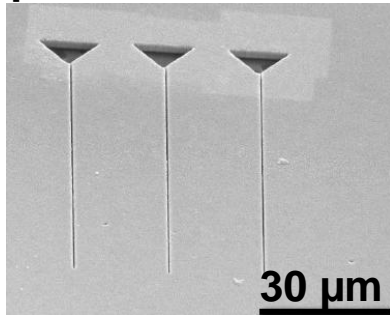
6 MeV C³⁺
F=4×10¹⁶ cm⁻²

Electrical features

High-resolution FIB-machined metal contact masks



2 μm thick metal mask



unpublished

-
- Diamond
 - IBL in diamond
 - Basic concepts
 - State of the art
 - Current research activities @ UniTo & INFN-To
 - **Electrical** features
 - Radiation detection
 - Biosensing
 - Quantum Optics
 - Conclusions

Radiation detection

“DIARAD” & “DIAMED” INFN projects



Coordinated Research Project F11016



Ettore Vittone

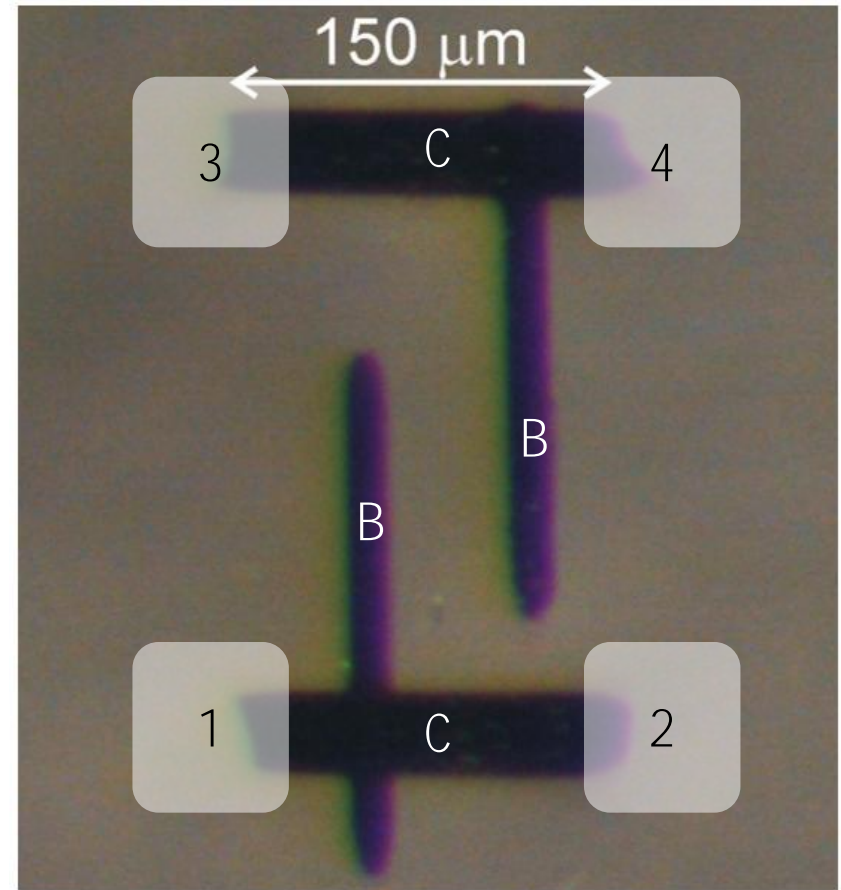
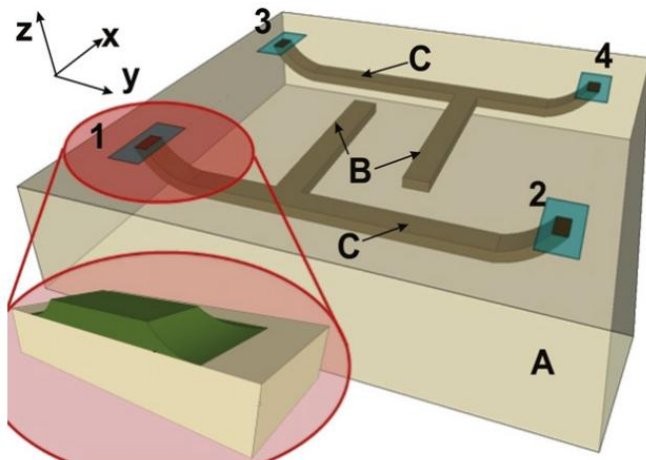
Radiation detection

Sample #1

- free-standing homoepitaxial single-crystal
“**electronic grade**” CVD diamond grown by ElementSix™
- [N], [B] < 5 ppb

Ion-beam microfabrication

- ion μ -beam line @ **Ruđer Bošković** Institute
- ions: 6 MeV C³⁺ (range $\sim 3 \mu\text{m}$)
- ion fluence: $4 \times 10^{16} \text{ cm}^{-2}$
- annealing: 2 hrs @ 950 °C in Ar

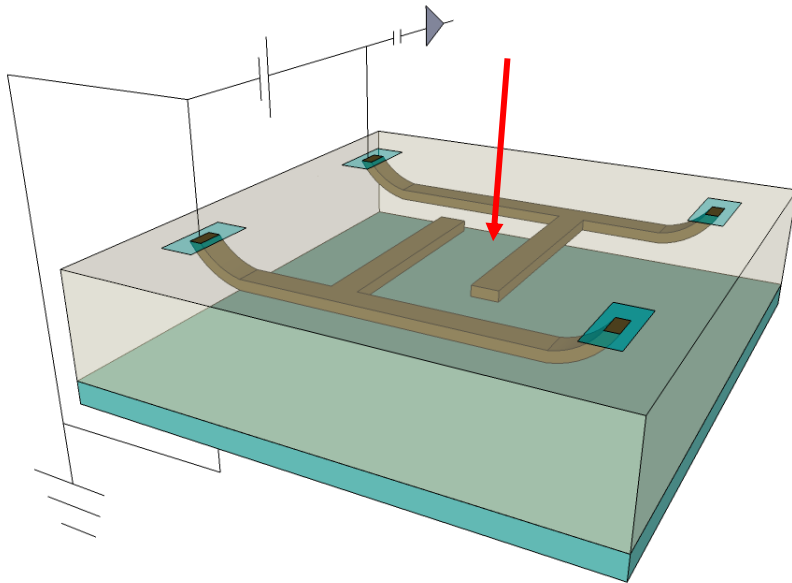


- $R_{1-3}, R_{2-4} \sim 10 \text{ T}\Omega$
 - $R_{1-2}, R_{3-4} \sim 1 \text{ k}\Omega$
 - ohmic contacts
- $\rightarrow \rho_C \sim 10 \text{ m}\Omega \text{ cm}$

Radiation detection

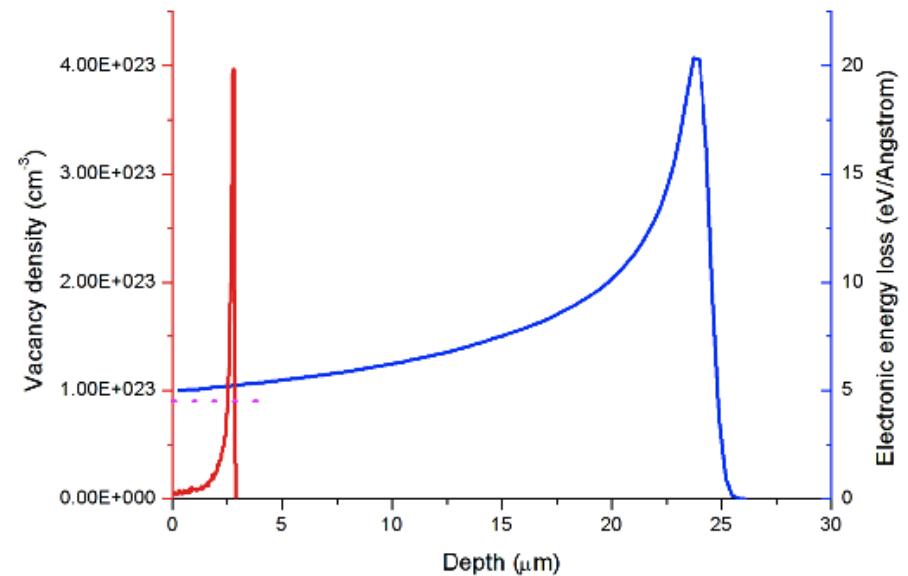
Sample #1

- free-standing homoepitaxial single-crystal
“**electronic grade**” CVD diamond grown by ElementSix™
- **[N], [B] < 5 ppb**



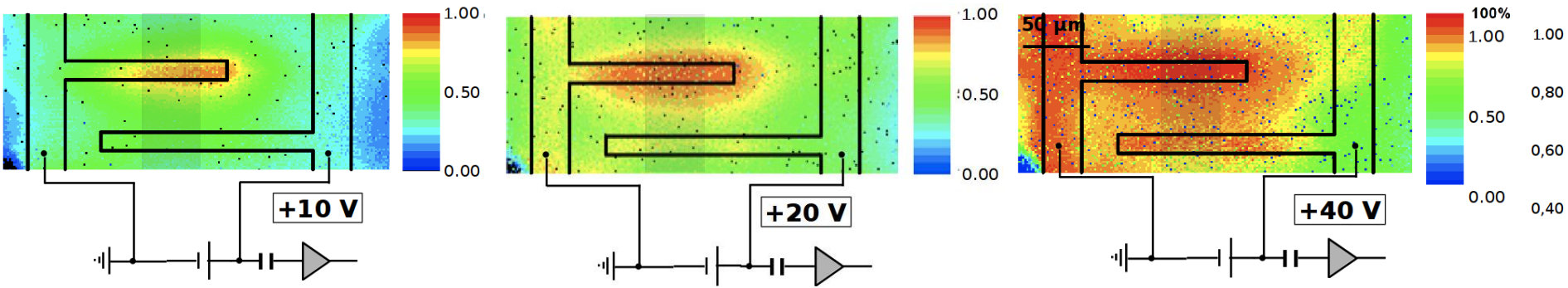
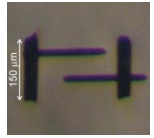
IBIC measurements

- ion μ -beam line @ **Ruđer Bošković** Institute
- ions: 2 MeV H⁺ (range $\sim 25 \mu\text{m}$)
- $\varnothing \sim 2 \mu\text{m}$
- frontal geometry

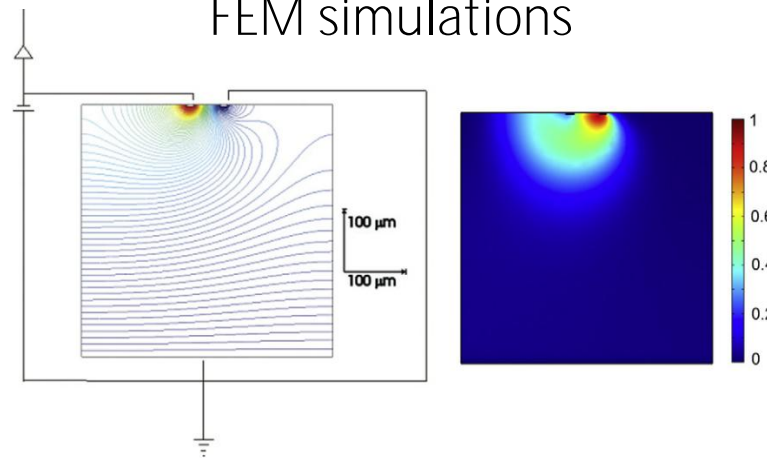


Radiation detection

IBIC maps @ different V_{bias}



FEM simulations



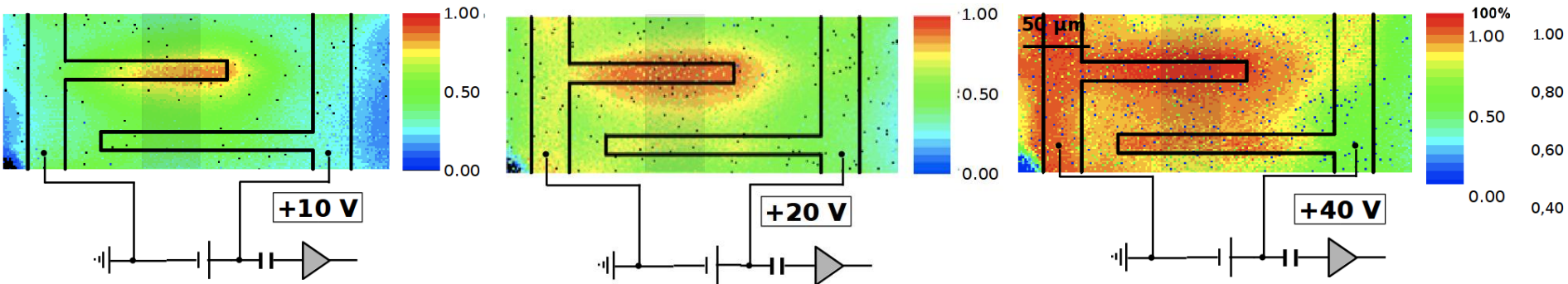
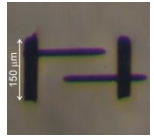
Gunn's weighting
potential

CCE

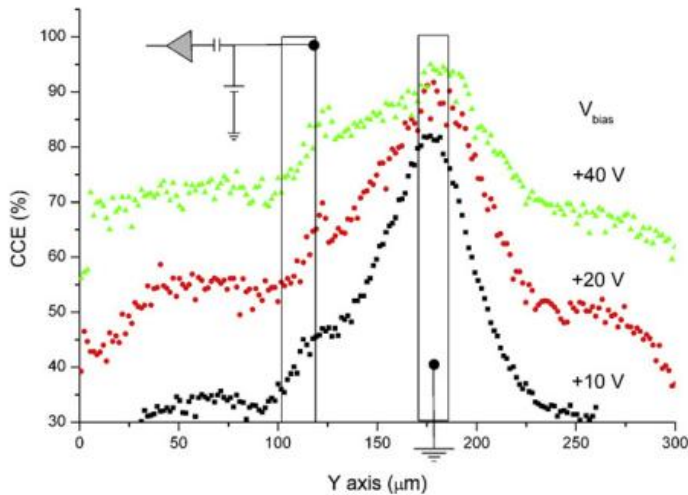


Radiation detection

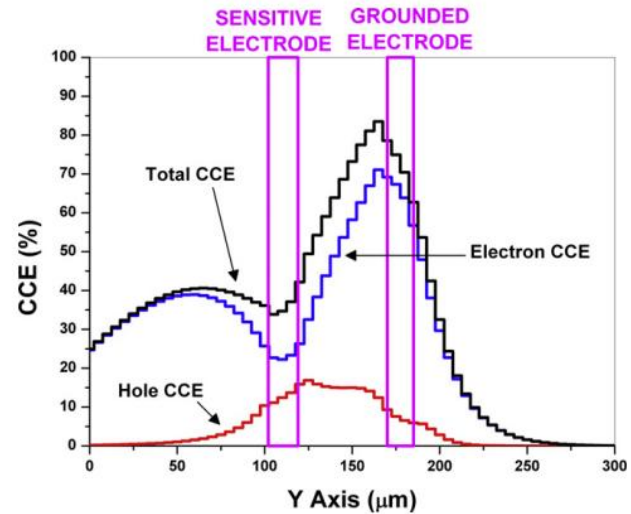
IBIC maps @ different V_{bias}



IBIC profiles @ different V_{bias}



Numerical predictions



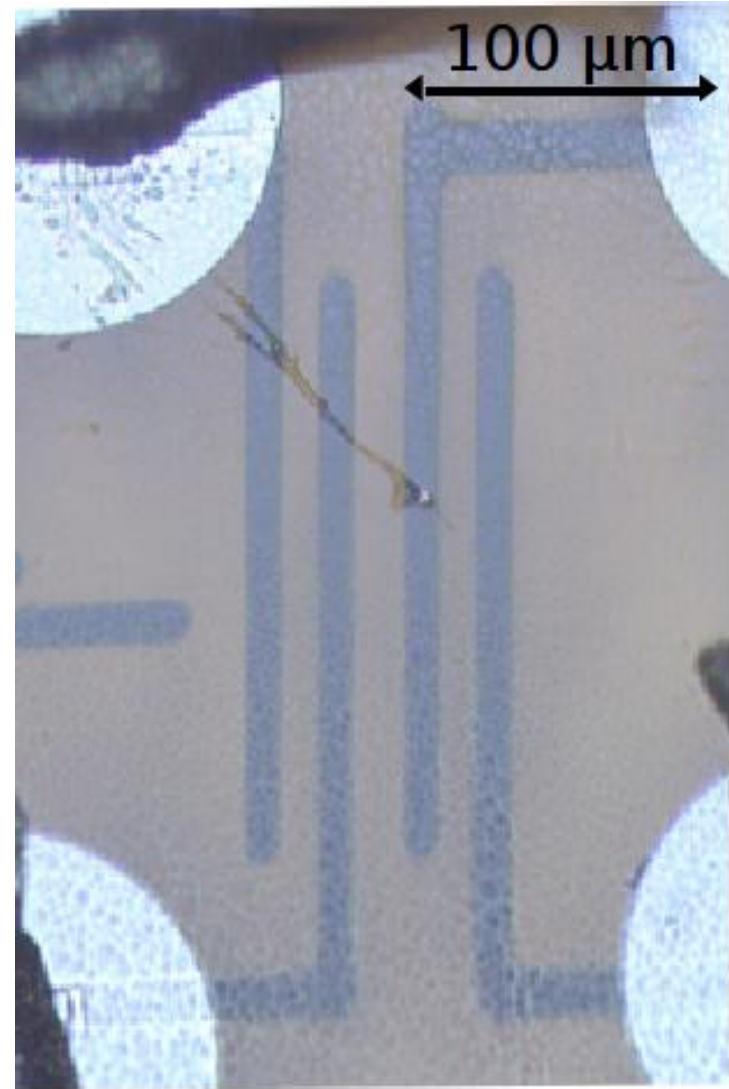
Radiation detection

Sample #2

- homoepitaxial single-crystal CVD diamond grown @ UniRoma “Tor Vergata”
- **50 μm** thick intrinsic layer on HPHT substrate
- $[\text{N}], [\text{B}] < 5 \times 10^{14} \text{ cm}^{-2}$

Ion-beam microfabrication

- ion μ -beam line @ Legnaro National Laboratories
- ions: 2 MeV He^+ (range $\sim 3 \mu\text{m}$)
- ion fluence: $1.5 \times 10^{17} \text{ cm}^{-2}$
- annealing: 2 hrs @ 1100 °C in vacuum



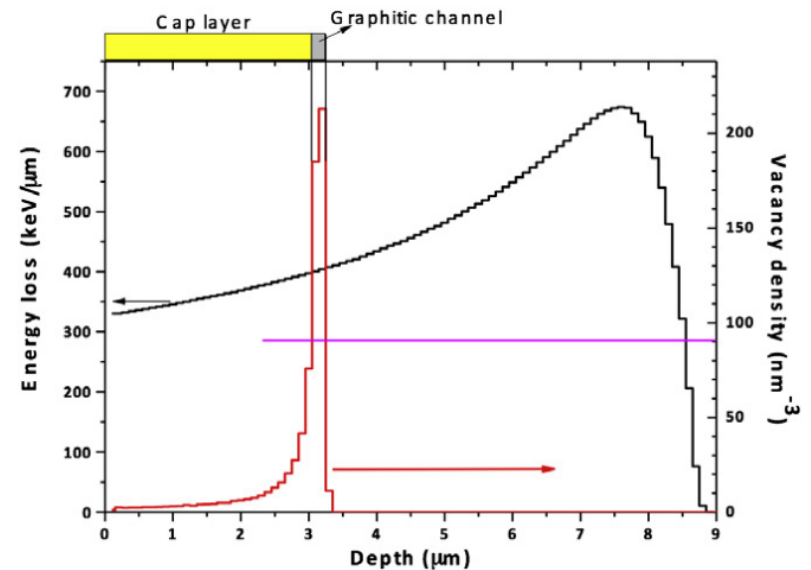
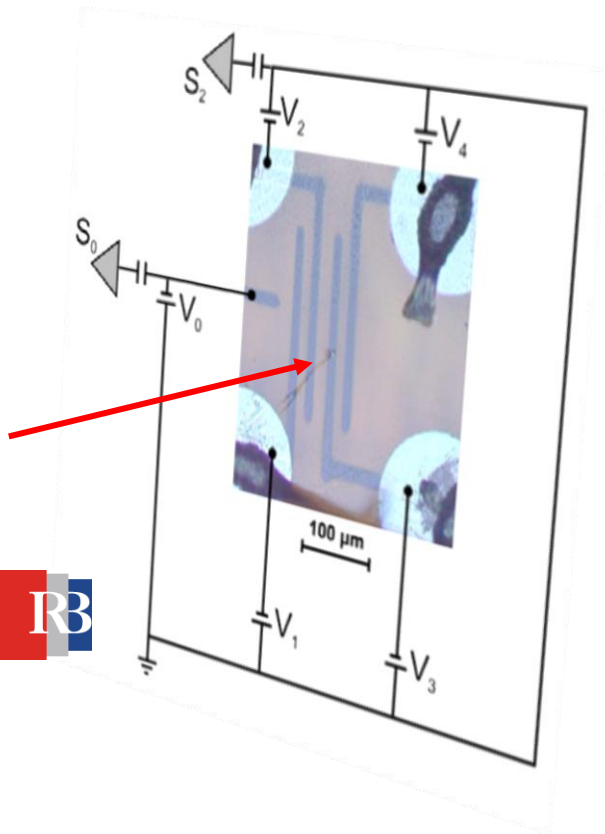
Radiation detection

Sample #2

- homoepitaxial single-crystal CVD diamond grown @ UniRoma “Tor Vergata”
- **50 μm** thick intrinsic layer on HPHT substrate
- $[\text{N}], [\text{B}] < 5 \times 10^{14} \text{ cm}^{-2}$

IBIC measurements

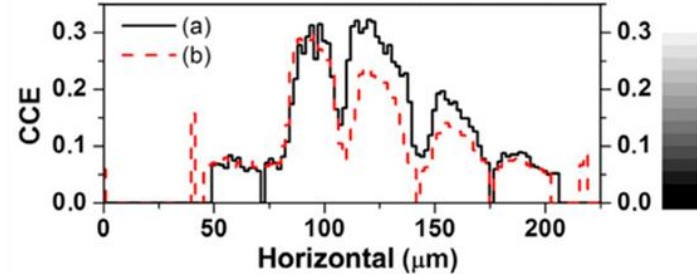
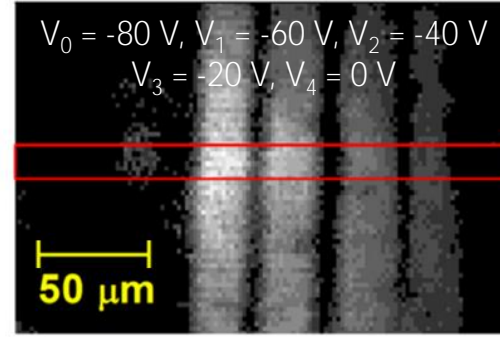
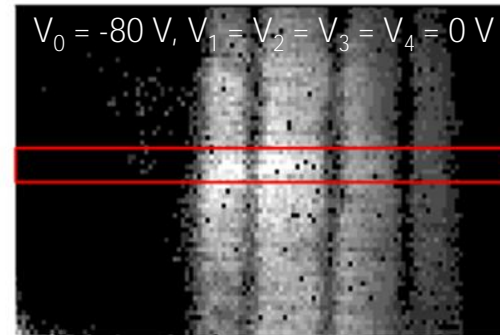
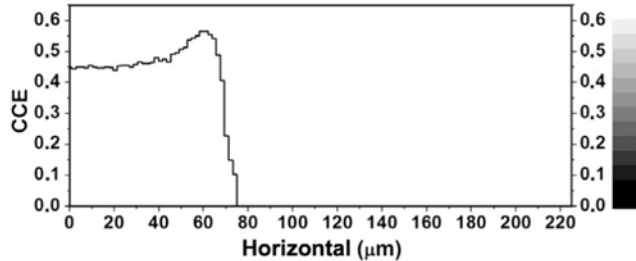
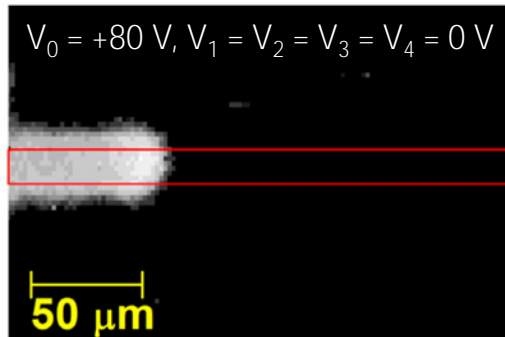
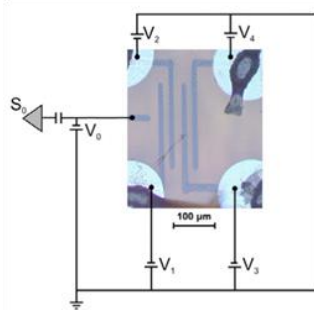
- ion μ -beam line @ **Ruđer Bošković** Institute
- ions: 4 MeV He^+ (range $\sim 8 \mu\text{m}$)
- $\varnothing \sim 4 \mu\text{m}$
- frontal geometry



Radiation detection

IBIC maps & profiles @ different V_{bias} configurations

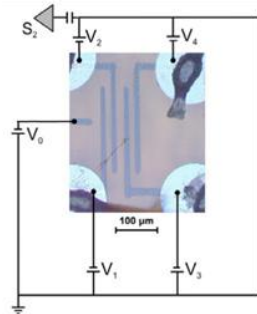
Sensitive electrode: S_0



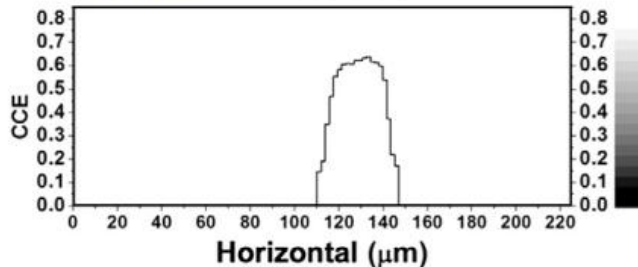
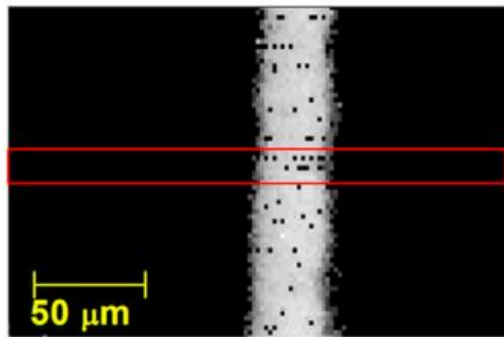
Radiation detection

IBIC maps & profiles @ different V_{bias} configurations

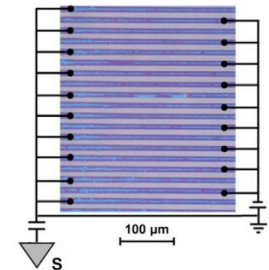
Sensitive electrode: S_2



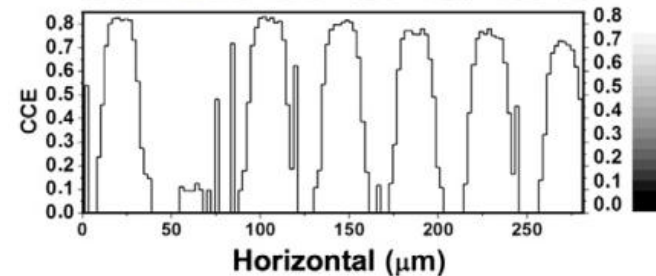
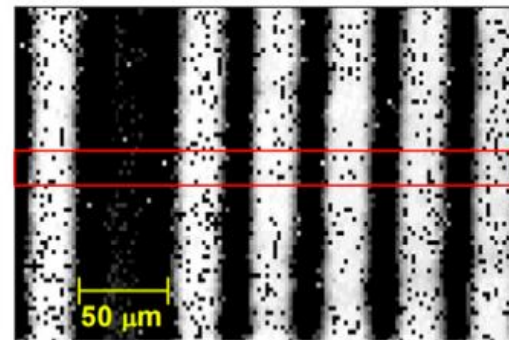
$$V_0 = V_2 = V_4 = 0 \text{ V}, V_1 = V_3 = -100 \text{ V}$$



Reference detector with planar Ti/Pt/Au electrodes

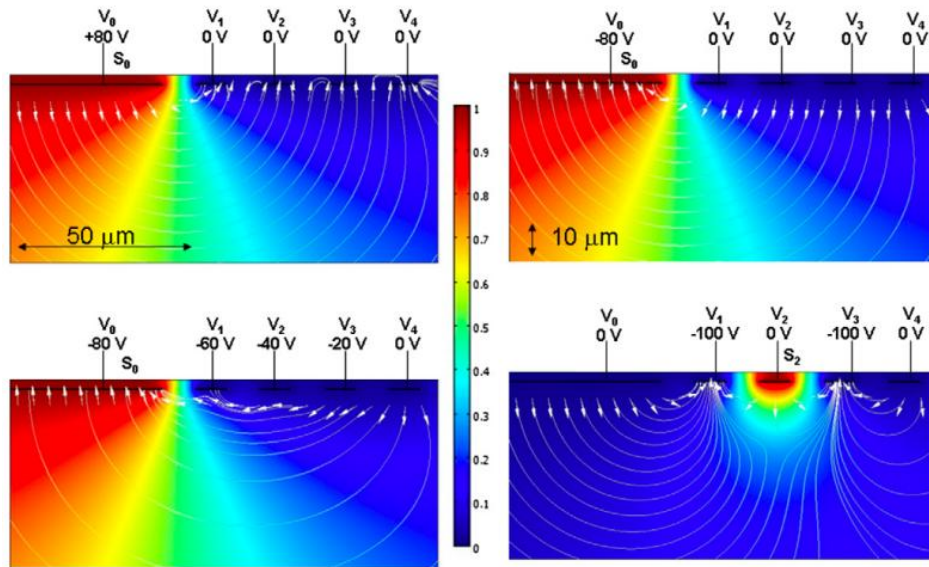


$$V_S = 0 \text{ V}, V = -100 \text{ V}$$



Radiation detection

FEM numerical simulations



Weighting potential and electric field lines

Remarks:

- good ohmic contacts
- good consistency with FEM simulations
- predominant hole contribution
- **residual damage in the “cap layer”**

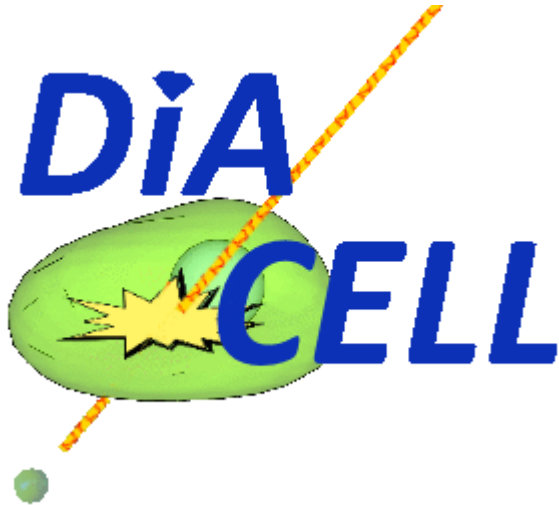


-
- Diamond
 - IBL in diamond
 - Basic concepts
 - State of the art
 - Current research activities @ UniTo & INFN-To
 - **Electrical** features
 - Radiation detection
 - Biosensing
 - Quantum Optics
 - Conclusions

Biosensing

INFN projects “DINAMO” & “DIACELL”

F. Picollo



Federico Picollo

Biosensing

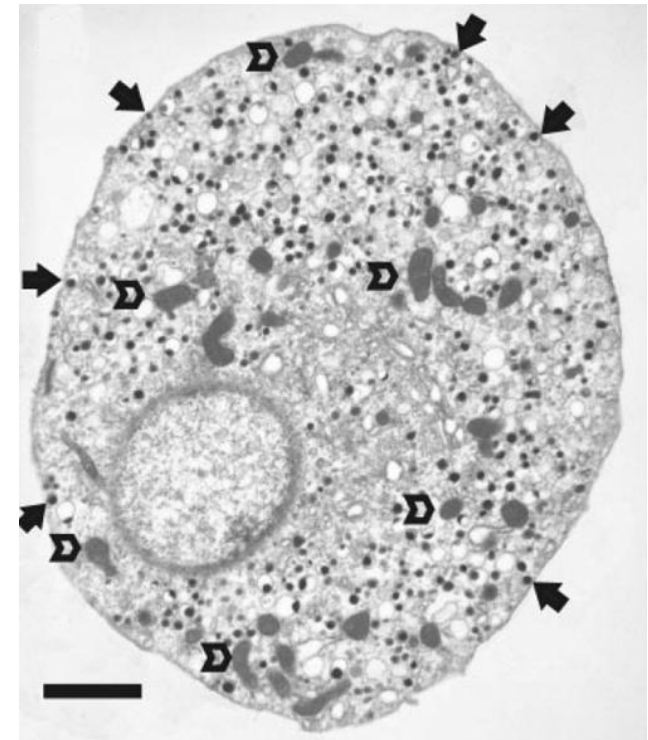
A viable model of neuronal excitation-secretion

- ✓ Easily available, large dimensions ($>10\ \mu\text{m}$)
- ✓ Voltage-gated Ca^{2+} channels
- ✓ Electrically excitable
- ✓ Containing chromaffin granules



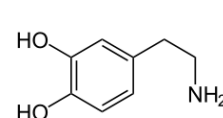
Diameter = 50-300 nm

Catecholamines concentration = 0.5-1 M
($\sim 10^6$ molecules each granule)

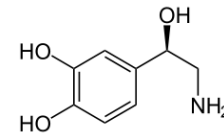


C. Grabner et al., J. Neurophysiol 94, 2093 (2005)

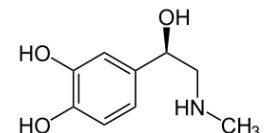
Catecholamines



dopamine



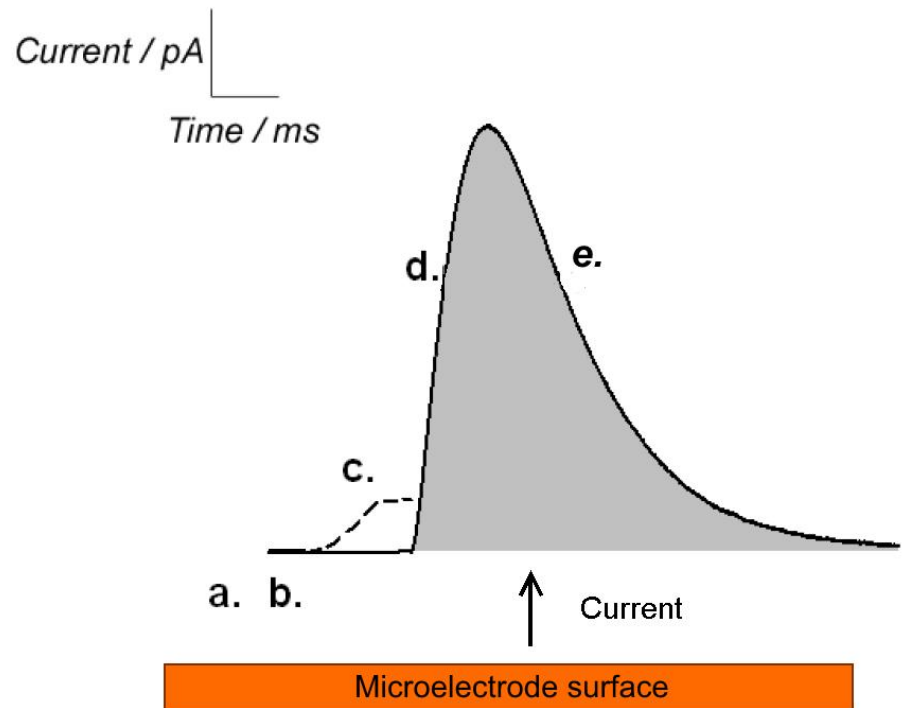
noradrenaline



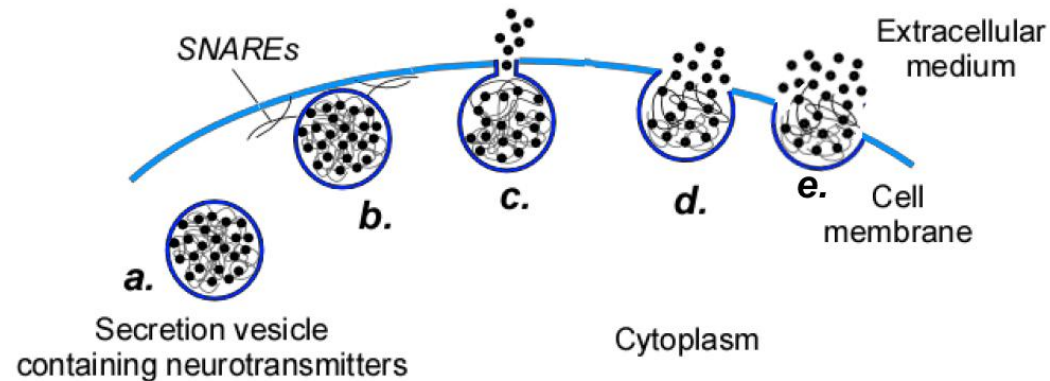
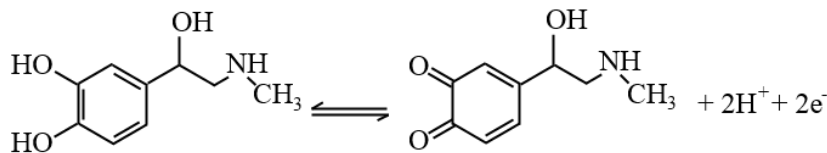
adrenaline

Biosensing

- ✓ Secretion of catecholamines from vesicles in which they are highly concentrated → strong signal
- ✓ Time duration: 50-100 ms
- ✓ Amperometric detection of the oxidized species in correspondence of a biased μ -electrode
- ✓ Electrical or chemical stimulation



Adrenaline oxidation

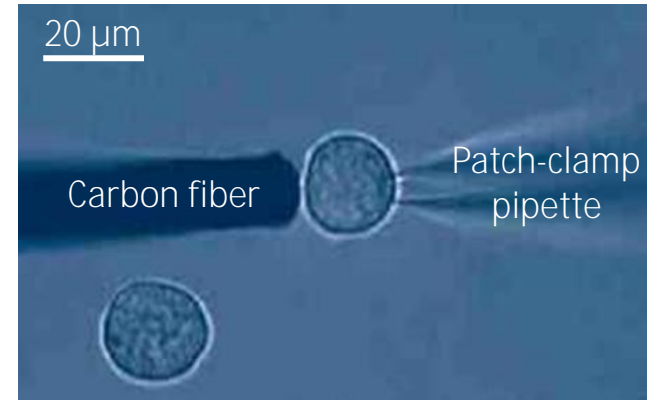


Biosensing

Carbon fibers

Biased carbon fiber microelectrode brought in close physical proximity of a single cell held by a patch-clamp pipette:

- ✓ not easily scalable
- ✓ **manipulation (→ stress) of the cell,**
and of the CF

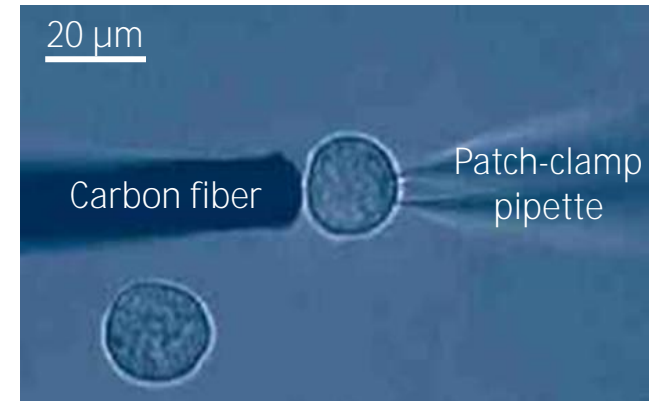


Biosensing

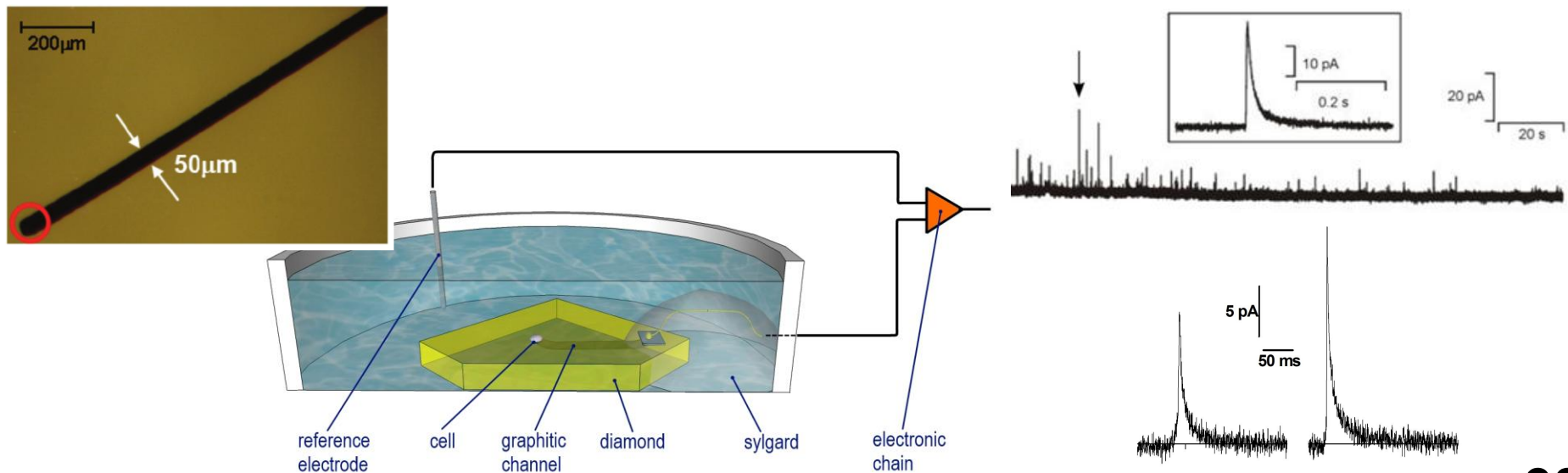
Carbon fibers

Biased carbon fiber microelectrode brought in close physical proximity of a single cell held by a patch-clamp pipette:

- ✓ not easily scalable
- ✓ **manipulation (→ stress) of the cell,**
and of the CF



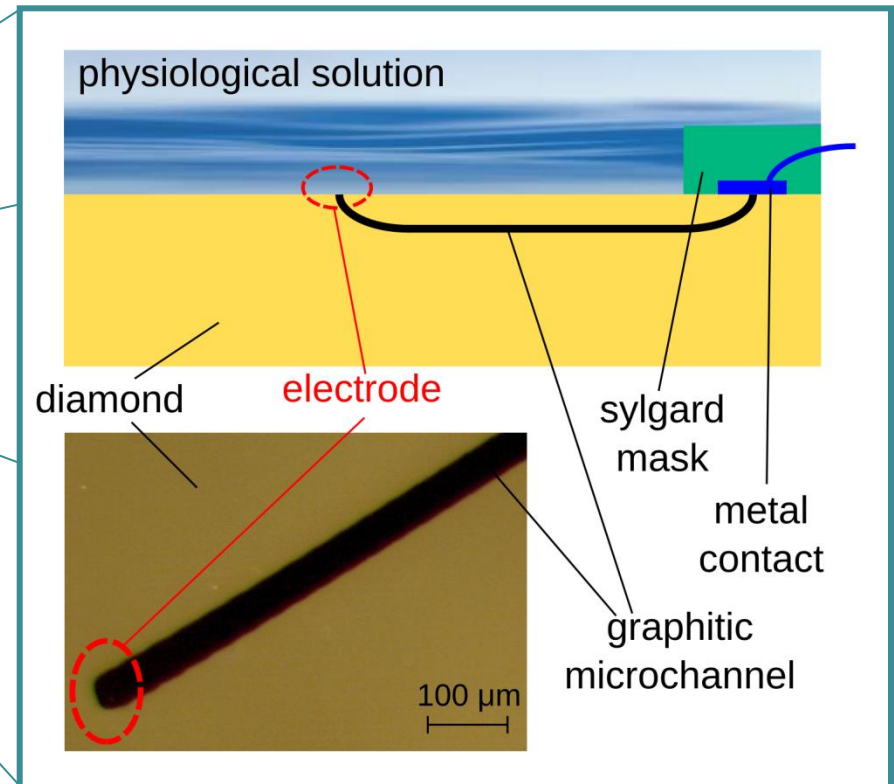
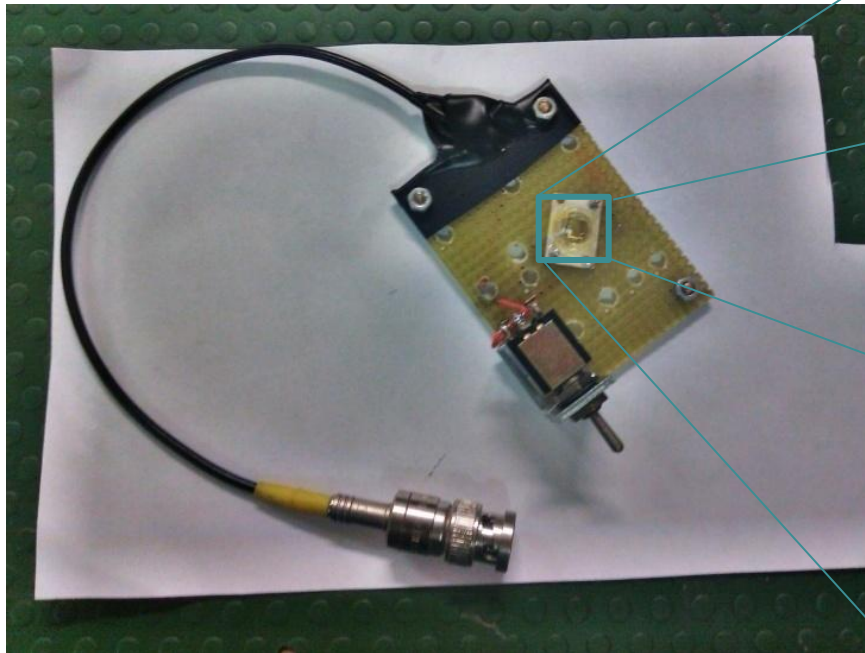
Single-electrode integrated device in diamond



Biosensing

Device fabrication

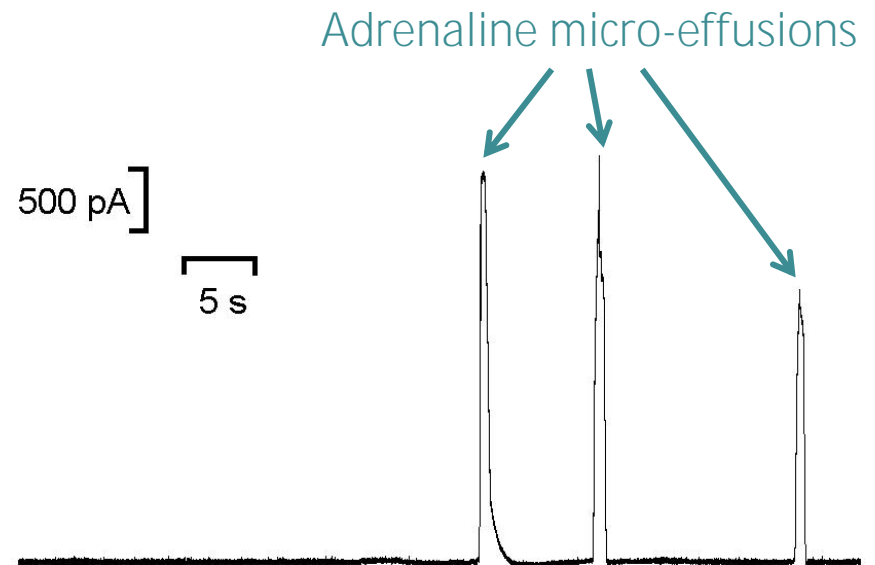
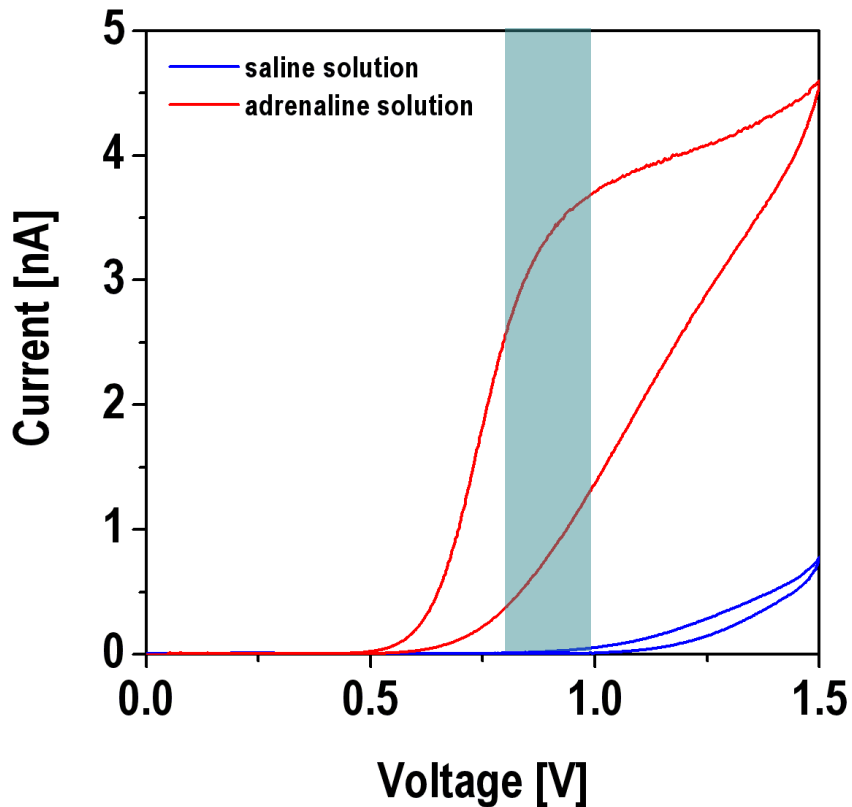
- $3 \times 3 \times 1.5 \text{ mm}^2$ type Ib single crystal HPHT diamond
- 1.8 MeV He^+ implantation at $5 \times 10^{17} \text{ cm}^{-2}$ fluence @ INFN Legnaro National Labs
- $1100 \text{ }^\circ\text{C}$ annealing for 2 hrs in vacuum
- mounting and contacting



Biosensing

Cyclic voltammetry: oxidation of **adrenaline** at the biased electrode

Preliminary sensitivity test: micro-effusion of adrenaline with a syringe



Saline solution (in mM): 128 NaCl, 2 MgCl₂, 10 glucose, 10 HEPES, 10 CaCl₂, 4 KCl

Adrenaline solution: saline solution + adrenaline (10 mM)

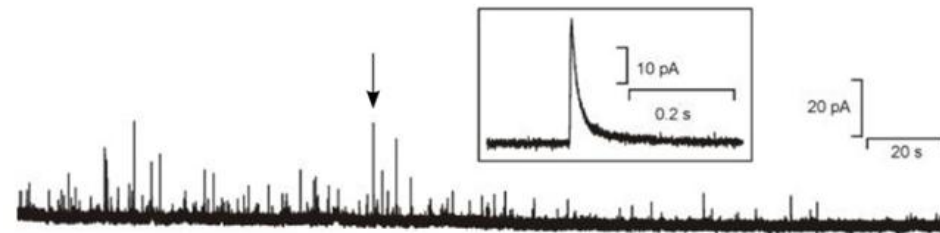
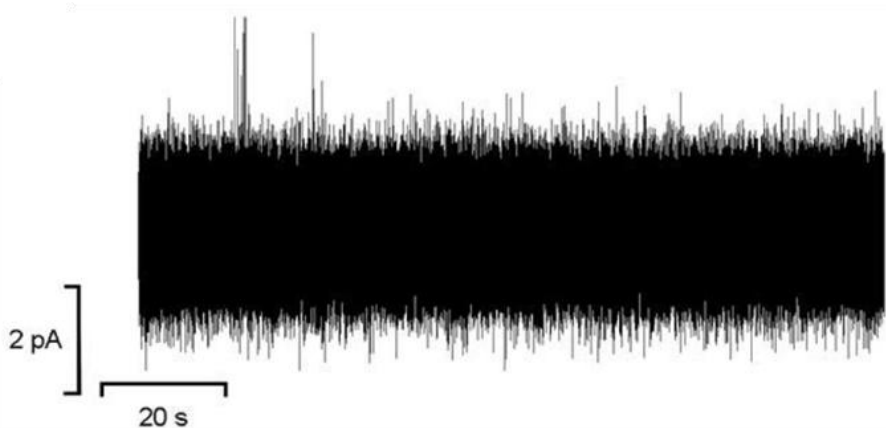
Biosensing

Exocytosis detection from a single chromaffin cell

Cell manipulation and positioning: glass patch-clamp pipette

Non-stimulated cell

Stimulated cell



Solution (in mM): 128 NaCl, 2 MgCl₂,
10 glucose, 10 HEPES, 10 CaCl₂, 4 KCl

Solution (in mM): 100 NaCl, 2 MgCl₂,
10 glucose, 10 HEPES, 10 CaCl₂, 30 KCl

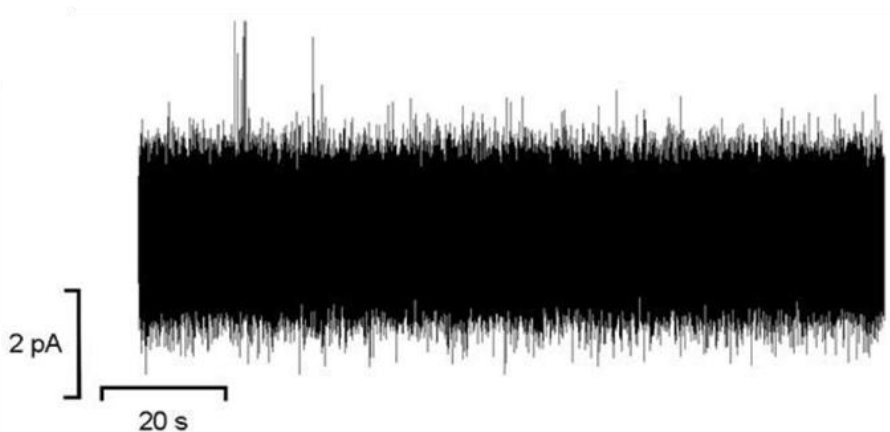
F. Picollo et al., *Advanced Materials* 25 (34), 4696-4700 (2013)

Biosensing

Exocytosis detection from a single chromaffin cell

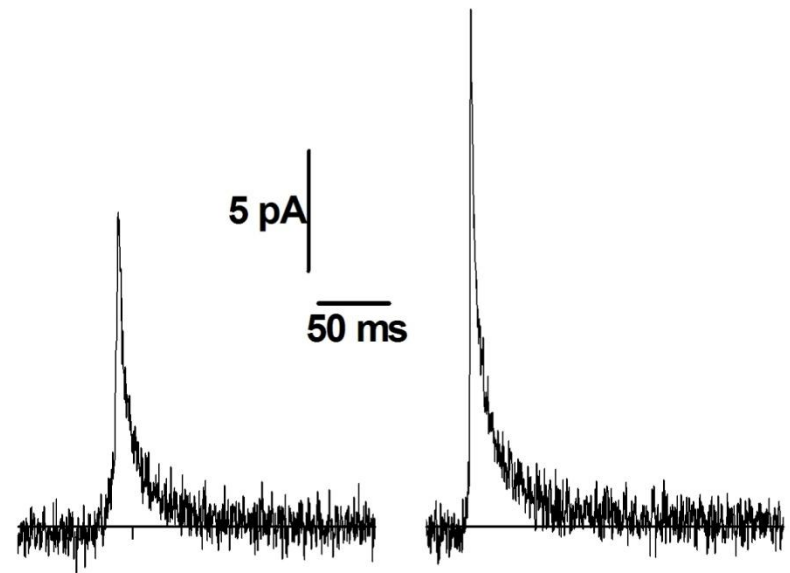
Cell manipulation and positioning: glass patch-clamp pipette

Non-stimulated cell



Solution (in mM): 128 NaCl, 2 MgCl₂,
10 glucose, 10 HEPES, 10 CaCl₂, 4 KCl

Stimulated cell



Solution (in mM): 100 NaCl, 2 MgCl₂,
10 glucose, 10 HEPES, 10 CaCl₂, 30 KCl

Biosensing

Samples:

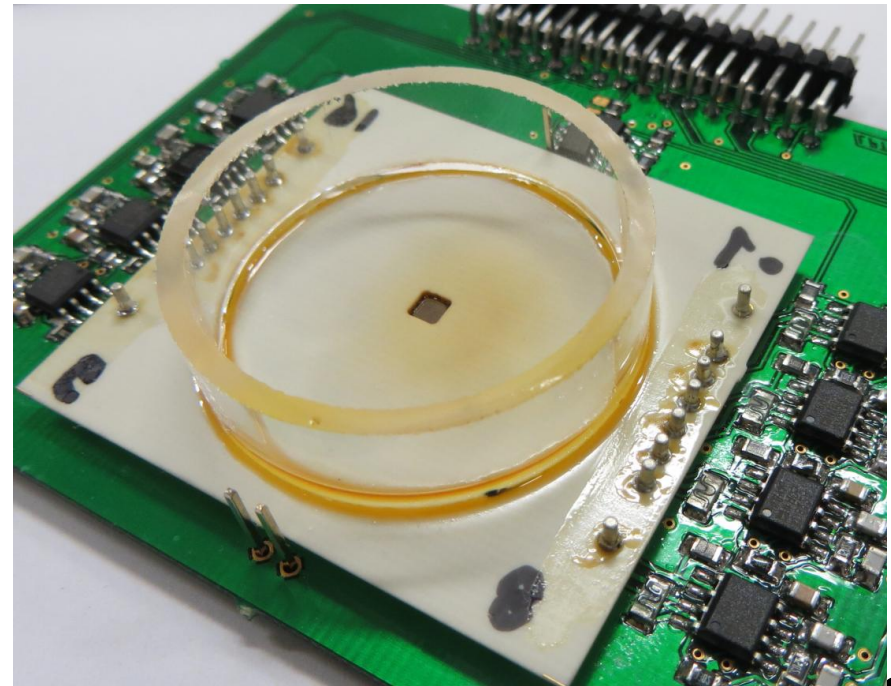
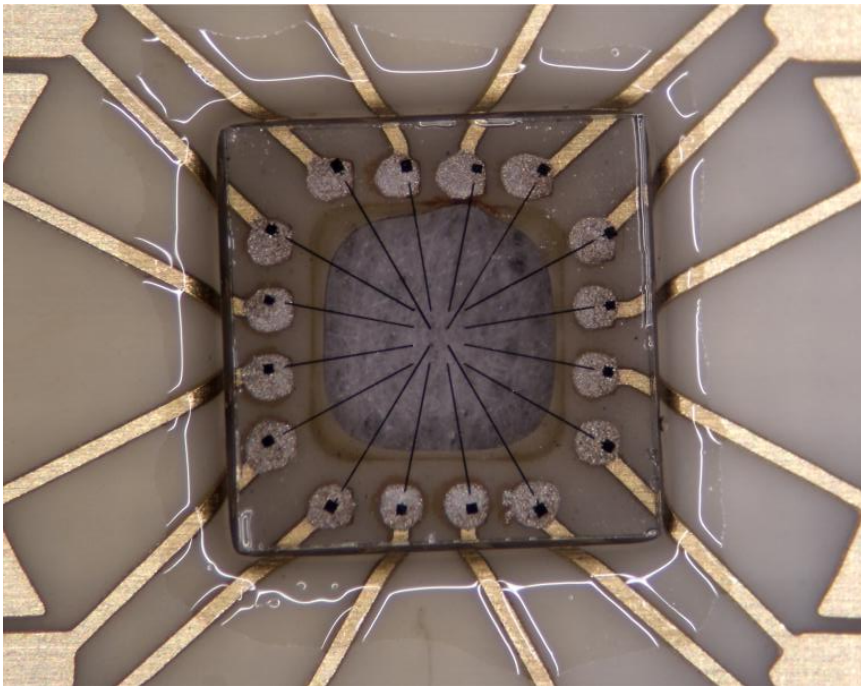
- single-crystal type IIa CVD from ElementSix™
- $4.5 \times 4.5 \times 0.5 \text{ mm}^3$

Ion implantation:

- He⁺ @ 1.2 MeV
- fluence $1.2 \times 10^{17} \text{ cm}^{-2}$
- penetration depth: $\sim 2 \mu\text{m}$

Thermal annealing:

- vacuum
- 950 °C
- 2 hrs

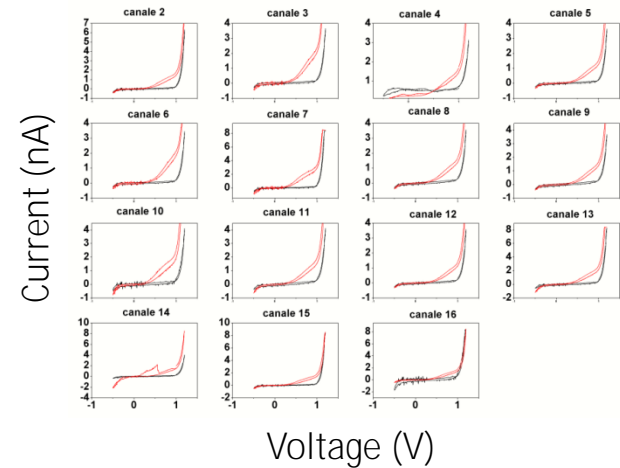


Biosensing

Exocytosis detection from a cultured chromaffin cells

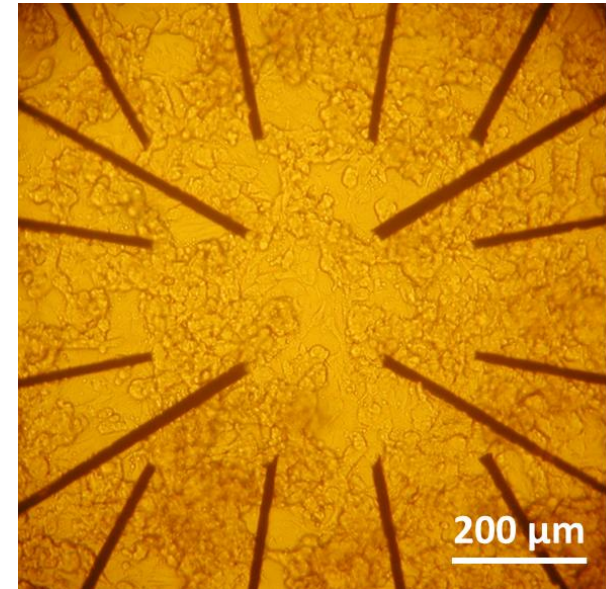
Cyclic voltammetry:

- solution: tyrode / tyrode + 100 μm adrenaline
- 0.8 V: adrenaline oxidation



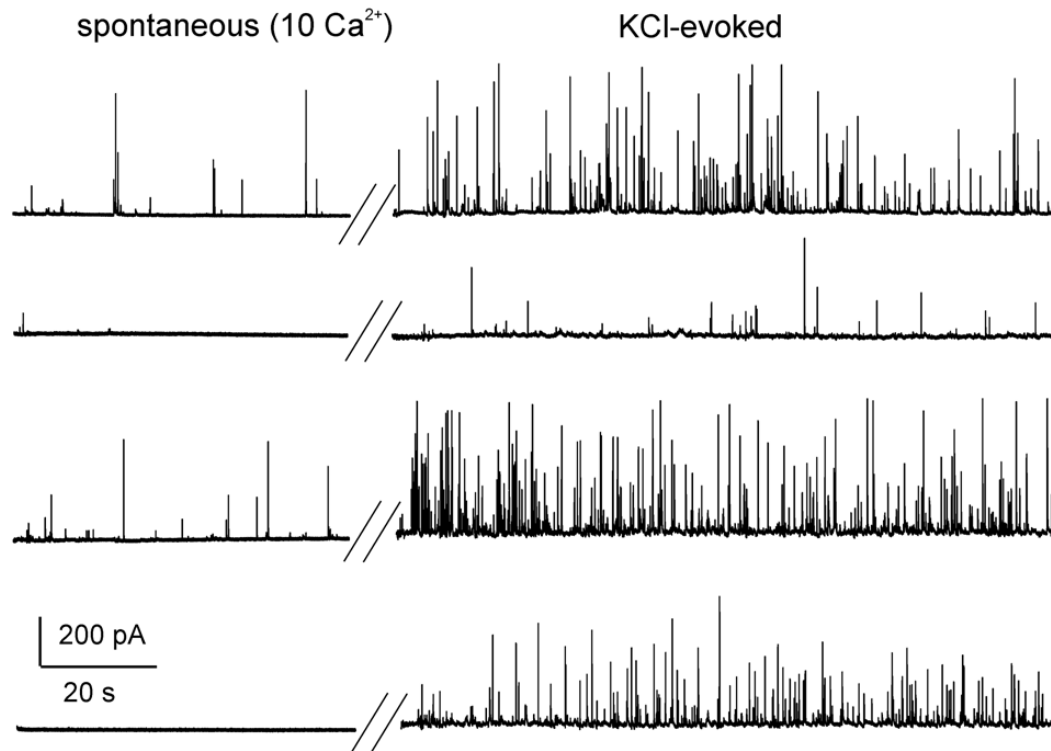
Plated chromaffin cells:

- from bovine adrenal glands
- ~150.000 cells plated on chip
- cultured for 4 days (37 °C, H₂O-saturated atmosphere with 5% CO₂)



Biosensing

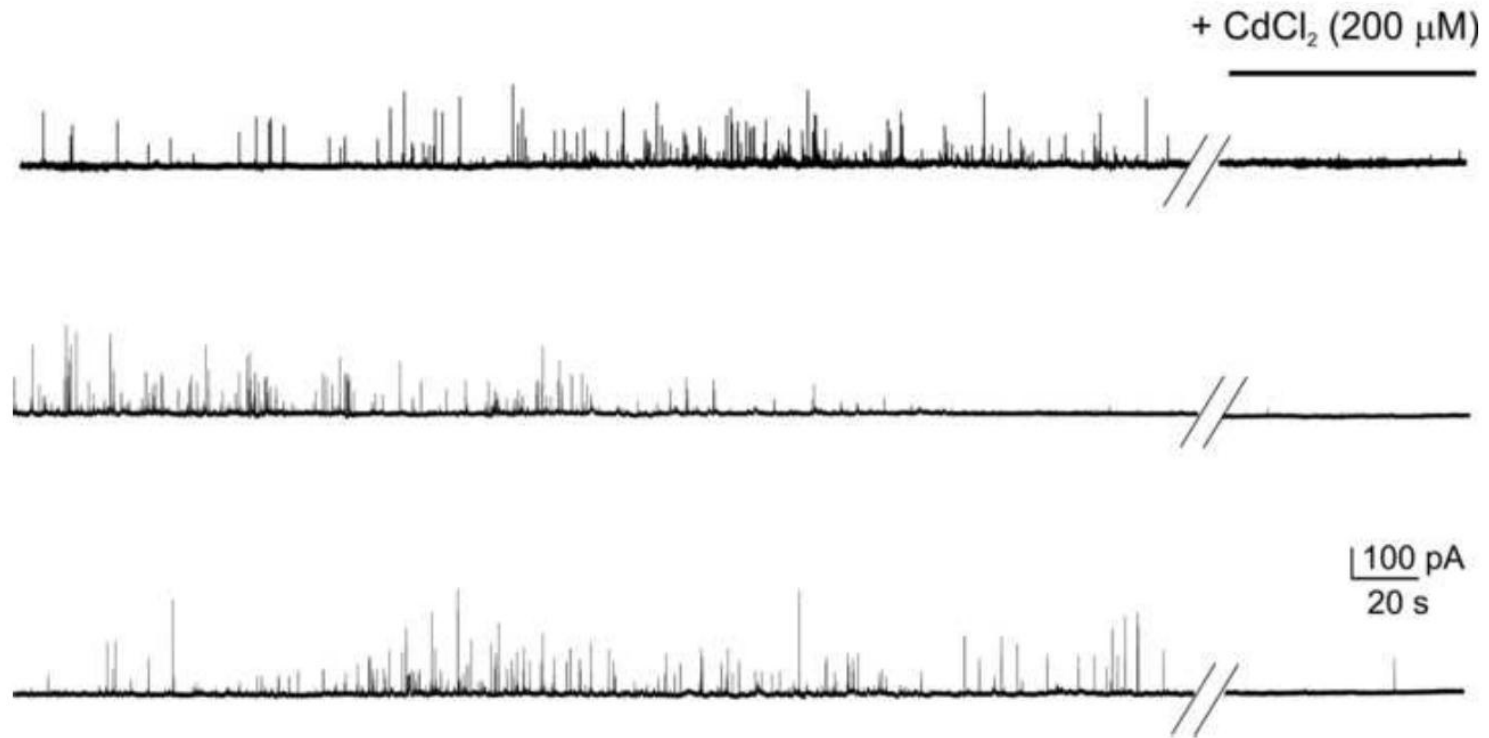
Chrono-amperometric recordings



- ✓ Bias voltage: +800 mV
- ✓ Individual cells in close proximity of the electrode
- ✓ Spontaneous activity in 10 mM Ca²⁺ solution (0.08 Hz)
- ✓ Chemical stimulation with 30 mM KCl solution (0.9 Hz)

Biosensing

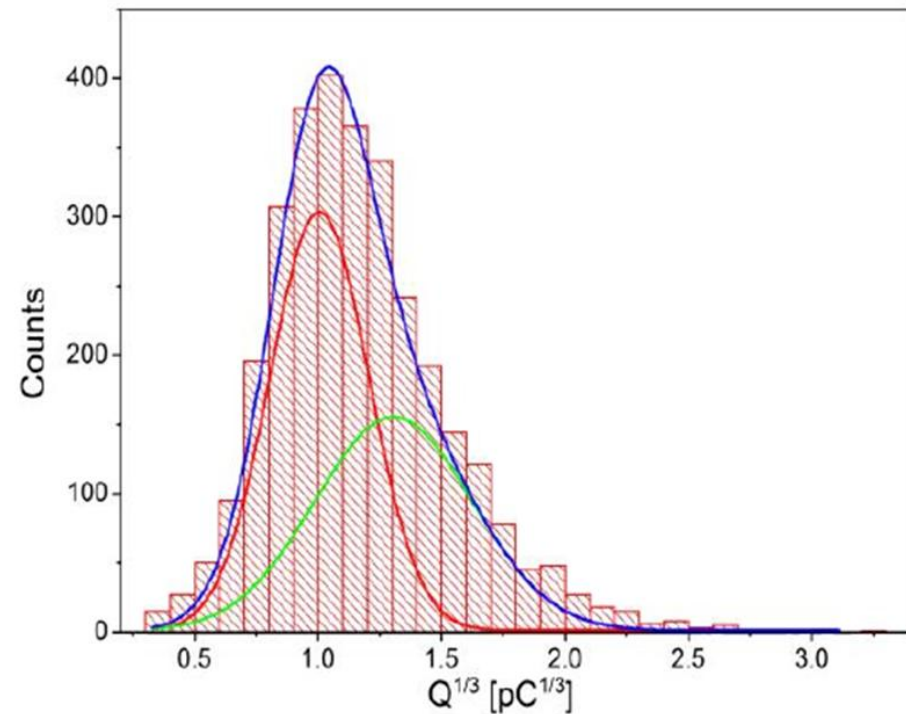
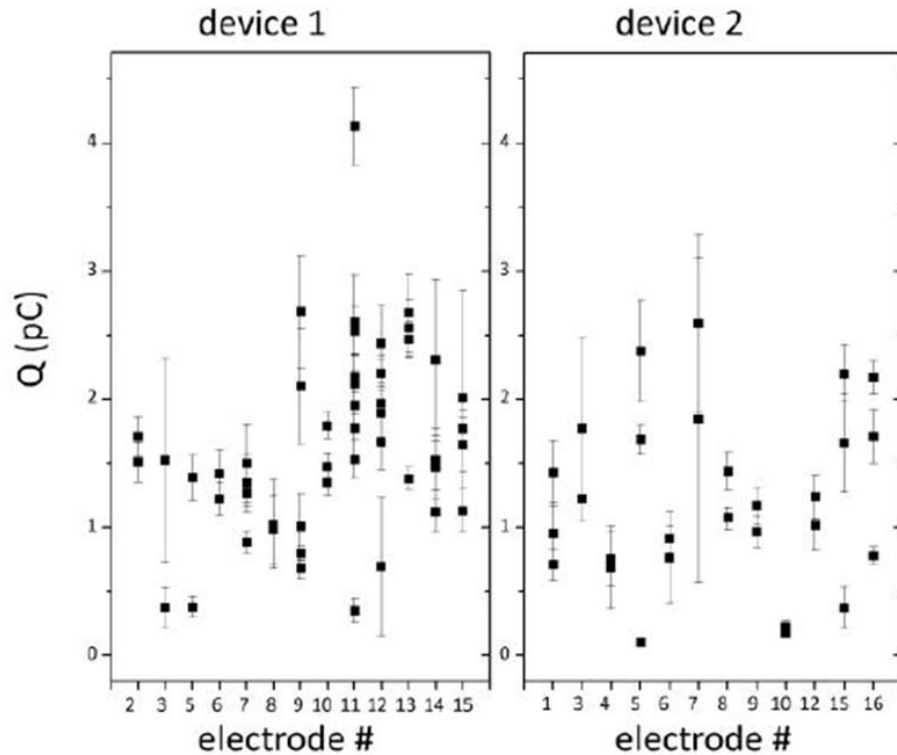
Chrono-amperometric recordings



- ✓ Bias voltage: +800 mV
- ✓ Individual cells in close proximity of the electrode
- ✓ Chemical suppression in 200 μm CdCl₂ solution

Biosensing

Signal statistics



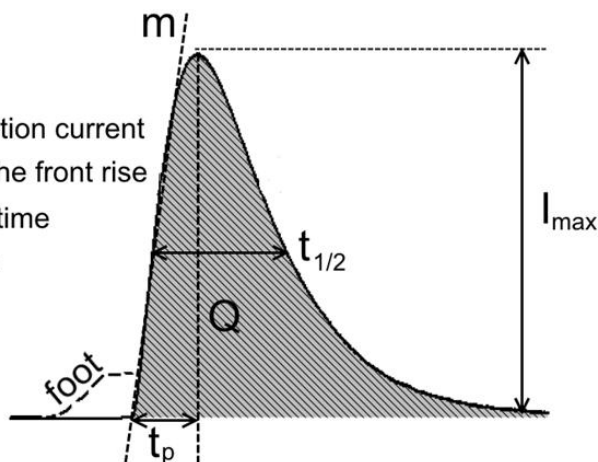
- ✓ Device reproducibility
- ✓ Variations due to cell behavior

- ✓ Full fusion events
- ✓ **“Kiss-and-run” events (smaller events with faster kinetics)**

Biosensing

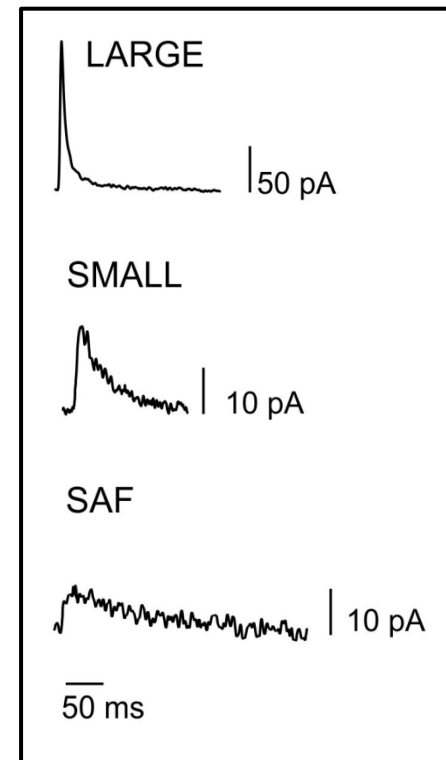
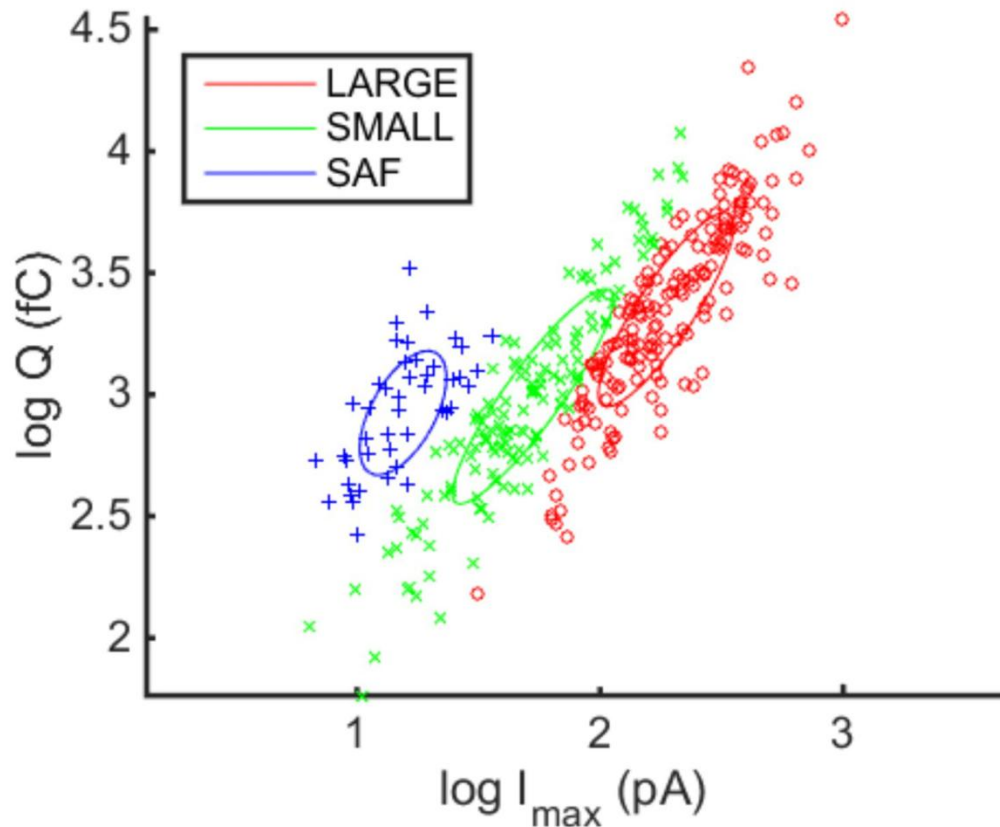
Signal statistics

	I_{\max} (pA)	Q (pC)	$Q^{1/3}$ (pC ^{1/3})	$t_{1/2}$ (ms)	m (nA s ⁻¹)	t_p (ms)	# spikes	# cells
SCD-MEA: cultured cells	74 ±5	1.56 ±0.09	1.06 ±0.02	17.0 ±0.7	21 ±2	8.3 ±0.4	3003	70
CFE (cultured cells on diamond plate)	82 ±13	1.4 ±0.2	0.97 ±0.05	17.2 ±1.6	33 ±6	8.0 ±0.8	495	14
Literature ‡ and §	73 ‡ ±3	1.40 ‡ ±0.06	1.06 § ±0.04	16.0 ‡ ±0.5	24.2 ‡ ±1.1	18.2 ‡ ±1.0	778 ‡	12 ‡



‡ J. D. Machado et al., Mol. Pharmacol. 60, 514 (2001)
 § J. M. Finnegan et al., J. Neurochem. 66, 1914 (1996)

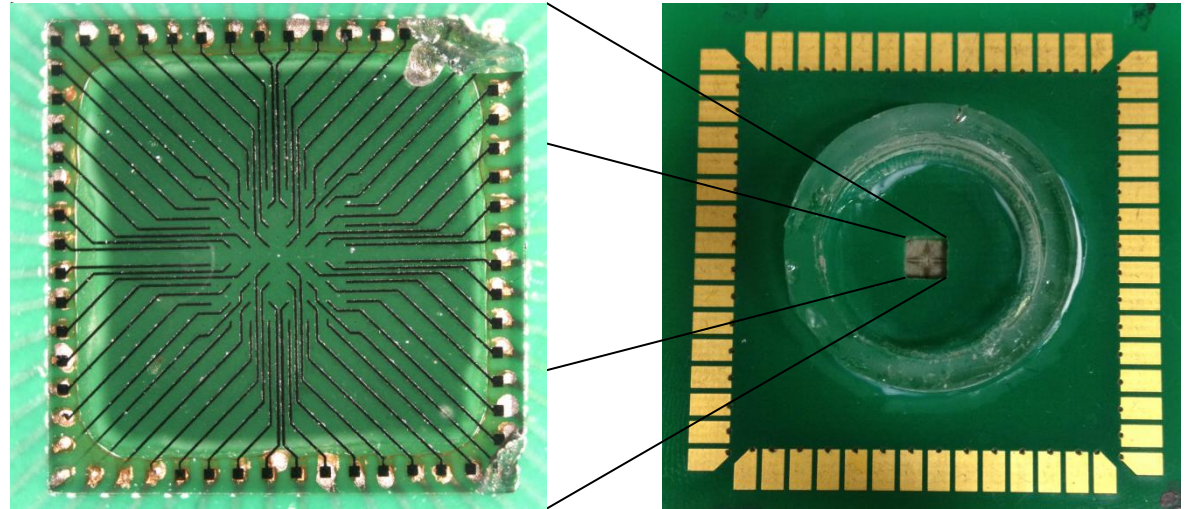
Signal statistics



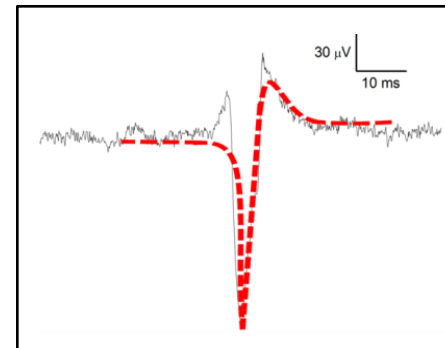
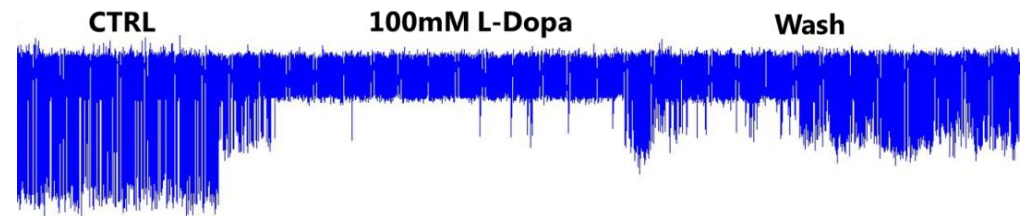
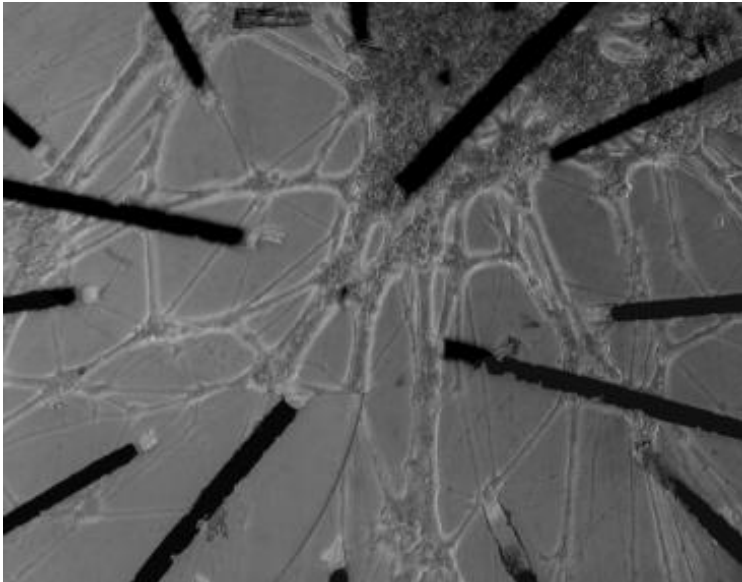
- ✓ 2D Gaussian mixture analysis
- ✓ 3-modal distribution: large (“full fusion”), small (“kiss-and-run”) and stand-alone foot (“kiss-and-stay”) events

Biosensing

64 channels
micro-electrode array

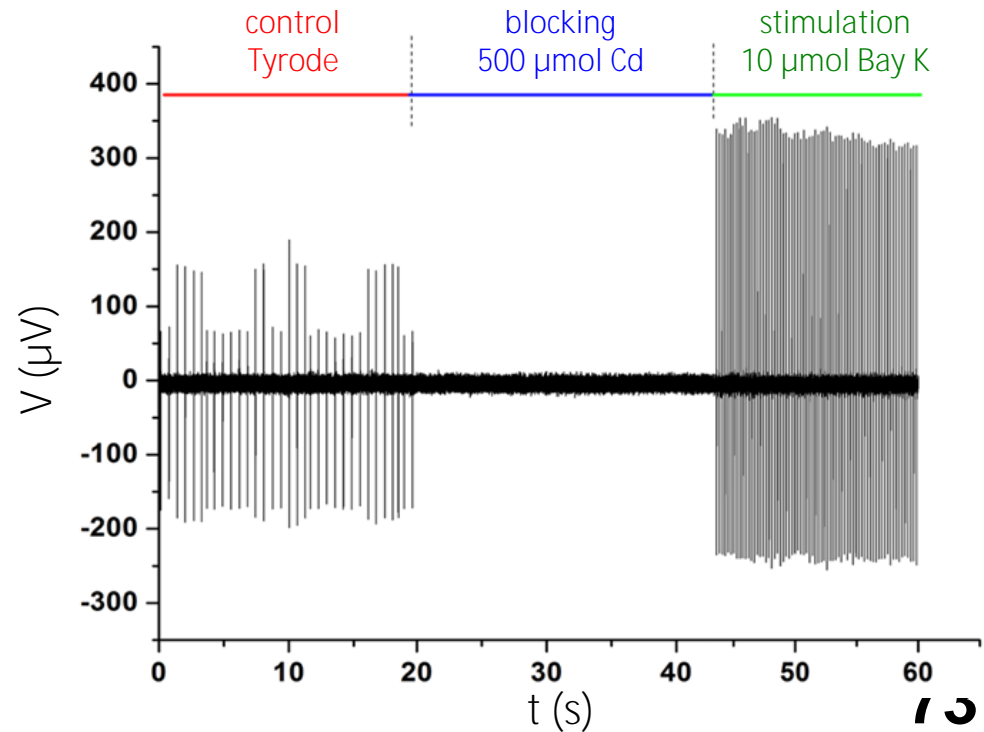
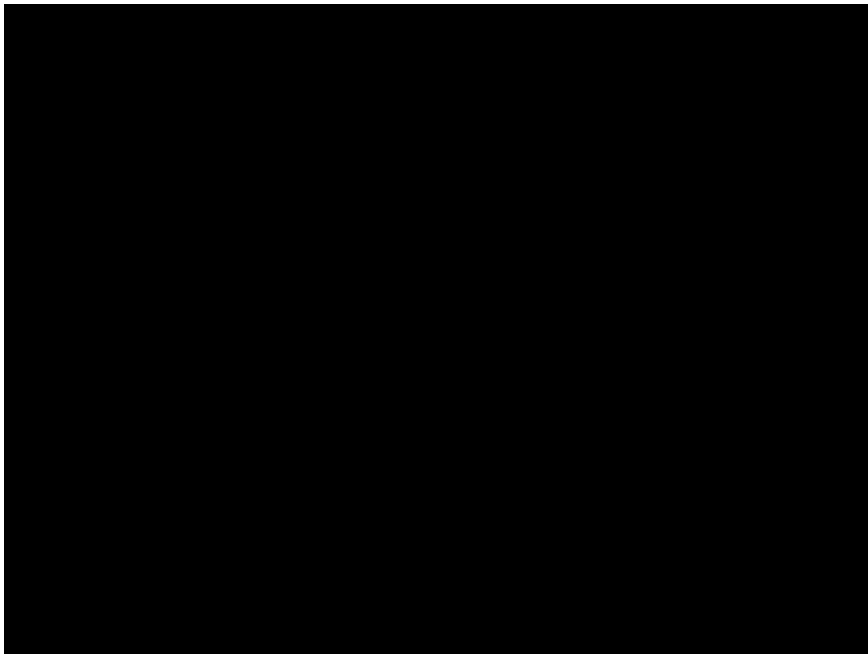
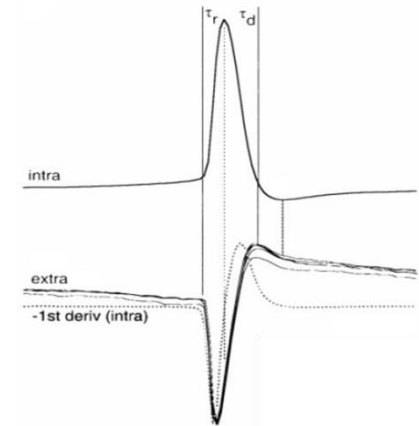
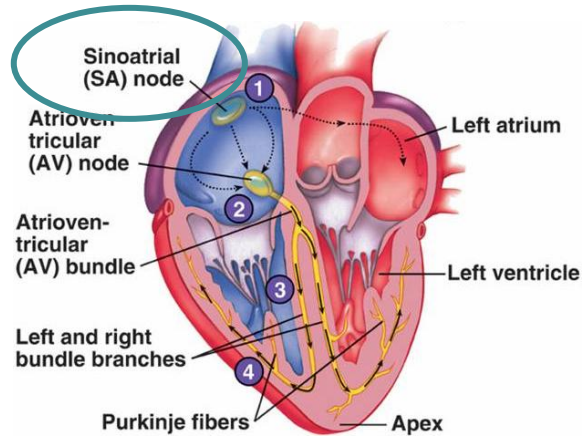


substantia nigra neurons



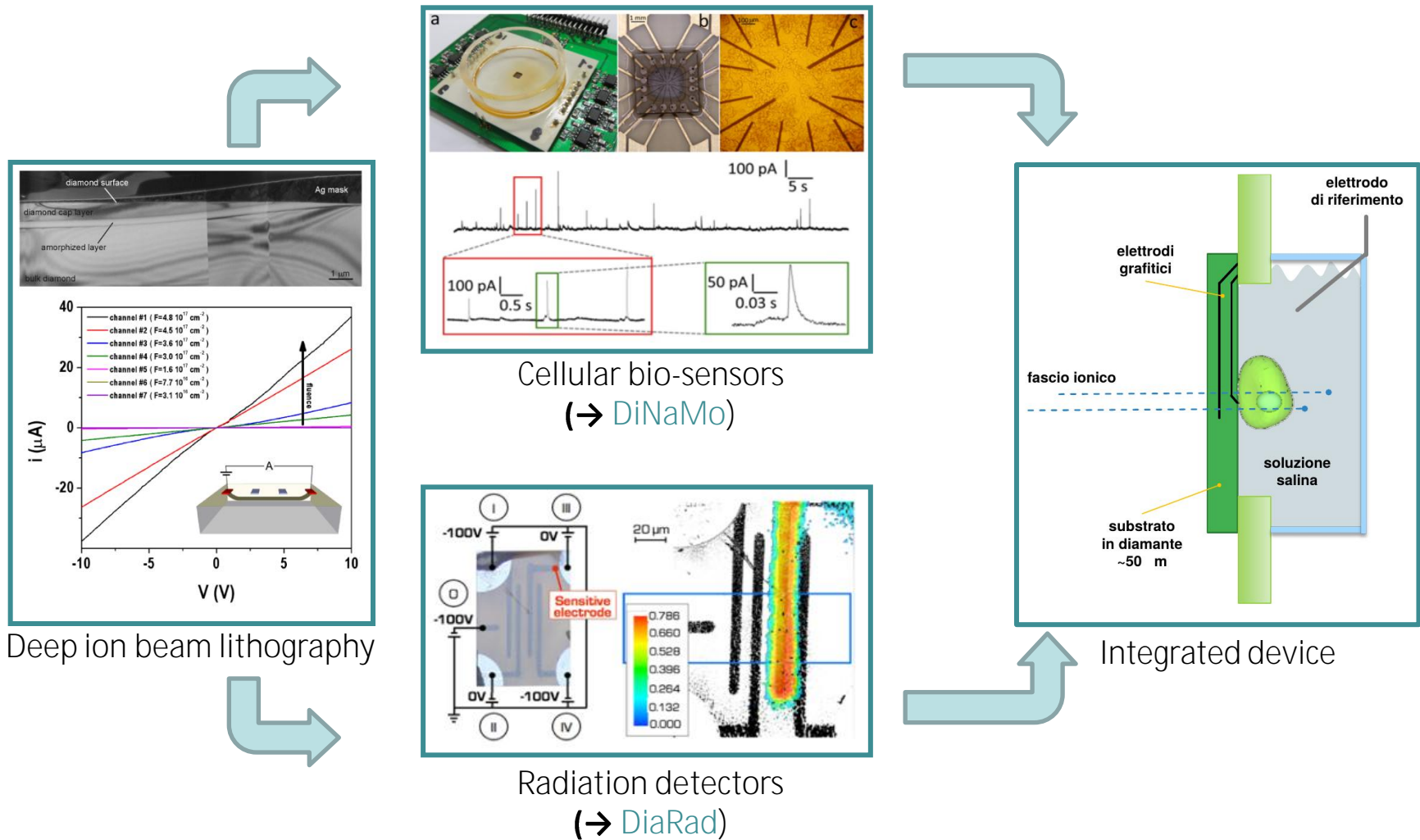
Biosensing

Detection of the action potential



Biosensing

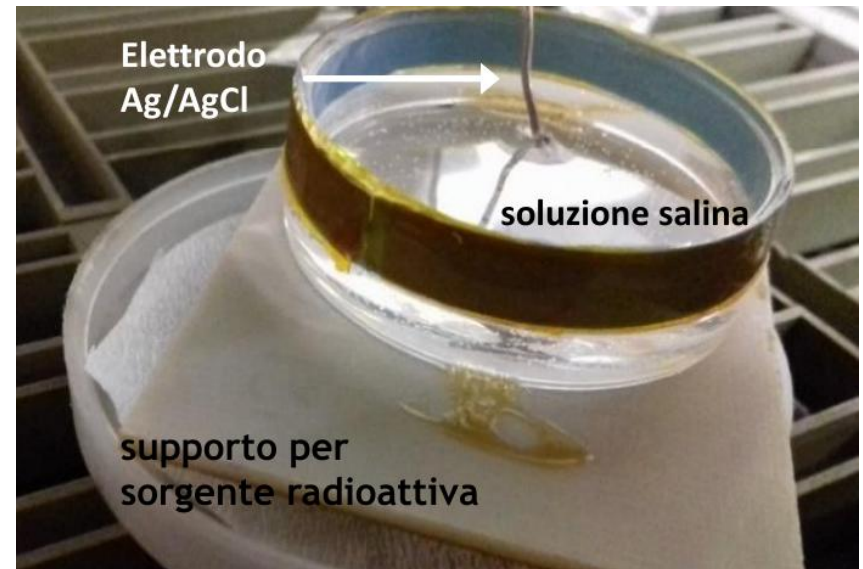
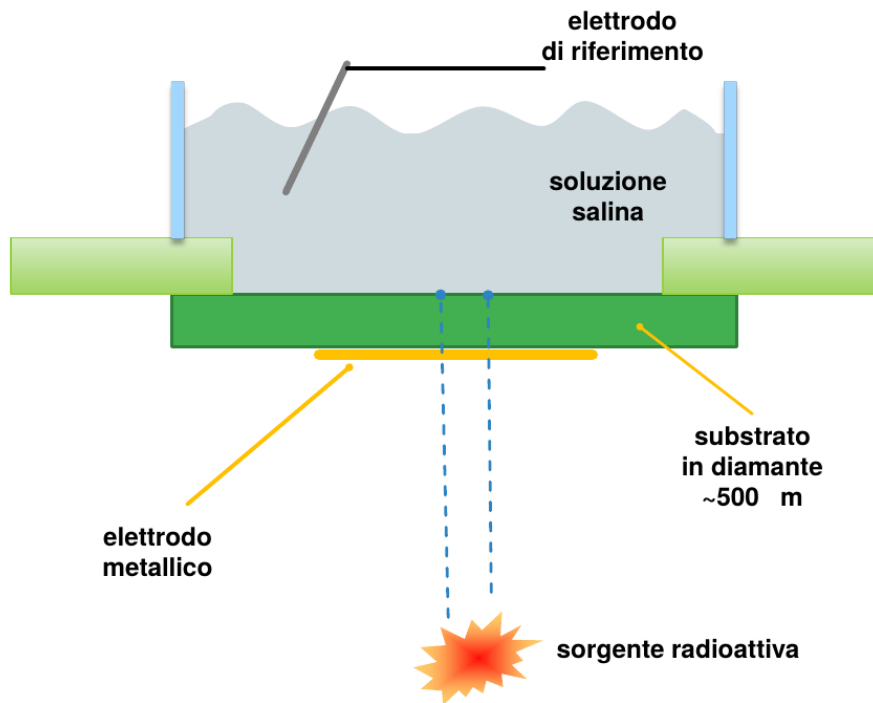
DIACELL: development of artificial diamond devices for the simultaneous detection of cell signals and ionizing radiation for applications in micro-radiobiology



Biosensing

DIACELL: preliminary results

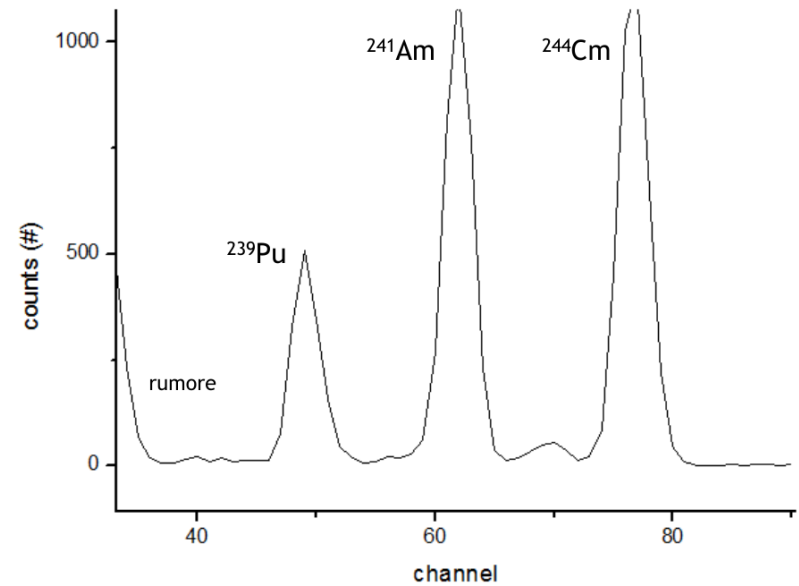
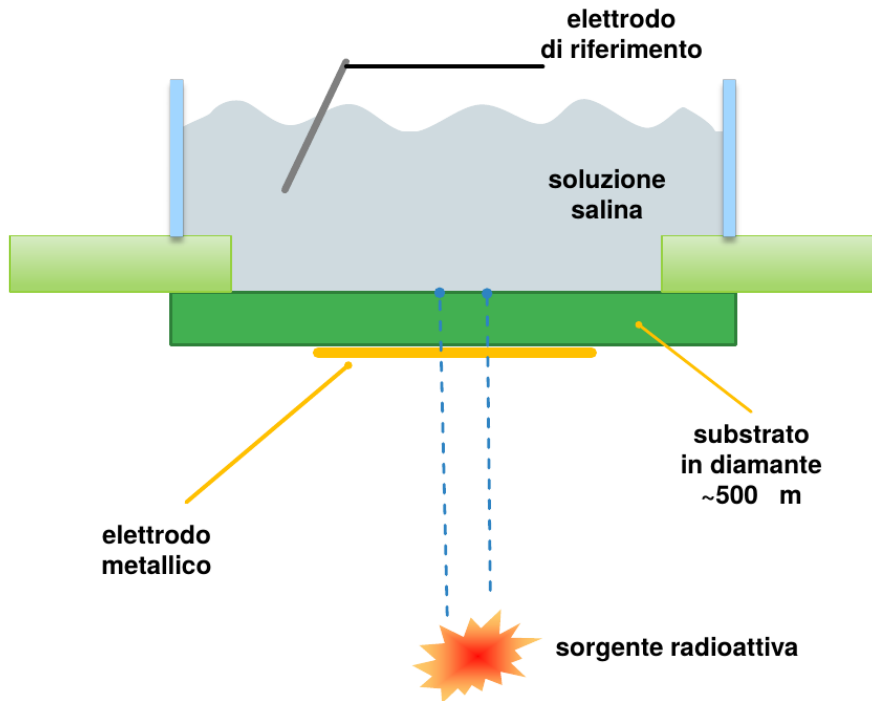
Counter-electrode in solution



Biosensing

DIACELL: preliminary results

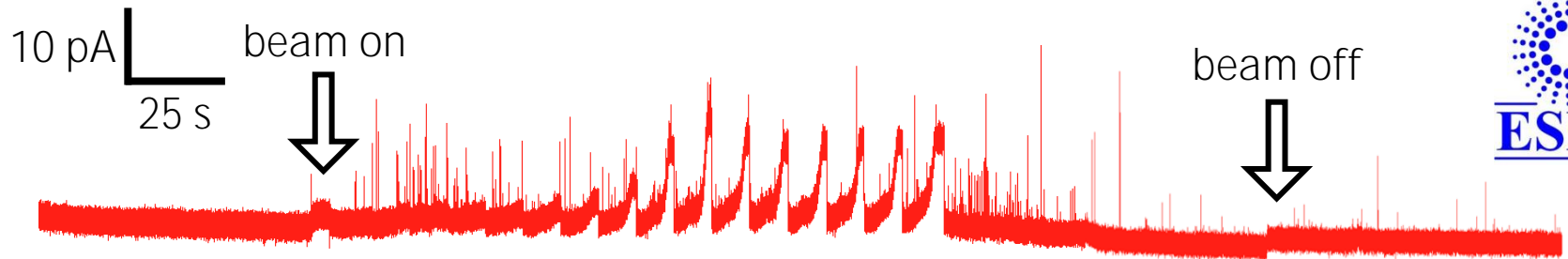
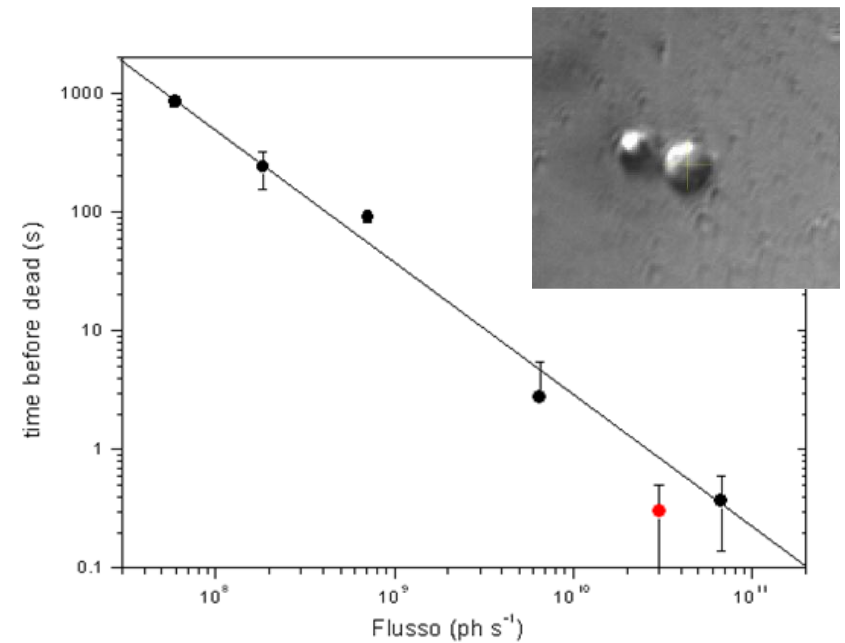
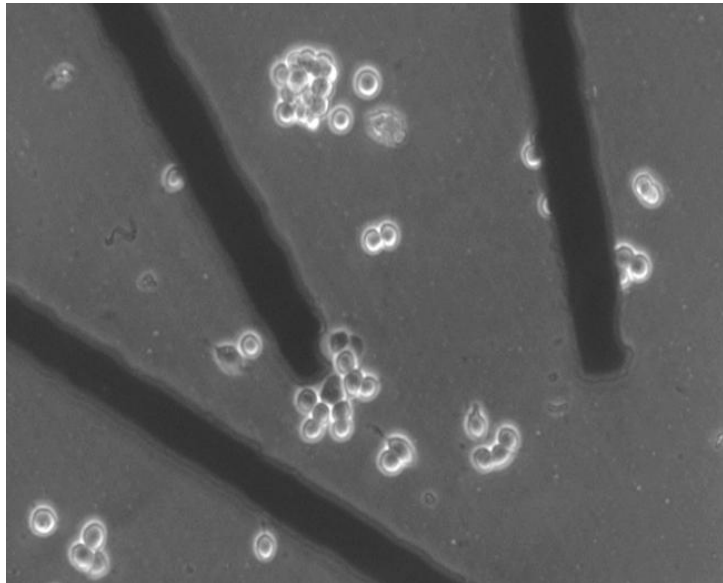
Counter-electrode in solution



Biosensing

DIACELL: preliminary results

Test run @ ESRF: 17 keV photons, $10^8 - 10^{11}$ photons s^{-1} , $\varnothing_{\text{beam}} = 20\text{-}200$ nm



-
- Diamond
 - IBL in diamond
 - Basic concepts
 - State of the art
 - Current research activities @ UniTo & INFN-To
 - **Electrical** features
 - Radiation detection
 - Biosensing
 - Quantum Optics
 - Conclusions

Quantum optics

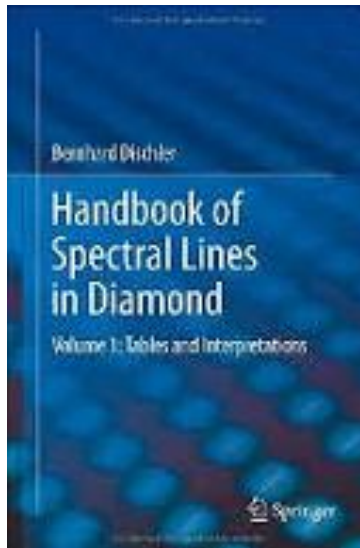
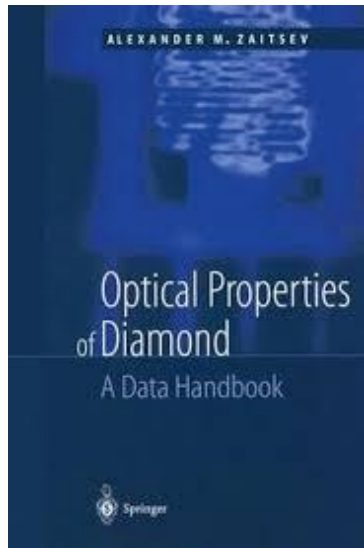
INFN project “DIESIS”

J. Forneris

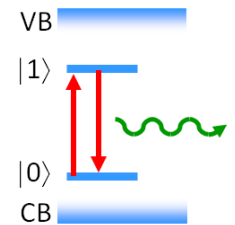


Jacopo Forneris

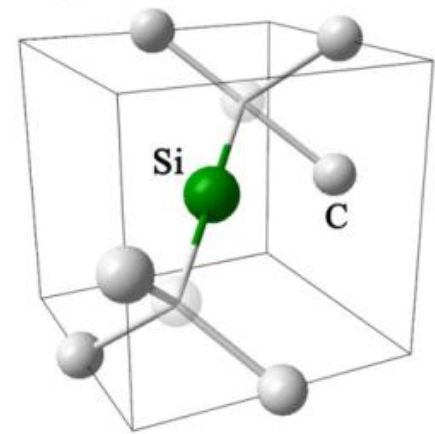
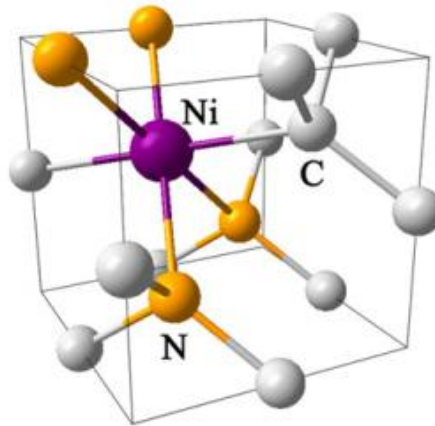
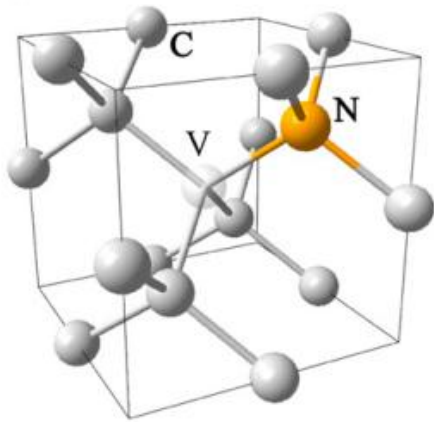
Quantum optics



$E_g = 5.49 \text{ eV}$
range of defects and impurities
low phonon density



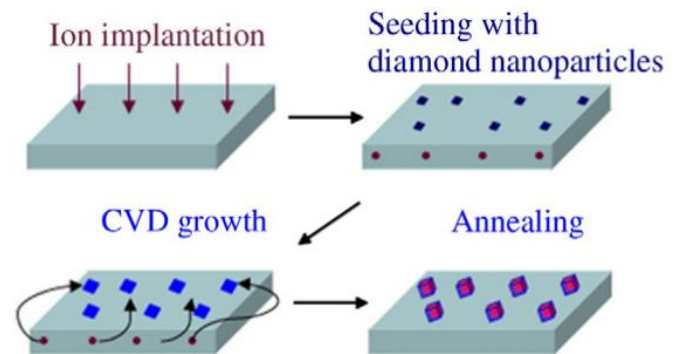
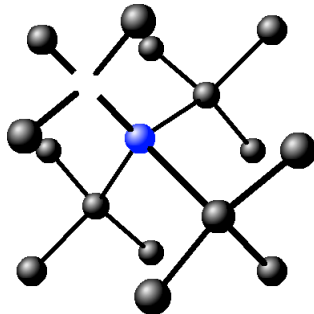
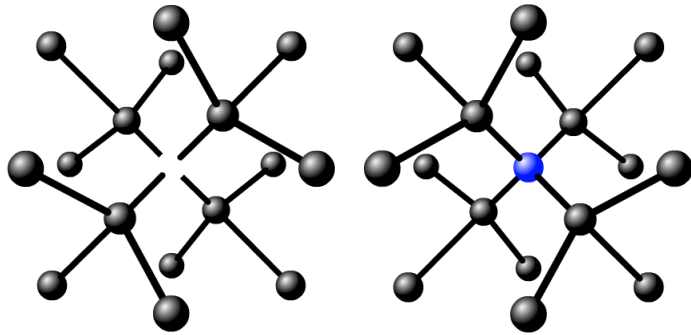
wide transparency from NUV to far IR
>150 vibrational & >500 electronic optically active centers
many centers are characterized by high quantum efficiency and photo-stability at room temperature
some centers display a convenient level structure for spintronics



→ single photon emitters (quantum cryptography, quantum optics)

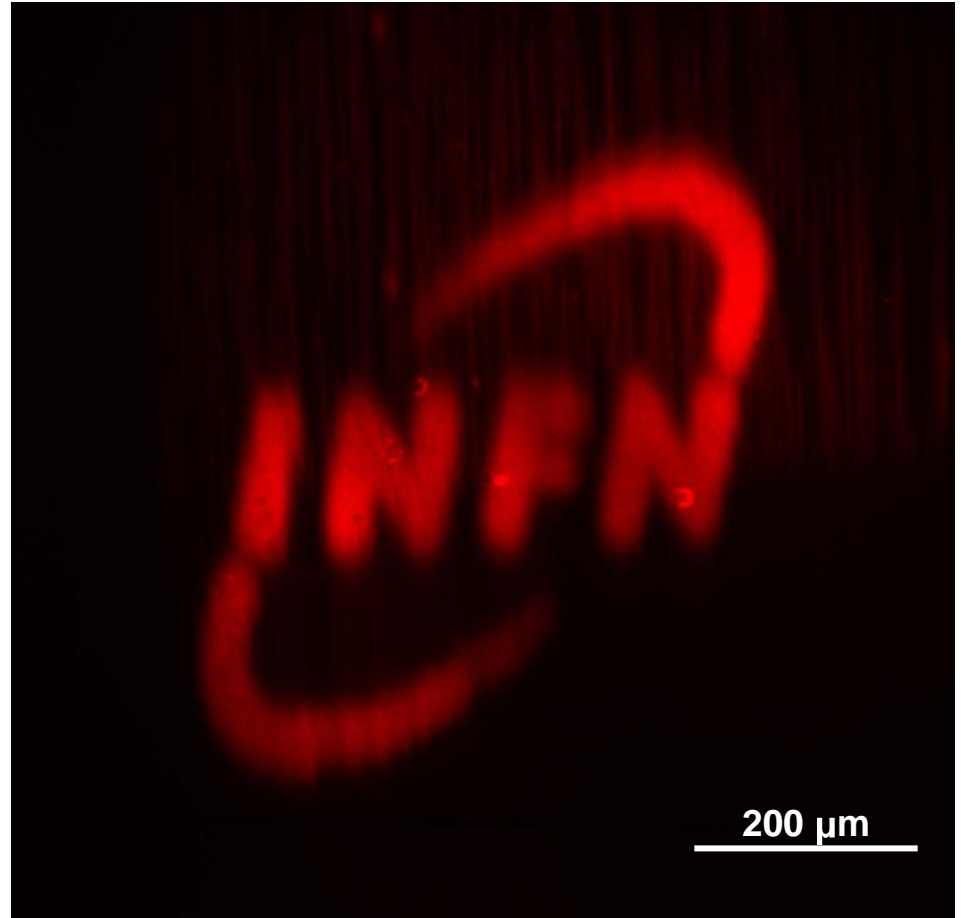
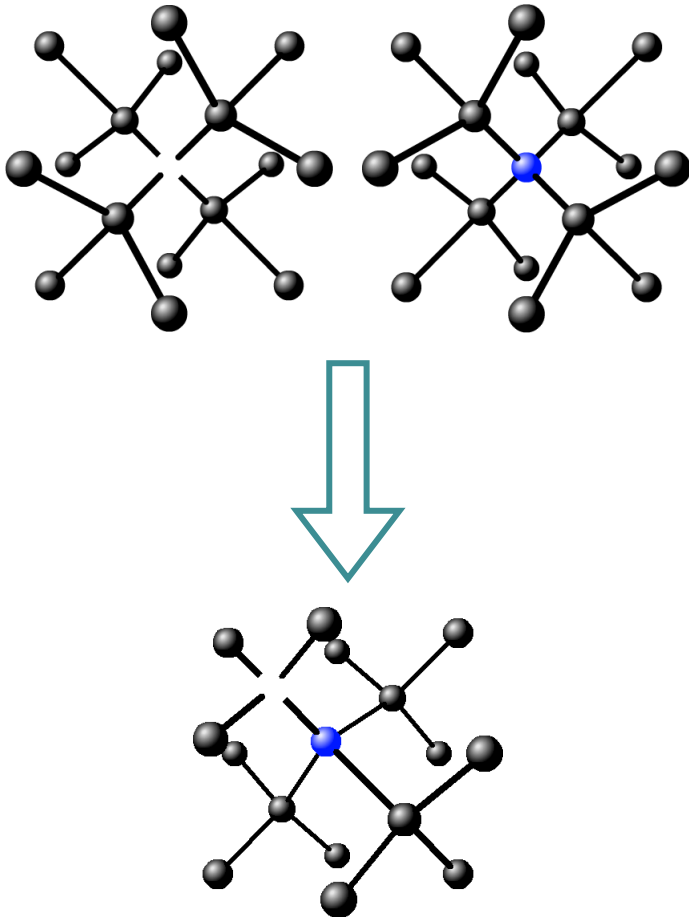
Quantum optics

Creation of NV centers via
CVD growth



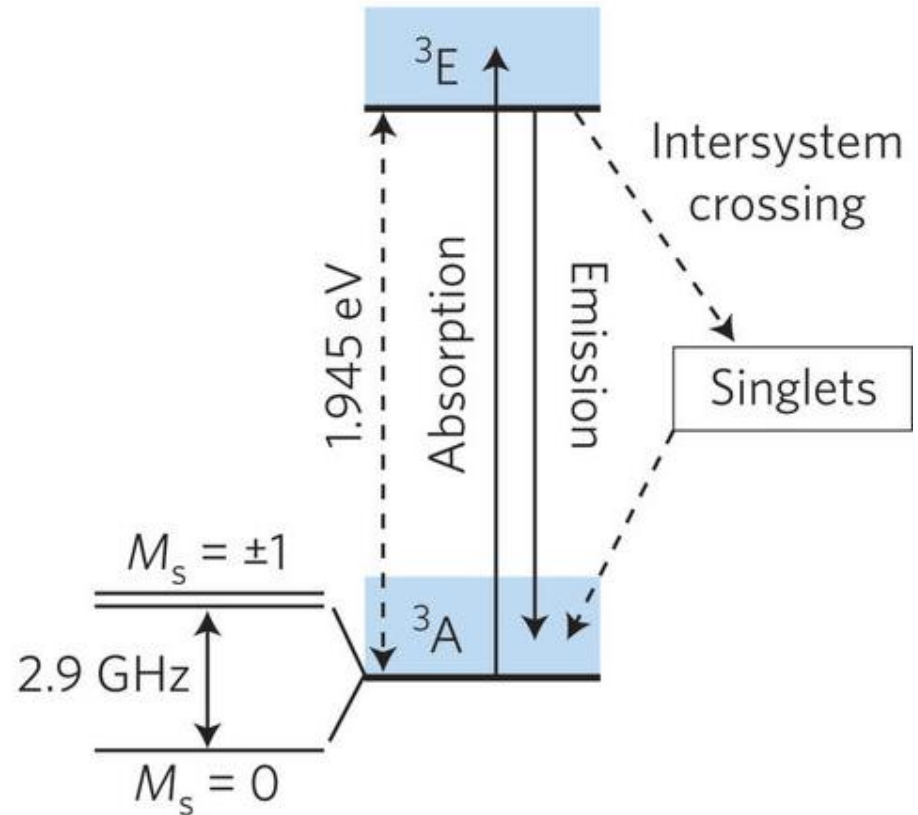
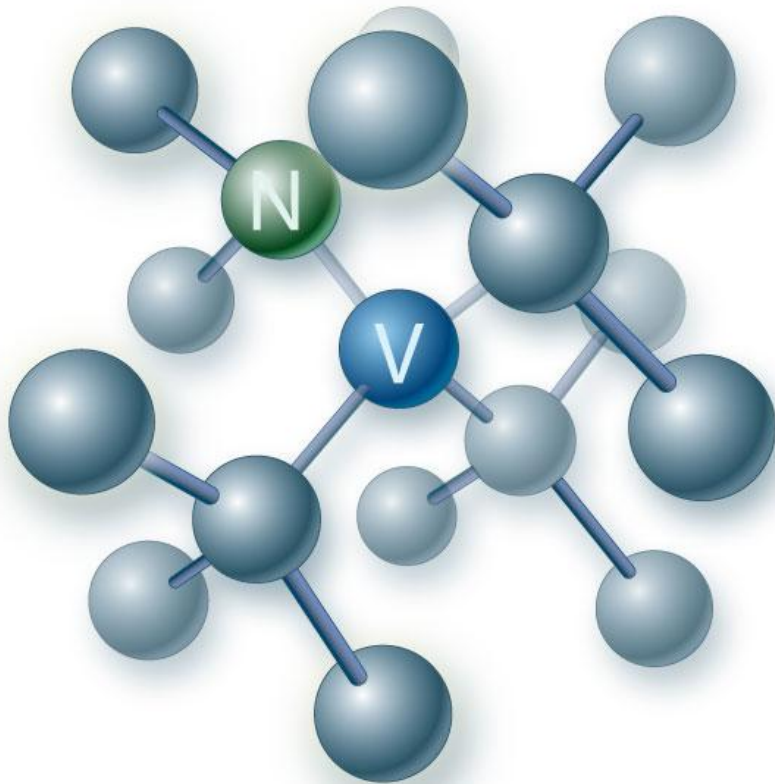
Quantum optics

Creation of NV centers via
ion implantation & annealing



Quantum optics

The negatively-charged nitrogen-vacancy (NV⁻) center

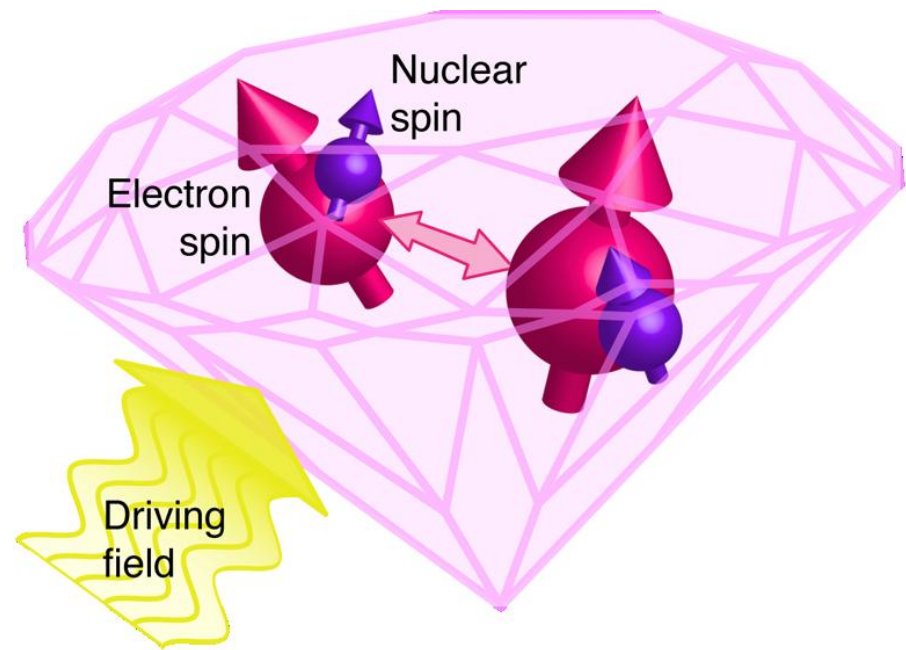
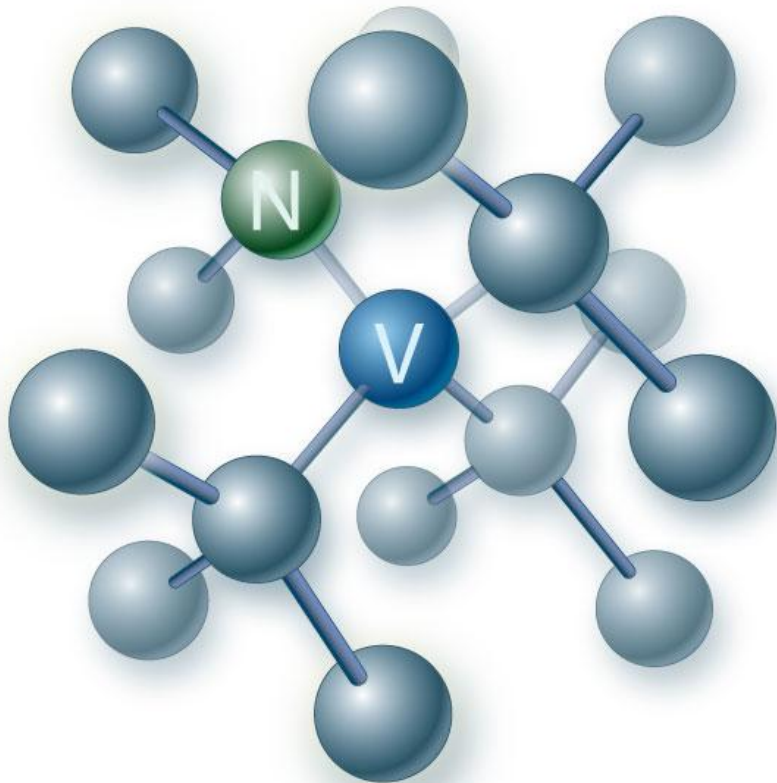


single-**spin selective transitions** →

optically detected magnetic resonance (ODMR)

Quantum optics

The negatively-charged nitrogen-vacancy (NV⁻) center

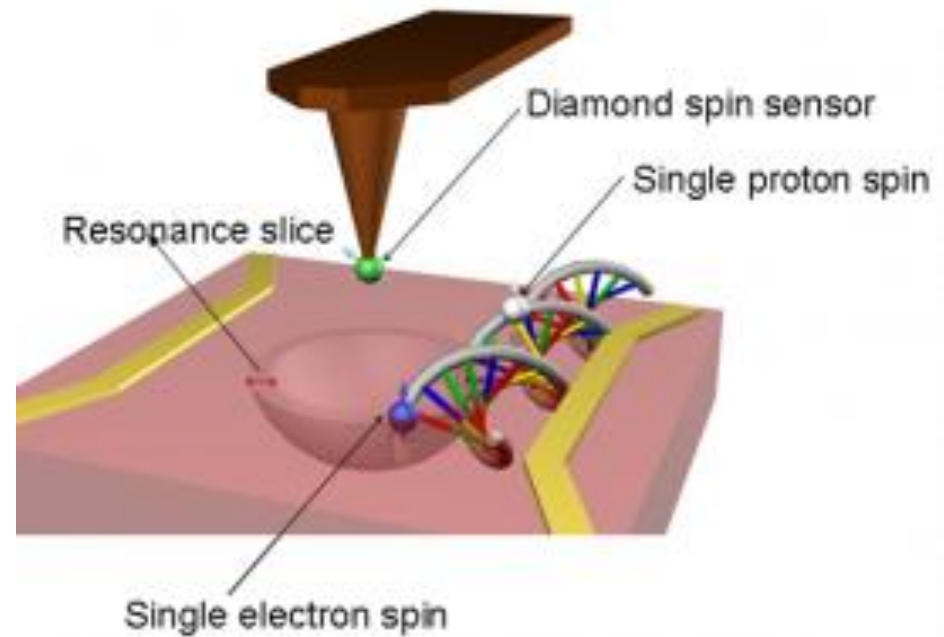
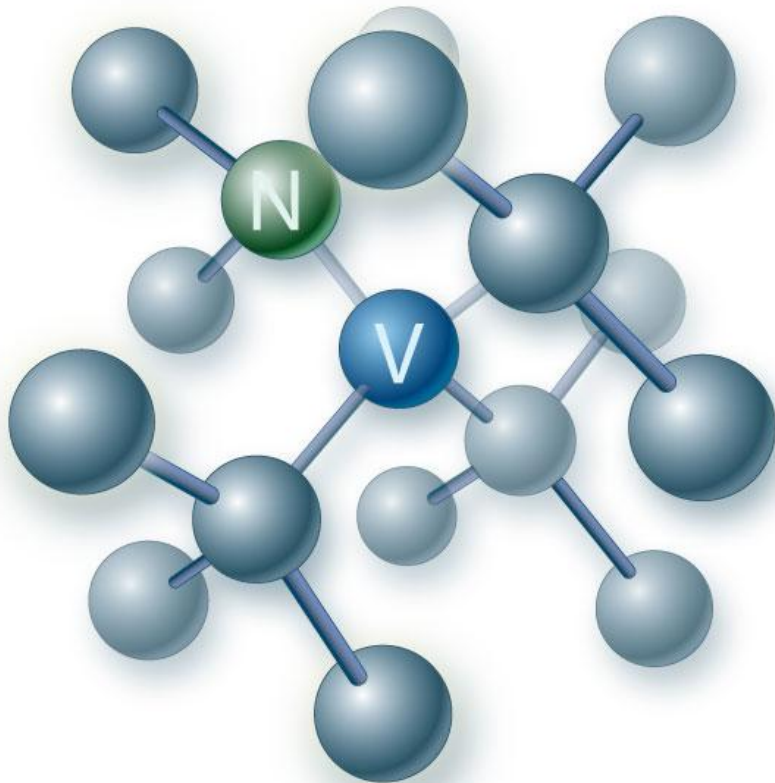


single-**spin selective transitions** →

optically detected magnetic resonance (ODMR)
quantum information processing

Quantum optics

The negatively-charged nitrogen-vacancy (NV⁻) center

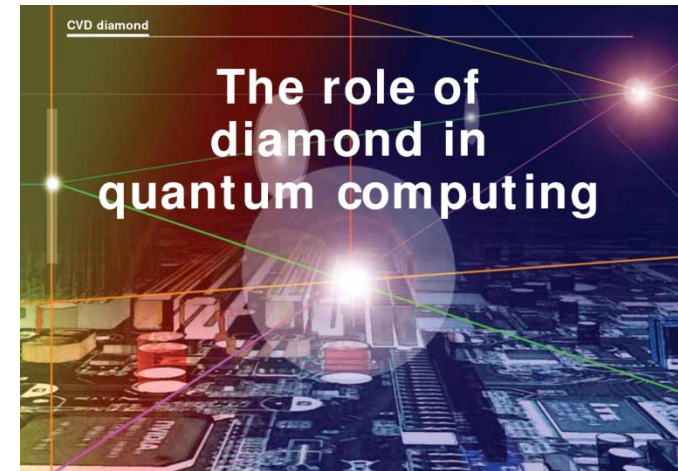
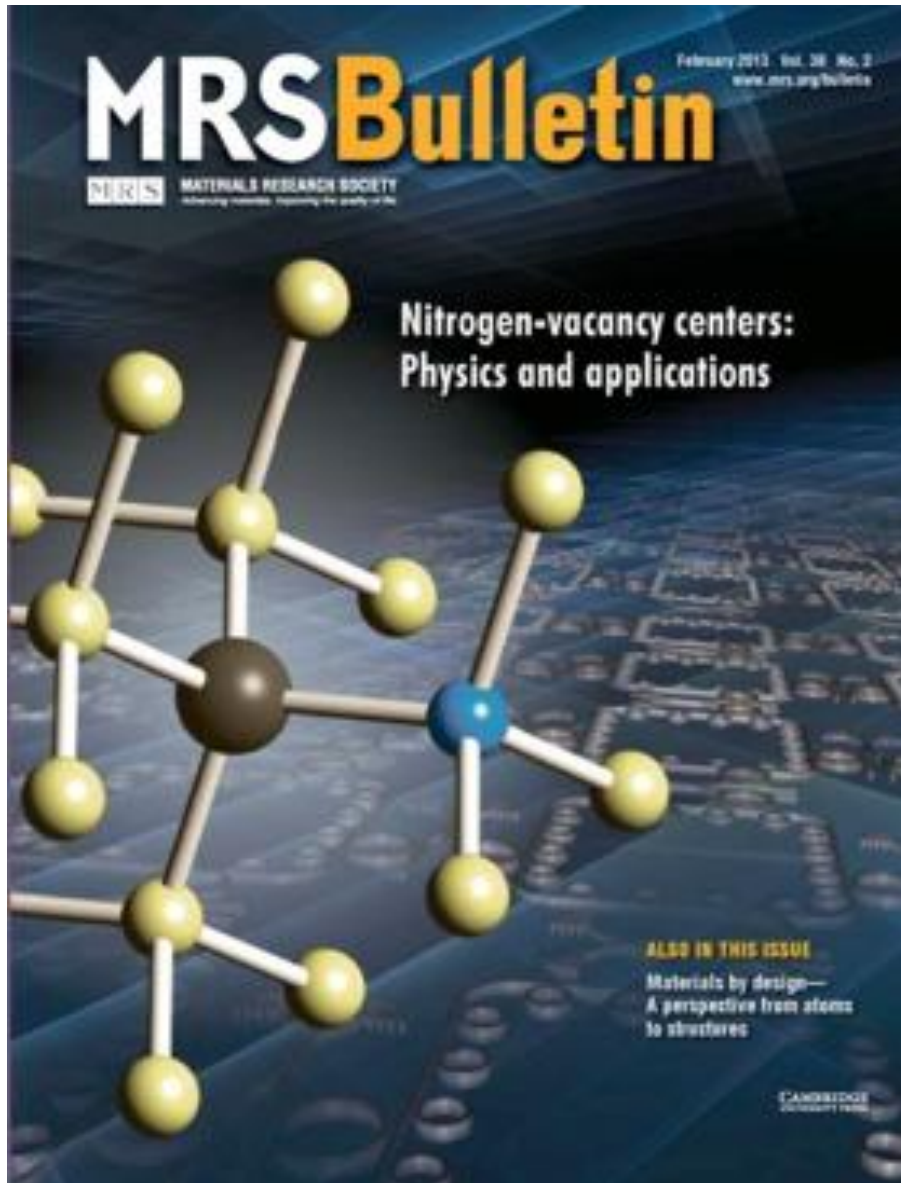


single-**spin selective transitions** →

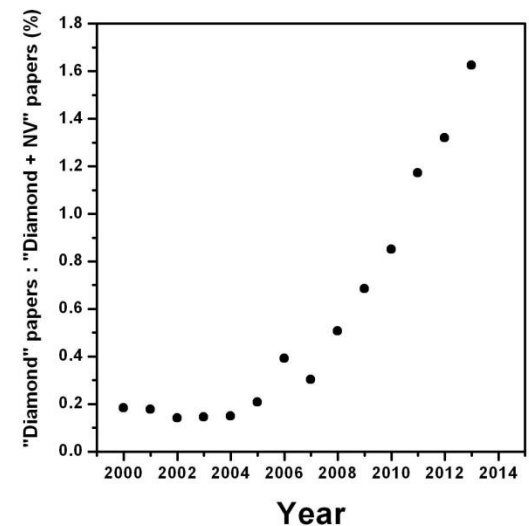
optically detected magnetic resonance (ODMR)
quantum information processing

high sensitivity & resolution magnetometry @ RT

Quantum optics

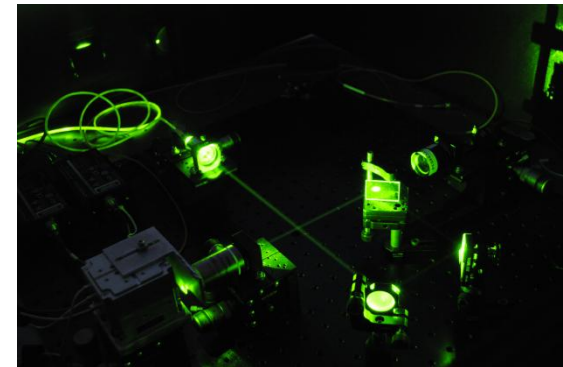
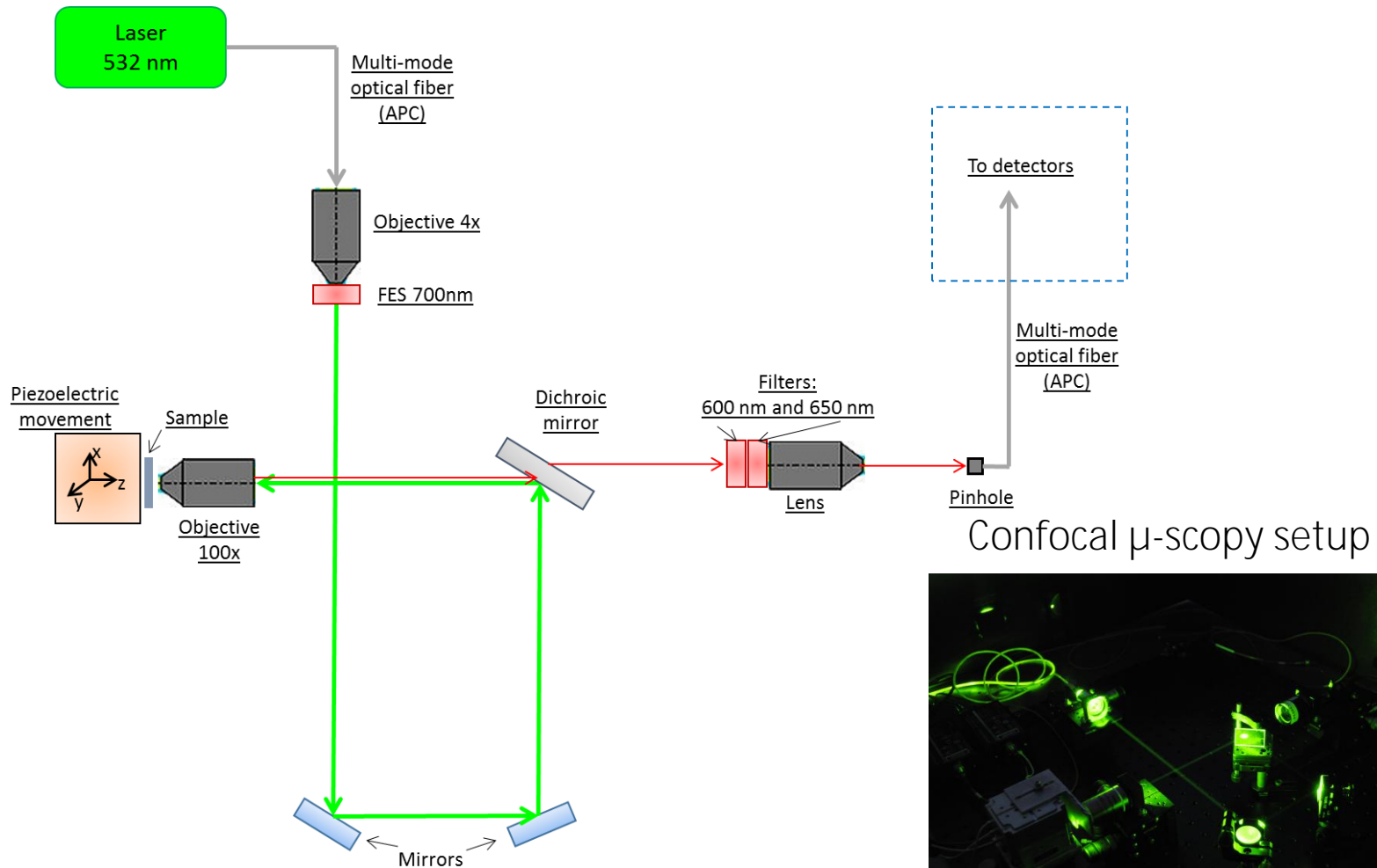


of “Diamond + nitrogen-vacancy” papers
: # of “Diamond” papers
(source: ISI Web)



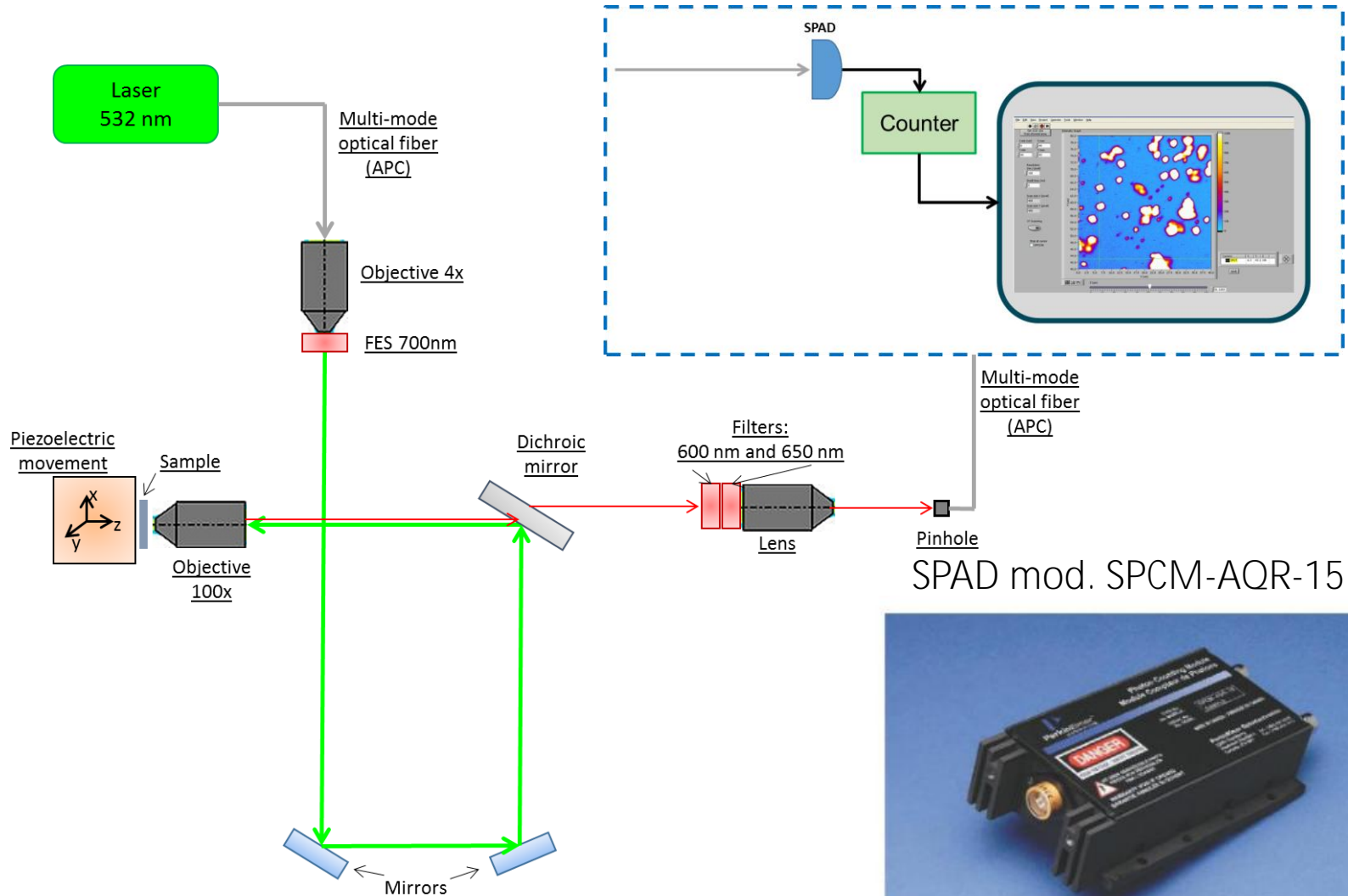
Quantum optics

Single-photon-sensitive confocal microscopy



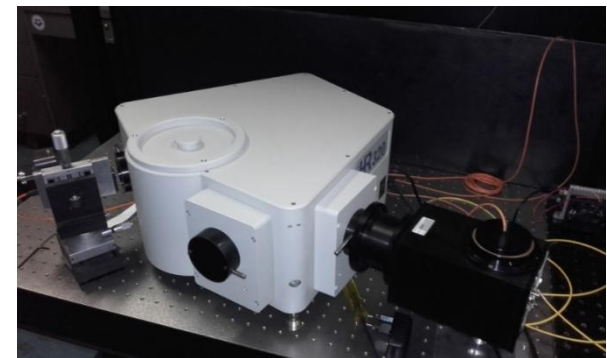
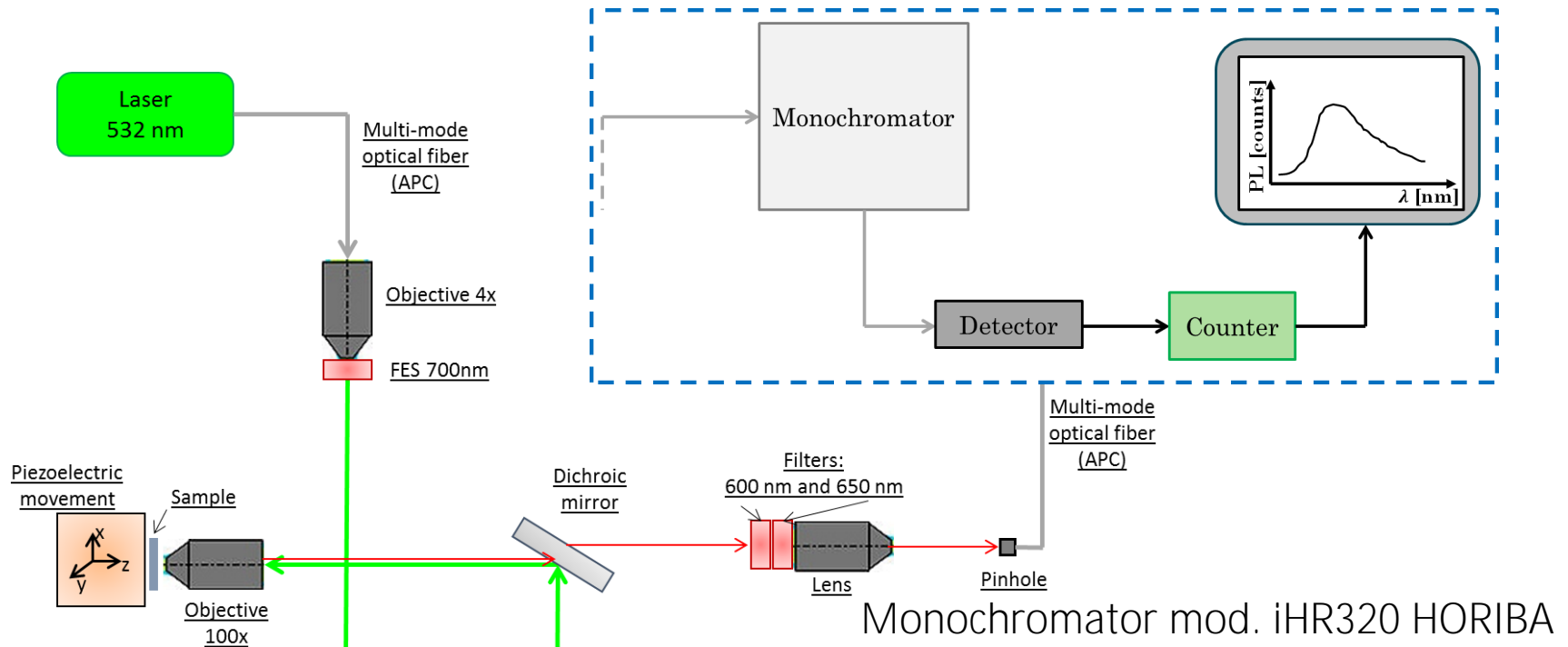
Quantum optics

Single-photon-sensitive confocal microscopy



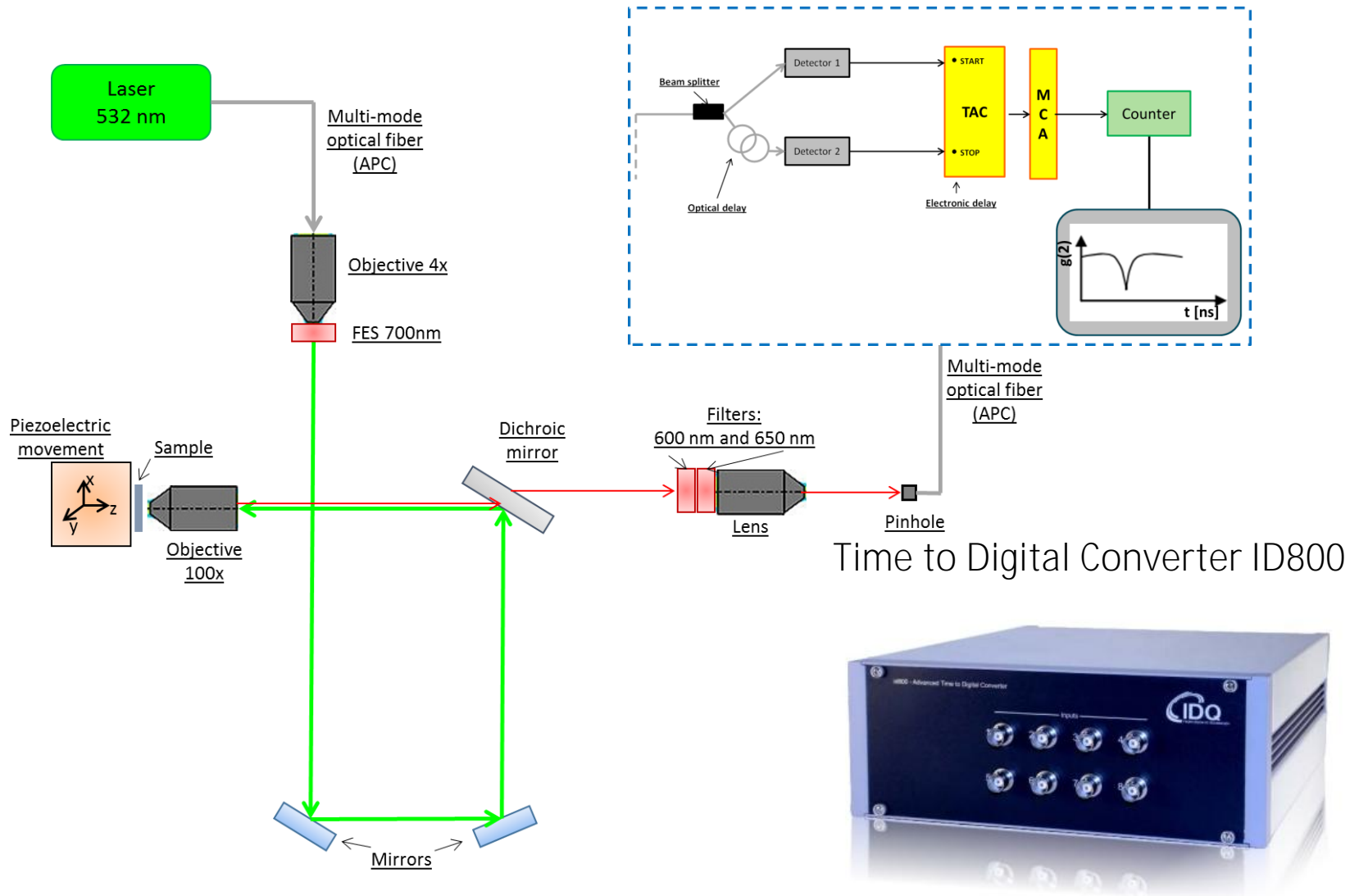
Quantum optics

Single-photon-sensitive confocal spectroscopy



Quantum optics

Hanbury-Brown-Twiss interferometry

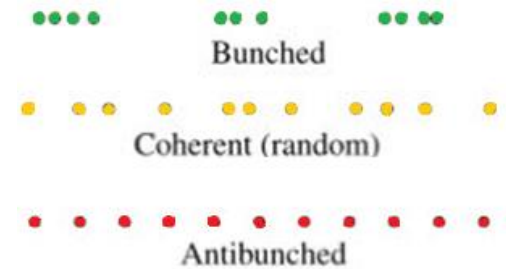
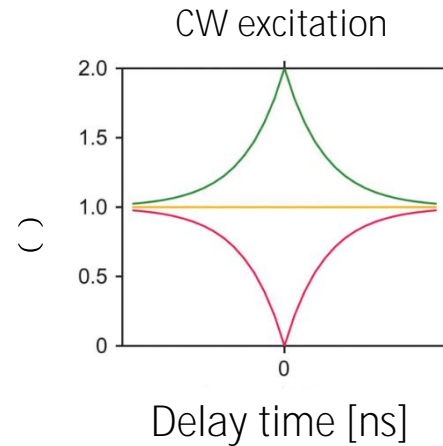


Quantum optics

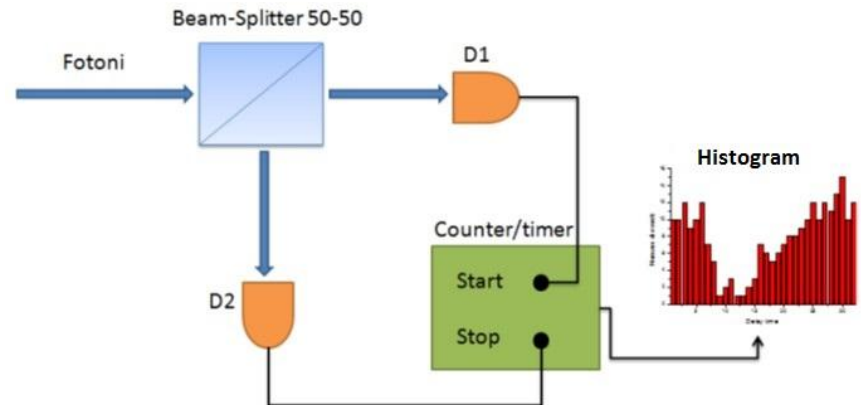
Hanbury-Brown-Twiss interferometry

$$g_2(\tau) = \frac{\langle I(t) \cdot I(t+\tau) \rangle}{\langle I(t) \rangle^2}$$

2nd order auto-correlation function

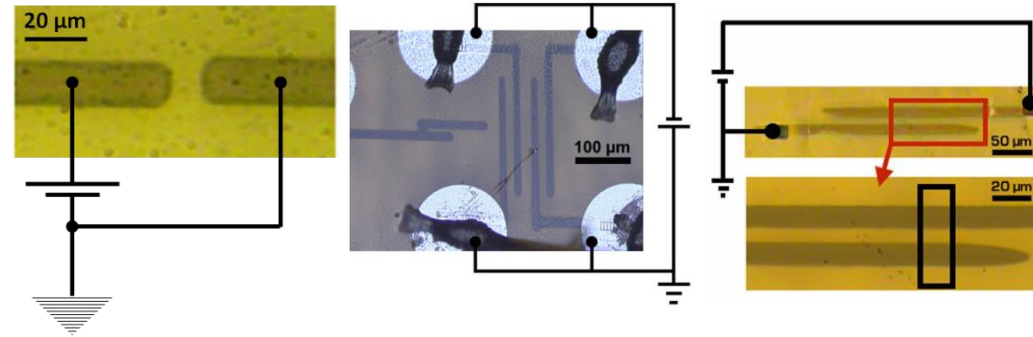
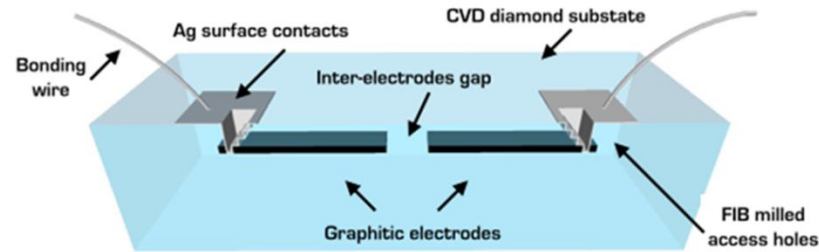


$g^{(2)}(0) < 0.5 \rightarrow$ **single-photon emitter**



Quantum optics

The devices

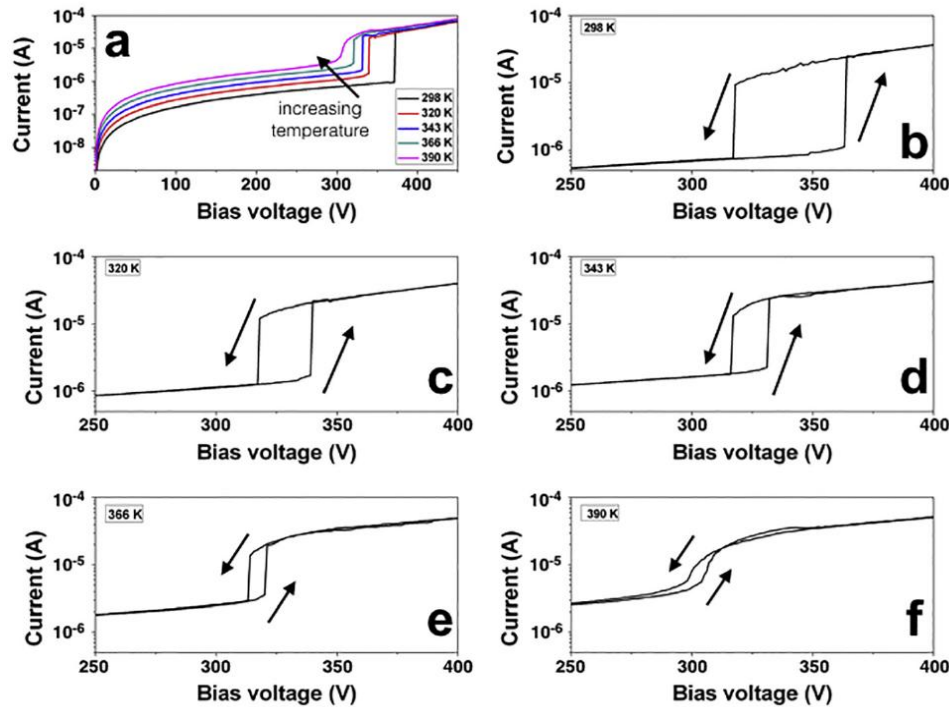


- Ila samples: optical / electronic grade from ElementSix, home grown
- ion beam lithography: 6 MeV C ions (RBI), 1.8 MeV He (INFN-LNL)
- penetration depth: $\sim 3 \mu\text{m}$
- post-implantation thermal processing: 950 °C, 2 hrs



Quantum optics

Electrical characterization



$V < \sim 350$ V: “low current”, Space Charge Limited Current

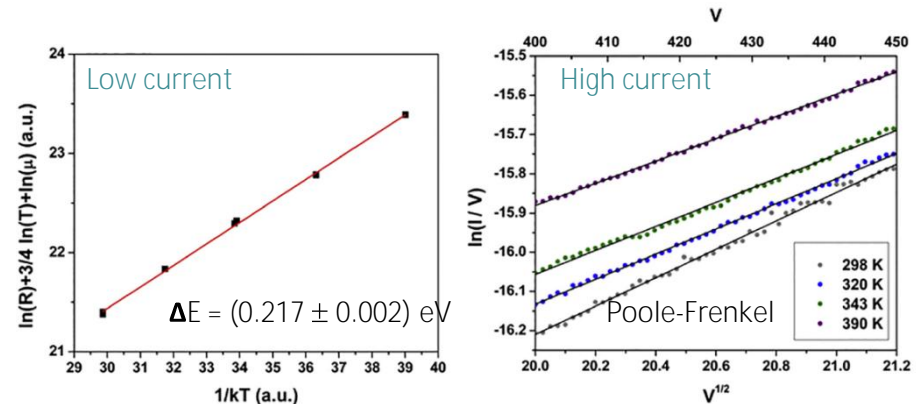
~ 350 V: abrupt current increase

$V > \sim 350$ V: “high current”, Poole-Frenkel

temperature-dependent study

“low-current” regime: NV charge state control, NV Stark shift

“high-current” regime: electroluminescence

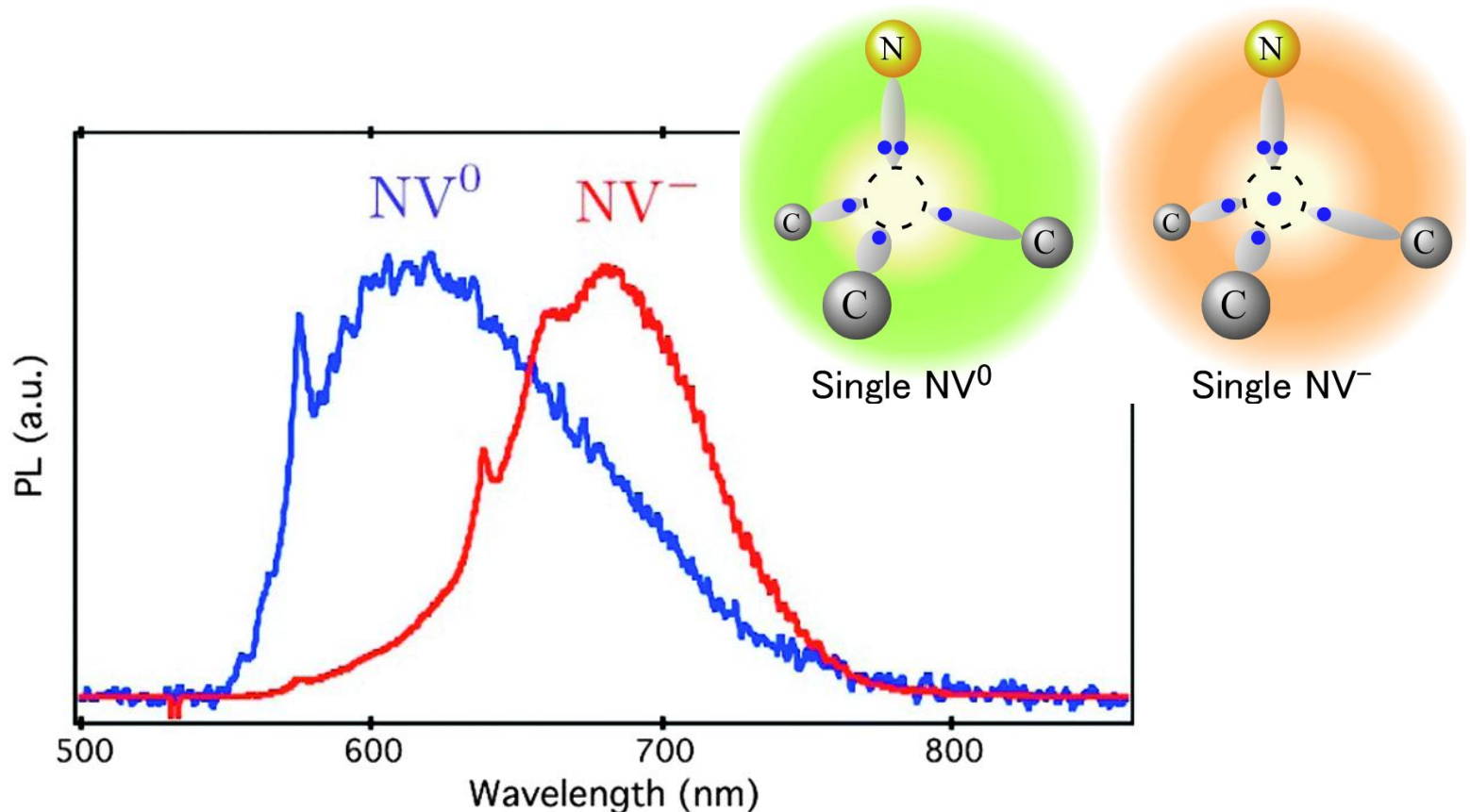


S. Ditalia et al., Diamond Relat. Mater. 74, 125 (2017)

Quantum optics

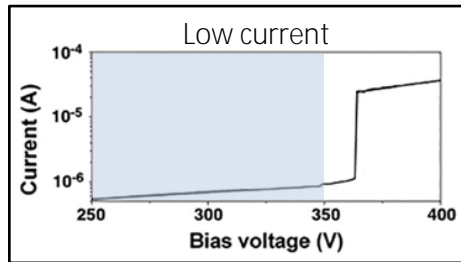
Open issues with NV defects:

- ✓ Efficiency in defect formation
- ✓ **Spectral properties (inhomogeneous broadening, phonon coupling, ...)**
- ✓ Charge state instability



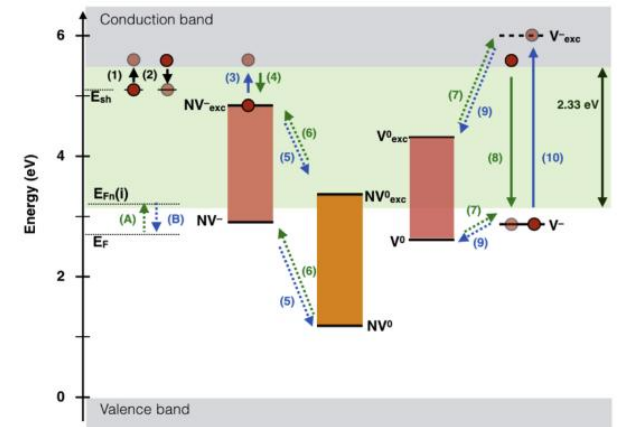
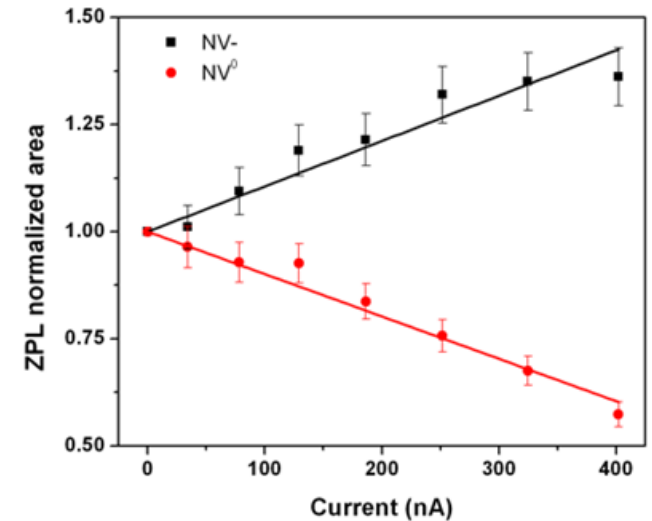
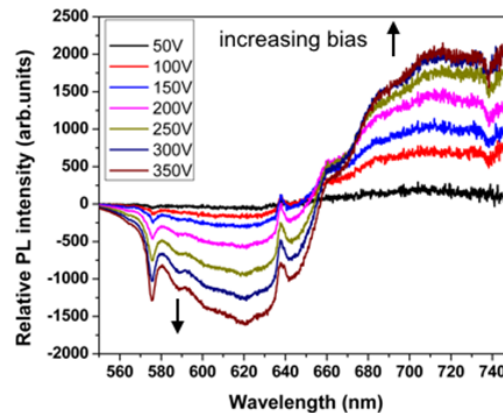
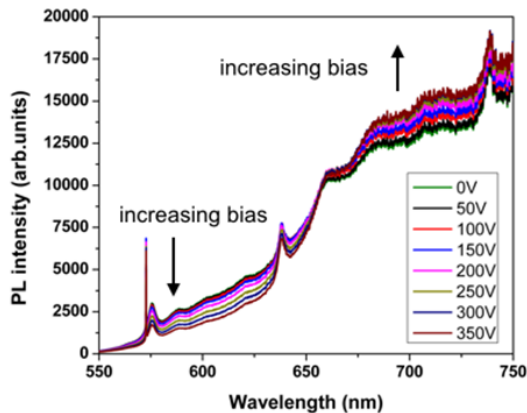
Quantum optics

NV charge state control



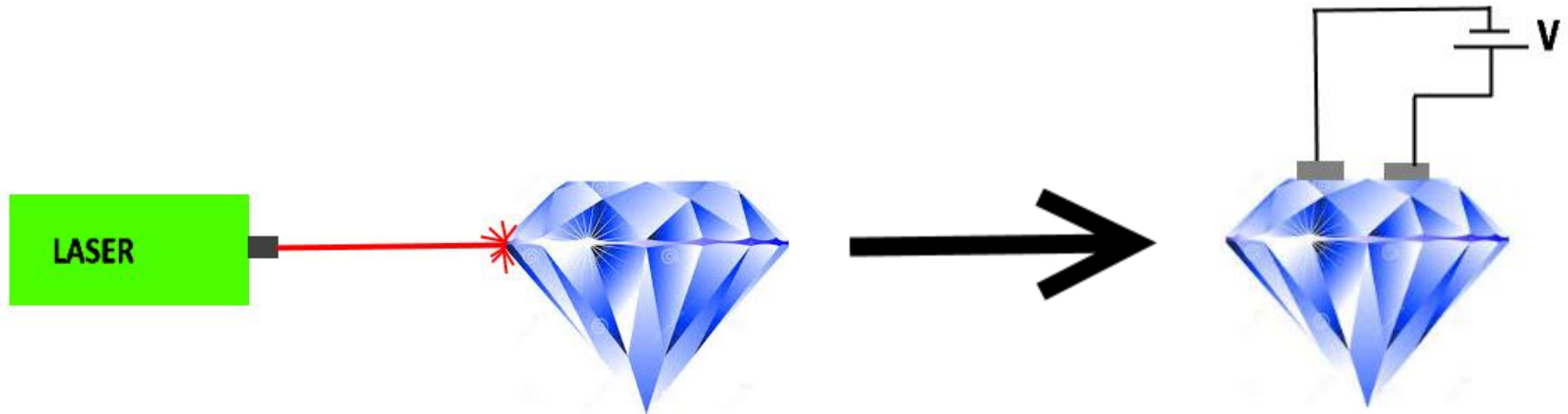
- optical grade sample, C ion beam
- steady laser excitation

- $\lambda = 532 \text{ nm}$
- $P = 21.6 \text{ mW}$



Quantum optics

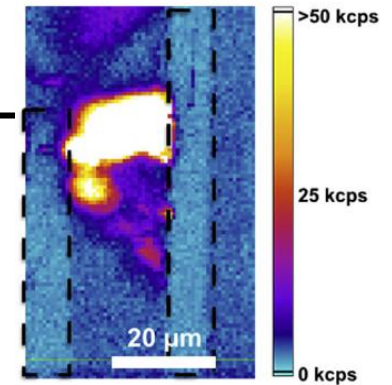
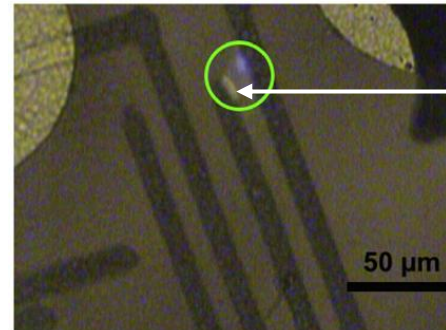
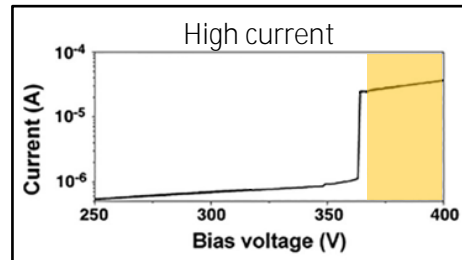
Electrical stimulation of luminescent emission



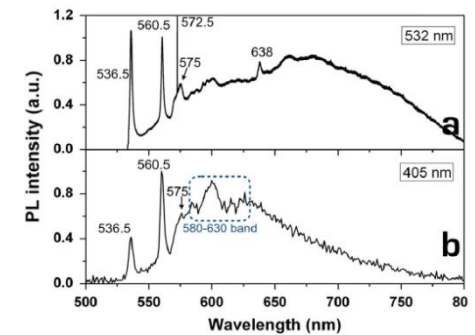
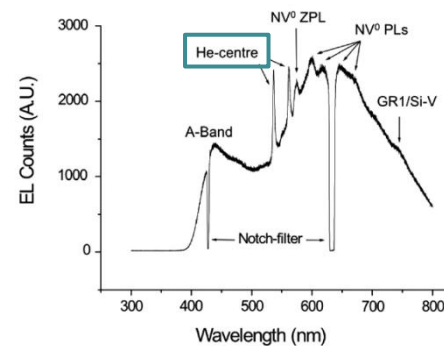
- ✓ Simpler device design
- ✓ No need for optical alignment
- ✓ Larger scalability and integrability

Quantum optics

Ensemble emission regime

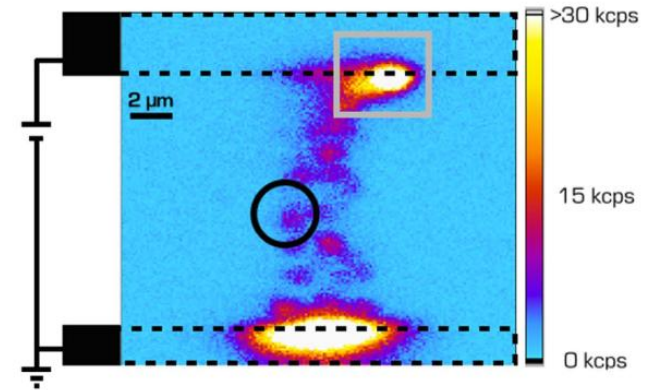
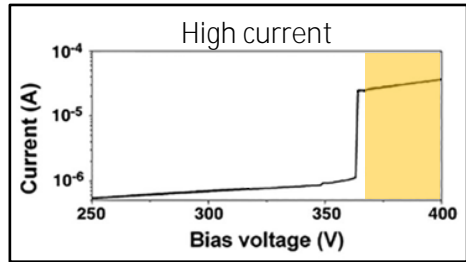


- CVD sample grown @Uni **Roma “Tor Vergata”**
- He ions irradiation with scanning μ -beam
- steady electrical stimulation
- observation of He-related color centers
- He-centers (536.5 nm, 560.5 nm) are both EL and PL active



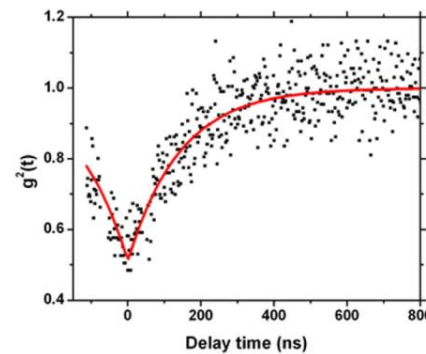
Quantum optics

Single-photon emission regime

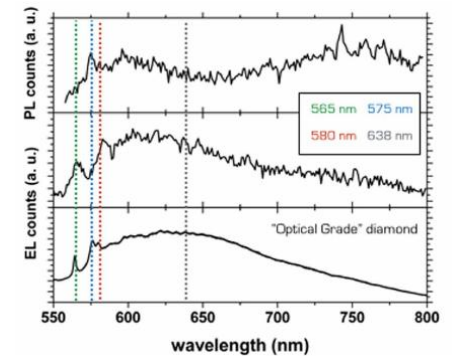


- electronic grade sample
- steady electrical stimulation
- $C_N(t) = 1 - a \cdot \exp(-\alpha |t|)$
- $\alpha^{-1} = (R + 1/\tau) = (143 \pm 5) \text{ ns}$

2nd order auto-correlation function



emission spectrum

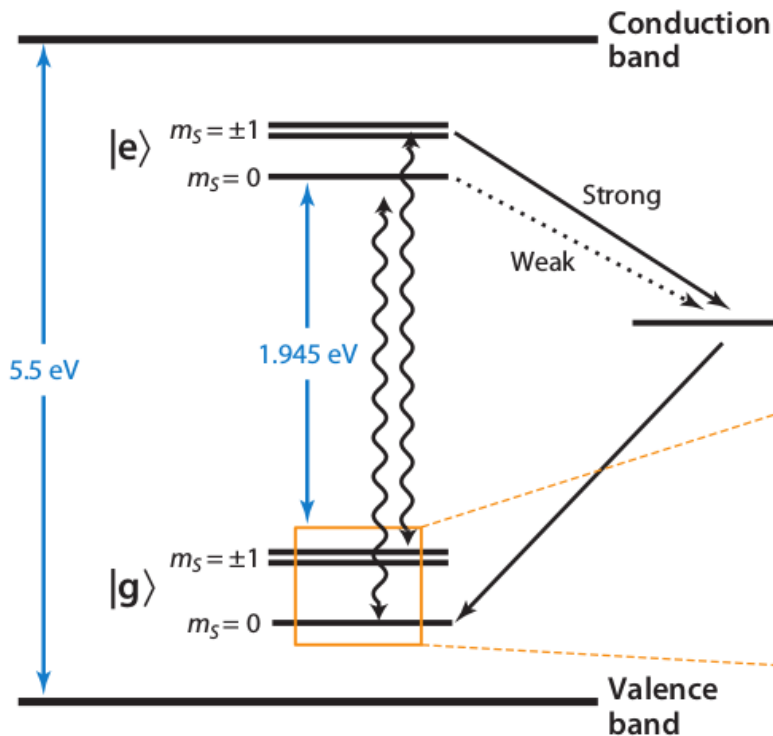


Quantum optics

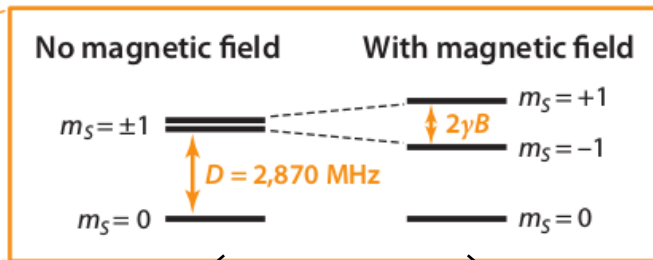
NV magnetometry

spin 1 system

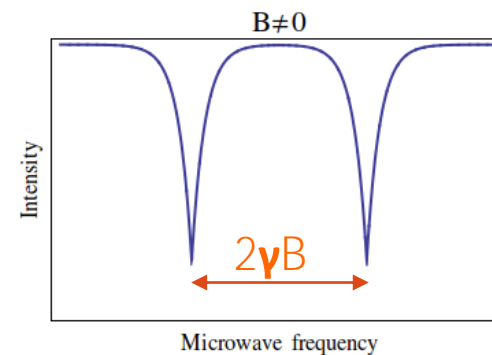
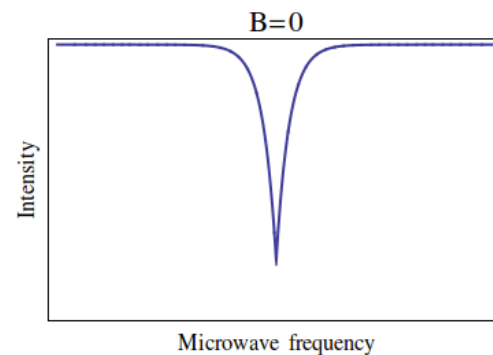
$m = \pm 1$ excited level: high probability of non-radiative relaxation



Microwaves promote transitions to the $m = \pm 1$ state.

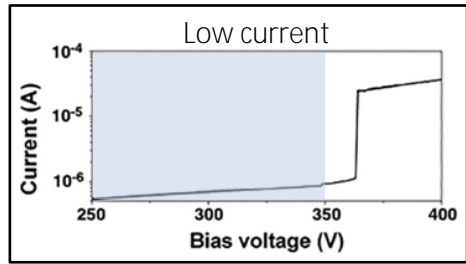


Zeeman effect
↓
Magnetometry



Quantum optics

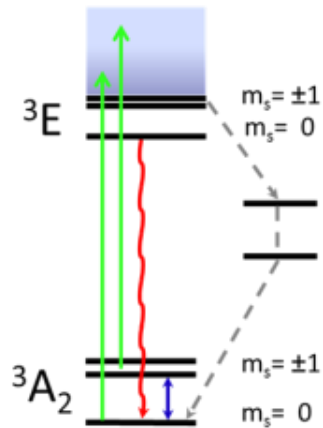
NV electrometry



- optical grade sample, C ions
- steady laser excitation

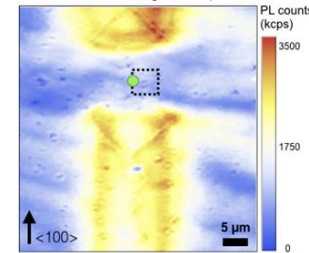
- $\lambda = 515 \text{ nm}$
- ODMR measurements

Stark shift of the $|\pm 1\rangle$ states

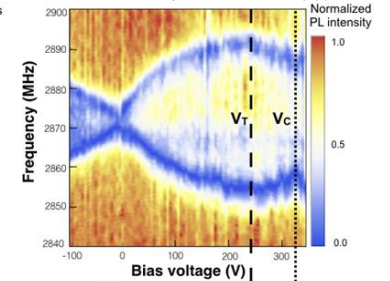


$$H = H_0 + \underbrace{g\mathbf{S} \cdot \mathbf{B}}_{\alpha} + \underbrace{d_{\parallel}(E_z + F_z)}_{\beta} [S_z^2 + S(S+1)/3] - \underbrace{d_{\perp}(E_x + F_x)(S_x S_y + S_y S_x)}_{\gamma} - \underbrace{d_{\perp}(E_y + F_y)(S_x^2 - S_y^2)}_{\delta}$$

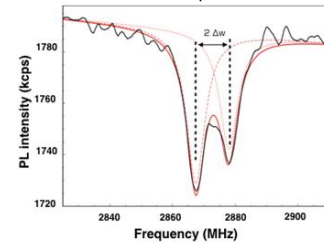
PL intensity map



ODMR spectra vs V_{bias}



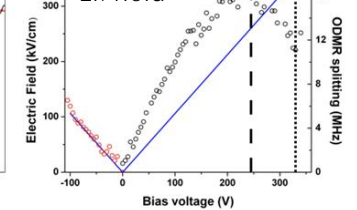
ODMR spectrum



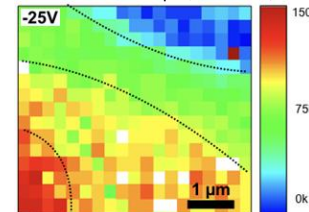
[C] (1)

[R] (2)

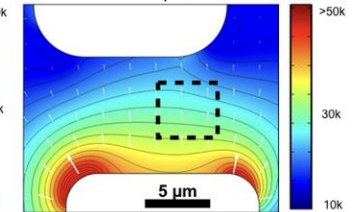
El. field



El. field map (ODMR)



El. field map (FEM sim.)



F. Forneris et al., arXiv:1706.07935 (2017)

-
- Diamond
 - IBL in diamond
 - Basic concepts
 - State of the art
 - Current research activities @ UniTo & INFN-To
 - **Electrical** features
 - Radiation detection
 - Biosensing
 - Quantum Optics
 - Conclusions

Conclusions

- Ion beam lithography: a powerful technique for microfabricating **“extreme” materials such as diamond**

Conclusions

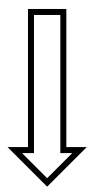
- Ion beam lithography: a powerful technique for microfabricating **“extreme” materials such as diamond**

Conclusions

- Ion beam lithography: a powerful technique for microfabricating

“extreme” materials such as diamond

- Nuclear damage:



point defect creation

→ **single color centers**

amorphization & graphitization

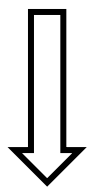
→ **buried electrodes**

Conclusions

- Ion beam lithography: a powerful technique for microfabricating

“extreme” materials such as diamond

- Nuclear damage:



point defect creation

→ **single color centers**

amorphization & graphitization

→ **buried electrodes**

- Device applications:

→ **particle detectors**

→ **cellular biosensors**

→ **quantum-optical devices**

Acknowledgments



Sample processing and characterization University of Torino

A. Battiato, F. Bosia, V. Carabelli, E. Carbone, J. Forneris, D. Gatto Monticone, A. Lo Giudice, S. Gosso, P. Olivero, F. Picollo, A. Re, A. Tengattini, E. Vittone



FIB micromachining and optical characterization National Institute of Metrologic Research

G. Amato, L. Boarino, G. Brida, I. Degiovanni, E. Enrico, M. Genovese, P. Traina

MeV ion implantation & IBIC measurements

National Laboratories of Legnaro (INFN)

D. Ceccato, L. La Torre, V. Rigato



LABEC laboratory (INFN)

S. Calusi, L. Giuntini, M. Massi

Ruđer Bošković Institute

V. Grilj, M. Jakšić, Ž. Pastuović, N. Skukan



RUBION Laboratory

S. Pezzagna, J. Meijer

FIB microfabrication, cross-sectional TEM MARC group, University of Melbourne

B. Fairchild, S. Praver, S. Rubanov

Optical / morphological characterization National Institute of Optics

R. Mercatelli, F. Quercioli, A. Sordini, S. Soria, M. Vannoni

Optical absorption characterization ENEA “La Casaccia”

A. Sytchkova

Optical modeling Department of Energetics, University of Florence

S. Lagomarsino, S. Sciortino

Waveguides characterization CIBA – National University of Singapore

A. Bettiol, V. S. Kumar

High-resolution X-ray diffraction Department of Physics, University of Padova

N. Argiolas, M. Bazzan

CVD diamond growth Department of Mechanical Engineering, University of Rome Tor Vergata

M. Marinelli, C. Verona, G. Verona-Rinati



Acknowledgments

Development of microfabrication techniques in diamond for applications in bio-sensing and photonics

Italian Ministry for Instruction, University and Research



A.Di.N-Tech. - Advanced Diamond-based Nano-technologies
CSP Foundation



Di.Na.Mo. – Diamond NanoModification
National Institute of Nuclear Physics



DIESIS – Electrically controlled diamond-based single photon sources

National Institut of Nuclear Physics



DIACELL – Diamond based detector for in vitro cellular radiobiology

National Institut of Nuclear Physics



MIRADS – New Micro-Radiobiology Devices for aeroSpace
CRT Foundation



Thanks for your attention!
